DNA-uptake pilus of *Vibrio cholerae* capable of kin-discriminated auto-aggregation

David W. Adams, Sandrine Stutzmann, Candice Stoudmann and Melanie Blokesch*

Laboratory of Molecular Microbiology, Global Health Institute, School of Life Sciences, Station 19, EPFL-SV-UPBLO, Swiss Federal Institute of Technology Lausanne (Ecole Polytechnique Fédérale de Lausanne; EPFL), CH-1015 Lausanne, Switzerland.

*For correspondence email: melanie.blokesch@epfl.ch.

Summary

Natural competence for transformation is a widely used and key mode of horizontal gene transfer that can foster rapid bacterial evolution. Competent bacteria take-up DNA from their environment using Type IV pili, a widespread and multi-purpose class of cell surface polymers. However, how pili facilitate DNA-uptake has remained unclear. Here, using direct labelling, we show that in the Gram-negative pathogen *Vibrio cholerae* DNA-uptake pili are abundant, highly dynamic and that they retract prior to DNA-uptake. Unexpectedly, these pili can self-interact to mediate auto-aggregation of cells into macroscopic structures. Furthermore, extensive strain-to-strain variability in the major pilin subunit PilA controls the ability to aggregate without affecting transformation, and enables cells producing pili composed of different PilA to discriminate between one another. Our results suggest a model whereby DNA-uptake pili function to promote inter-bacterial interactions during surface colonisation and moreover, reveal a simple and potentially widespread mechanism for bacterial kin recognition.

Keywords

Auto-aggregation, DNA uptake, natural transformation, pilus dynamics, type IV pilus, *Vibrio cholerae*

29 **Introduction**

30 How bacteria physically sense and interact with their environment is a fundamental problem
31 in biology. Type IV pili (T4P) are thin 'hair-like' cell surface polymers ideally suited to this task
32 and are widely distributed throughout the bacteria. Composed of thousands of copies of a
33 single major pilin and assembled by broadly conserved machinery, T4P exhibit extensive
34 functional versatility, with roles in motility, adhesion, DNA-uptake and are especially
35 important for surface sensing and colonisation (Ellison *et al.*, 2017; Maier and Wong, 2015;
36 Persat *et al.*, 2015). Consequently, T4P are critical virulence factors for a number of
37 important human pathogens including *Escherichia coli*, *Neisseria meningitidis*, *Pseudomonas*
38 *aeruginosa* and *Vibrio cholerae*. T4P are also evolutionarily related to the type II secretion
39 system and indeed, share some homologous components (Berry and Pelicic, 2015; Giltner *et*
40 *al.*, 2012). Understanding how T4P function may thus yield insights valuable for
41 understanding mechanisms of environmental survival and pathogenicity.

42 T4P have been extensively studied revealing a largely conserved assembly pathway
43 (Berry and Pelicic, 2015; Giltner *et al.*, 2012; Leighton *et al.*, 2015). Pilins are produced as
44 precursors and processed in the inner membrane by a pre-pilin peptidase. Mature pilins
45 resemble a 'lollipop' with a globular domain on top of a long N-terminal α-helix. They are
46 extracted by the assembly machinery and polymerised into a helical pilus fibre that in Gram-
47 negative bacteria is extruded from the cell surface through a gated outer membrane pore;
48 the secretin (Chang *et al.*, 2017; Chang *et al.*, 2016; Craig *et al.*, 2006; Gold *et al.*, 2015;
49 Kolappan *et al.*, 2016). The N-terminal domains of pilins, which contain the signal sequence
50 required for membrane insertion, cleavage, and that forms the core of the pilus fibre, are
51 well conserved. In contrast, variation within the globular domain is common and is thought
52 to underpin the functional diversity of T4P (Giltner *et al.*, 2012). A key feature of T4P is the
53 ability to undergo dynamic cycles of extension and retraction, which is essential for many
54 pilus functions *e.g.* twitching motility (Merz *et al.*, 2000; Skerker and Berg, 2001). Rotation of

55 an IM 'platform' protein in opposite directions, driven by the cytoplasmic ASCE (Additional
56 Strand Catalytic 'E') ATPases PilB and PilT, controls pilus extension and retraction,
57 respectively, by either adding or liberating pilin subunits at the base (Chang *et al.*, 2016;
58 Jakovljevic *et al.*, 2008; McCallum *et al.*, 2017).

59 *V. cholerae* causes the pandemic disease Cholera, which remains an on-going threat
60 to human health worldwide, especially in areas without access to basic sanitation (Clemens
61 *et al.*, 2017). Pandemic strains of *V. cholerae* typically encode three distinct T4P systems –
62 two of which are well characterised. First, toxin co-regulated pili (TCP) serve a dual role as
63 both a receptor for CTXϕ bacteriophage, which carries the cholera toxin genes (Waldor and
64 Mekalanos, 1996), and also as the primary human colonisation factor, with multiple
65 essential roles in infection that involves adhesion and auto-aggregation of cells on the
66 intestinal cell surface (Chiang *et al.*, 1995; Taylor *et al.*, 1987). Second, Mannose-sensitive
67 haemagglutinin (MSHA) pili mediate attachment to biotic and abiotic surfaces (Chiavelli *et*
68 *al.*, 2001; Meibom *et al.*, 2004; Watnick *et al.*, 1999). Together with flagellar motility, the
69 surface sensing activity of MSHA pili is critical for the initiation of biofilm formation
70 (Moorthy and Watnick, 2004; Utada *et al.*, 2014; Watnick and Kolter, 1999). These are dense
71 surface-associated multicellular communities, held together by an extracellular matrix
72 composed of polysaccharides and matrix proteins (Teschler *et al.*, 2015). Biofilms represent
73 a key adaptation to survival in hostile environments and provide a physical barrier to defend
74 against predators such as bacteriophages and protozoan grazers.

75 Outside of its role in disease *V. cholerae* is a natural inhabitant of the aquatic
76 environment and is commonly found in association with chitinous surfaces *e.g.* zooplankton
77 and their molts (Tamplin *et al.*, 1990). These surfaces provide nutrition, foster biofilm
78 formation, and likely play a role in environmental dissemination and transmission to humans
79 (Blokesch, 2015; Colwell *et al.*, 2003; Huq *et al.*, 1996; Meibom *et al.*, 2004). Growth on
80 chitin also activates natural competence for transformation (Meibom *et al.*, 2005), a key

81 mode of horizontal gene transfer that is widely used by bacteria to take up DNA from their
82 environment, and which can thus, foster rapid bacterial evolution (Johnston *et al.*, 2014).
83 This involves production of the third T4P, the Chitin-Regulated pilus (ChiRP) or DNA-uptake
84 pilus, as it was later renamed due to its role in natural competence (Matthey and Blokesch,
85 2016; Meibom *et al.*, 2005).

86 We previously showed that the DNA-uptake pilus forms a *bona fide* pilus, composed
87 of the major pilin subunit PilA, and that transformation was dependent on the putative
88 retraction ATPase PilT (Seitz and Blokesch, 2013). However, the pilus itself is not sufficient
89 for DNA uptake and requires the combined action of a periplasmic DNA binding protein,
90 ComEA. Moreover, upon addition of transforming DNA, ComEA switches from a diffuse to
91 focal localisation pattern (Seitz *et al.*, 2014). These findings, together with work in other
92 organisms, led to a model in which pilus retraction facilitates entry of DNA into the
93 periplasmic space (Wolfgang *et al.*, 1998), wherein ComEA-DNA binding acts as a ratchet to
94 pull the remaining DNA into the cell (Seitz *et al.*, 2014). Subsequently, DNA transport across
95 the cytoplasmic membrane occurs via a spatially coupled channel, ComEC (Seitz and
96 Blokesch, 2014). Although this model is well supported by genetic experiments and is
97 consistent with the similarly combined action of T4P and ComEA in other organisms, direct
98 evidence is lacking (Gangel *et al.*, 2014; Laurenceau *et al.*, 2013). Indeed, the affinity tag and
99 immuno-fluorescent approaches commonly used to visualise pili preclude the observation of
100 pilus dynamics and so how the pilus functions has remained unclear.

101 Here, we set out to visualise the DNA-uptake pilus directly using a cysteine labelling
102 approach, which was recently validated as a tool for labelling pili (Ellison *et al.*, 2017). We
103 demonstrate that the pilus is highly dynamic and that these dynamics are PilT-dependent.
104 Unexpectedly, we discovered that DNA-uptake pili are also capable of mediating auto-
105 aggregation and that PilA diversity controls this ability but has no impact on transformation.

106 Remarkably, specific interactions between DNA-uptake pili allow cells to recognise pili
107 composed of the same PilA subunit, enabling a simple mechanism for kin recognition.
108
109 **Results**
110 **Direct observation of pilus dynamics by cysteine labelling**
111 In order to visualise the DNA-uptake pilus, but avoid the limitations imposed by immuno-
112 fluorescent methods, a direct cysteine labelling approach was employed using a thiol-
113 reactive dye (Blair *et al.*, 2008; Ellison *et al.*, 2017). Six different PilA cysteine variants were
114 created along the αβ–loop, which is predicted to be surface exposed on the assembled pilus
115 fibre and is therefore an ideal target for labelling (Craig *et al.*, 2006; Kolappan *et al.*, 2016).
116 These variants were tested for functionality and labelling in cells grown under chitin-
117 independent competence induction (Figure 1A and Figure S1A), using an arabinose-inducible
118 copy of *tfoX* (Tn*tfoX*), the master regulator of competence (Lo Scrudato and Blokesch, 2012).
119 PilA[S67C] and PilA[T84C] were both produced at similar levels and were fully transformable,
120 as compared to the unmodified parent, and when stained exhibited visible pili (Figure 1A
121 and Figure S1A and B). However, since PilA[T84C] produced only occasional, weakly stained
122 pili, it was not studied further.
123 In contrast, cells producing PilA[S67C] exhibited abundant pili (Figure 1C and D).
124 Quantification showed that on average 27 ± 3 % of cells were piliated and the majority of
125 these displayed 1 or 2 pili per cell (Figure 1 I and J). The length of pili was clustered around 1-
126 2 µm, although some cells were capable of producing pili of up to 10 µm (Figure 1K). In
127 addition, numerous detached pili were visible in the media and intriguingly, some of these
128 pili appeared to self-interact to form large structures composed of networks of pili (Figure
129 S2A). When examined by time-lapse microscopy cells exhibited rapid pilus dynamics with
130 multiple assembly and retraction events immediately apparent (Figure 1L; Movie S1-4).
131 Indeed, within the 1 minute time frame studied 66 ± 3 % cells were piliated, with most cells

132 producing 1-2 pili per minute (Figure 1N). Notably, a small subpopulation of cells was even
133 more dynamic, elaborating ≥5 pili per min. Interestingly, and in support of the idea that pilus
134 retraction precedes DNA uptake, when competent cells were incubated with purified
135 genomic DNA it was also possible to concurrently visualise pilus retraction followed by DNA-
136 uptake, as monitored by the re-localisation of ComEA-mCherry, which binds incoming DNA
137 in the periplasm (Figure S3; Movie S5).

138 Control experiments showed that, as expected, deletion of either *pilB* or *pilQ*,
139 encoding respectively the assembly ATPase and outer-membrane secretin, abolished
140 piliation (Figure 1E and F). Surprisingly, however, the cell body did stain with the dye,
141 despite the absence of obvious pili. This was not the case for uninduced cells encoding
142 PilA[S67C] (Figure 1C). However, cells engineered to produce PilA[S67C] but not PilA[WT]
143 independently of the pilus assembly machinery also stained similarly, indicating that this
144 effect likely results from non-specific uptake of the dye across the outer-membrane and its
145 subsequent binding to the inner-membrane pool of PilA[S67C] (Figure S1C). This staining was
146 also independent of the MSHA pilus and the outer membrane porin OmpA (Figure S1C). As
147 in other species, *V. cholerae* encodes two potential retraction ATPases, PilT and PilU.
148 Deletion of *pilU* did not affect piliation (Figure 1G, I and J), in agreement with its
149 dispensability for transformation ((Seitz and Blokesch, 2013) and below). In contrast, cells
150 lacking the presumed retraction ATPase PilT were hyper-piliated, with essentially all cells
151 displaying multiple static pili (Figure 1H-J and M; Movie S6-7). Taken together with the
152 dynamics described above, these data are consistent with the presence of multiple assembly
153 complexes scattered across the cell, which normally might serve to facilitate rapid switching
154 of pilus location, as previously hypothesised based on the mobility of PilB and the presence
155 of multiple PilQ foci (Matthey and Blokesch, 2016; Seitz and Blokesch, 2013). Unexpectedly,
156 cells deleted for *pilT* exhibited a second phenotype. Cells were often grouped into small
157 clusters within dense mesh-like networks of pili and occasionally large aggregates of pili-

158 encased cells could also be detected (Figure S2B and C). Indeed, when grown in liquid
159 culture cells appeared to auto-aggregate.
160
161 **Competent cells auto-aggregate in the absence of pilus retraction**
162 To test directly whether the aggregation phenotype was an inherent property of hyper-
163 piliated cells or merely an artefact introduced by the cysteine variant, cells containing
164 unmodified *pilA* were examined (Figure 2A-C). Remarkably, competence-induced cells
165 lacking *pilT* readily formed large spherical aggregates, with a multi-layered and well-ordered
166 architecture on the order of ≥100 µm, which went on to form macroscopic aggregates that
167 rapidly sediment (Figure 2B, +Ara). This sedimentation phenotype was used to quantify the
168 extent of auto-aggregation by determining the ratio of cells remaining in solution to those in
169 the settled aggregates (Figure 2D). Importantly, neither WT cells nor those harbouring the
170 inducible-*tfoX* formed aggregates, irrespective of the presence of inducer. However, in the
171 absence of pilus retraction ≥90% of cells were present in aggregates and this phenotype was
172 strictly dependent on competence-induction (Figure 2D). Notably, the PilA[S67C] variant
173 used for labelling also aggregates similarly (Figure 1B). To rule out the possibility that the
174 deletion of *pilT* has either a polar or otherwise non-specific effect, an intact copy of *pilT*
175 driven by its native promoter was placed at an ectopic locus. Importantly, complementation
176 of Δ*pilT* was sufficient to fully restore the ~1000-fold defect in transformation frequency and
177 abolished the aggregation phenotype (Figure 1D and E). Complementation also fully
178 counteracted the enhanced motility phenotype of Δ*pilT* (Figure S4), which occurs due to loss
179 of function in the adhesive MSHA pilus and is in agreement with the previously established
180 role of PilT in MSHA pilus function (Jones *et al.*, 2015; Watnick and Kolter, 1999).
181 To investigate how the aggregates formed their assembly was followed over time.
182 These kinetic experiments revealed that aggregation occurs abruptly, suggesting that rather
183 than gradually increasing in size, the large aggregates form via the accumulation of smaller

184 ones (Figure S5A and B). In support of this hypothesis, when two otherwise isogenic Tn*tfoX*
185 Δ*pilT* strains, one of which constitutively produces GFP, were allowed to aggregate
186 separately (Figure S5C and D) before being mixed, they formed large composite aggregates
187 consisting of a patchwork of labelled and unlabelled cells (Figure S5F). Indeed, fusion events
188 between aggregates of various sizes were frequently observed. In contrast, when the strains
189 were grown together from the start only well-mixed aggregates were obtained (Figure S5E).
190 Finally, although cells continued to grow within the aggregates they remained stable and did
191 not disperse, even after prolonged culture overnight.
192
193 **Aggregates form via pilus-pilus interactions**
194 To determine the nature of the interaction(s) that underpin aggregate assembly, Δ*pilT* (*i.e.*
195 retraction-deficient cells) was combined with deletions of genes in various related pathways
196 that could potentially be involved. Deletion of *tcpA* and *mshA*; which respectively encode
197 the major pilins of the TCP and MSHA pili, *vpsA;* which encodes an enzyme required for
198 production of the *Vibrio* polysaccharide (VPS) matrix that is necessary for efficient biofilm
199 formation (Fong *et al.*, 2010), and *flaA*; which encodes the major subunit of the flagellum,
200 were all dispensable for aggregation, both individually and in combination (Figure 2F).
201 Similarly, additional genes tested with roles in biofilm formation (*bap1*, *rbmA*, *rbmEF*, *vpsT*)
202 (Absalon *et al.*, 2011; Berk *et al.*, 2012), adhesion (*gbpA*) (Kirn *et al.*, 2005), cell shape (*crvA*)
203 (Bartlett *et al.*, 2017) and an O-linked glycosylase (*VC0393* or $pglL_{Vc}$) (Gebhart *et al.*, 2012)
204 that could be involved in pilin modification all aggregated at levels indistinguishable from
205 the unmodified parent (Figure S6A). Furthermore, deletion of *VC0502*, an 'orphan' type IV
206 pilin encoded on the *Vibrio* seventh pandemic island II, had no effect on transformation,
207 aggregation or motility (Figure S6B-D). In contrast to these results, cells lacking PilQ or PilA
208 were unable to aggregate (Figure 2F) indicating that the DNA-uptake pilus is itself necessary
209 for aggregation.

210 To investigate how the pilus mediates auto-aggregation *e.g.* pilus-pilus, pilus-cell or
211 otherwise, a Tn*tfoX* Δ*pilT* strain constitutively producing GFP was co-inoculated with either
212 cells of the Tn*tfoX* WT, Tn*tfoX* Δ*pilT* or Tn*tfoX* Δ*pilA* Δ*pilT* and grown with and without
213 inducer (Figure 2G-L). As expected, in the absence of inducer, and hence pili, all cells were
214 equally distributed (Figure 2G-I). Similarly, upon competence induction the unlabelled
215 Tn*tfoX* Δ*pilT* cells formed well-mixed aggregates with those of the isogenic, labelled strain
216 (Figure 2K). However, the other unlabelled cells were largely excluded from the aggregates
217 (Figure 2J and L), indicating that first, aggregation occurs via pilus-pilus interactions and
218 second, that these interactions require non-retractile pili. Importantly, aggregation was not
219 affected by growth under high salt concentrations (*i.e.* LB-S 20 g/L NaCl), which are often
220 used to better reflect the natural aquatic environment of *Vibrio sp*. (Figure S6E). Similarly,
221 growth in the presence of Bovine serum albumin, which has previously been reported to
222 inhibit pilus-pilus interactions in *Neisseria gonorrhoeae* (Biais *et al.*, 2008), also had no effect
223 (Figure S6E).
224 The aggregates described above are reminiscent of those formed by TCP during
225 virulence induction. To directly compare the two types of aggregate, strains carrying an
226 arabinose-inducible copy of the transcriptional activator *toxT* were created. In the presence
227 of inducer, cells of this strain aggregate in a TcpA-dependent manner to similar levels as
228 those formed by the DNA-uptake pilus (Figure S7A). Interestingly, though both types of
229 aggregate are morphologically similar, those formed by TCP often appeared less tightly
230 packed, likely a result of the increased length of *toxT*-induced cells (Figure S7C). In
231 agreement with the results above and previous work on TCP, when grown together the two
232 types aggregates did not intermix (Figure S7B-D).
233

234 **MSHA pili do not form aggregates**

235 MSHA pili are important for surface sensing and attachment during the switch to the sessile
236 lifestyle that precedes biofilm formation, and pilus retraction is thought to be required for
237 their function. Given that MSHA pili are produced during normal growth but that retraction
238 deficient cells only aggregate upon competence induction, the results above suggest that
239 MSHA pili are unable to mediate auto-aggregation. To test this hypothesis directly we took
240 advantage of the report that increased levels of the second messenger c-di-GMP, leads to
241 enhanced assembly of MSHA pili on the cell surface (Jones *et al.*, 2015). As a control, we first
242 tested strains engineered to decrease c-di-GMP levels cells but did not observe aggregation
243 under any condition tested (Figure S8A and B). In contrast, strains engineered to increase c-
244 di-GMP levels produced large clumps of cells that appeared similar to the aggregates
245 described above and had a modest sedimentation phenotype (Figure S8A and B).
246 Nevertheless, the assembly of these structures occurred independently of *pilT*, *pilA* and
247 *mshA*, but was abolished by the loss of *vpsA* (Figure S8C). Thus, these structures are not
248 aggregates held together by pili but rather biofilms held together by the matrix
249 polysaccharide, VPS.

250

251 **ATPase deficient PilT variants are sufficient for aggregation and reveal a role for PilU**

252 PilT, like its homologue PilU and the assembly ATPase PilB are ASCE ATPases that contain
253 conserved Walker A and atypical Walker B box motifs (Figure S9), which are required for ATP
254 binding and hydrolysis, respectively. To investigate the role of ATPase activity in pilus
255 retraction, *pilT* mutants were created encoding Walker A (PilT[K136A]) and Walker B
256 (PilT[E204A]) variants predicted to abolish ATPase activity and tested for their ability to
257 support transformation, aggregation and motility (Figure 3A-C). Surprisingly, however, both
258 variants showed only a 25-50-fold reduction in transformation frequency (Figure 3A).
259 Moreover, the Walker A variant did not aggregate and had normal motility (Figure 3B and C).

260 In contrast, the Walker B variant aggregated, albeit at slightly reduced levels, and exhibited
261 an enhanced motility phenotype indistinguishable from a *pilT* deletion (Figure 3B and C).
262 The function of the PilT homologue PilU is unknown, and when absent has no
263 obvious effect on transformation or surface motility. Thus, one explanation for the confusing
264 and intermediate phenotypes described above, is that under certain circumstances PilU is
265 either able to substitute for or otherwise complement PilT function. If correct, then loss of
266 *pilU* or else the production of an ATPase impaired PilU variant would be expected to abolish
267 any remaining functionality. To test this hypothesis PilU Walker A (PilU[K134A]) and B
268 (PilU[E202A]) box variants were created. As expected, cells deleted only for *pilU* and those
269 producing the PilU variants were neither affected for transformation nor motility and did not
270 aggregate (Figure 3A-C). In contrast, combination of the PilT Walker A or B box variants with
271 either Δ*pilU* or either of the PilU Walker box variants all produced phenotypes in
272 transformation, aggregation and motility equivalent to that of the Δ*pilT* (Figure 3A-C). Taken
273 together, these data suggest that PilU has a redundant role in pilus retraction and moreover,
274 that it must interact with PilT to fulfil this role. Indeed, bacterial two-hybrid experiments
275 detected both self and cross-interactions between PilT and PilU (Figure 3D).
276
277 **A clinical *V. cholerae* isolate with a naturally occurring *pilT* mutation**
278 To determine whether the ability to aggregate is conserved among other clinical isolates we
279 investigated a set of six additional O1 El Tor strains, representative of the on-going seventh
280 Cholera pandemic. In the absence of *pilT* all were capable of aggregating at similar levels as
281 the frequently studied O1 El Tor A1552 used here (Figure 4A), as might be expected, given
282 the closely related nature of these strains. Notably, however, N16961 did not aggregate,
283 unless its well-characterised *hapR* frame-shift mutation (Joelsson *et al.*, 2006) was first
284 repaired (Figure 4A). Since the transcription of the genes required for pilus assembly are not

285 regulated by quorum sensing (QS) (Lo Scrudato and Blokesch, 2012) this finding suggests
286 that there may be an additional layer of post-transcriptional control.

287 To extend these results we also investigated strain MO10, a representative of the
288 O139 serogroup, which beginning in 1992 caused a severe Cholera epidemic that spread
289 rapidly throughout the Indian subcontinent. Unexpectedly, competence-induced cells of
290 MO10 aggregated in an otherwise unmodified background (Figure 4B and C). Indeed,
291 deletion of *pilT* did not affect the level of aggregation (Figure 4B). Although, similar to
292 N16961, the aggregation phenotype was further enhanced when we repaired the QS
293 defective HapR variant encoded by MO10 (Figure 4B and C). However, in line with the
294 results above, deletion of *pilA* abolished aggregation (Figure 4B). Introduction of the
295 PilA[S67C] substitution revealed that competence-induced cells of MO10 were hyper-
296 piliated, irrespective of the *hapR* repair, suggesting that they are defective for pilus
297 retraction (Figure 4D). Indeed, inspection of the *pilTU* locus detected a single bp mutation in
298 *pilT,* resulting in the substitution of a widely conserved arginine (R206S) that sits in proximity
299 to the Walker B motif (Figure S9B), suggesting that PilT[R206S] is either catalytically inactive
300 or otherwise impaired. The evidence for this assertion is three-fold. First, repairing the *pilT*
301 mutation (*i.e.* PilT[S206R]) abolished the ability of MO10 to aggregate (Figure 4B). Second,
302 recreating the *pilT* mutation in A1552 reduced transformation frequency and allowed
303 competence-induced cells to aggregate (Figure 4E and F). Third, similar to the PilT Walker A
304 and B box variants described above, the transformation of cells carrying the MO10 PilT
305 variant is PilU-dependent (Figure 4E). Taken together these data show that the naturally
306 occurring *pilT* mutation carried by MO10 encodes an ATPase deficient form of PilT and thus,
307 competence-induced cells of this strain have an inherent ability to aggregate.
308

309 **A1552 PilA is sufficient for aggregation in a non-O1/O139 strain**

310 PilA is known to vary considerably between different environmental strains of *V. cholerae*,
311 whereas the majority of clinical isolates carry an identical *pilA* (Aagesen and Häse, 2012).
312 One interesting exception is the well-studied toxigenic O37 serogroup strains, ATCC25872
313 and V52, which in turn caused local outbreaks of a cholera-like illness in the then
314 Czechoslovakia (1965) and in Sudan (1968) (Aldova *et al.*, 1968; Chun *et al.*, 2009). These
315 strains are thought to derive from a pandemic O1-Classical strain through the exchange of
316 the O-antigen cluster by horizontal gene transfer (Blokesch and Schoolnik, 2007; Li *et al.*,
317 2002). However, they both encode the same PilA that is only 50% identical to that typically
318 carried by pandemic strains (Figure S10). Since V52 is QS deficient, and transformation is QS
319 dependent, we investigated the functionality of this PilA in ATCC25872, which has a
320 functional QS pathway. Indeed, ATCC25872 is transformable at similar levels to that of
321 A1552, and as expected, transformation is PilT-dependent (Figure 5A). However, in contrast
322 to A1552, competence-induced cells lacking *pilT* did not aggregate and were excluded from
323 aggregates formed by A1552 (Figure 5B-D, G and H).

324 Given that all the other known components required for pilus assembly and
325 transformation are highly conserved in ATCC25872, we tested whether PilA itself was
326 responsible for this phenotype by exchanging the endogenous *pilA* open reading frame for
327 that of A1552 (*pilA*ex). As expected, the ATCC25872 *pilA*ex strain was fully transformable
328 (Figure 5A). Importantly, however, in the absence of *pilT*, competence-induced cells of this
329 strain were now able to form large aggregates, albeit at lower levels than in A1552 (Figure B,
330 E and F), and intermix within aggregates formed by A1552 (Figure 5I and J).

331

332 **PilA variability governs auto-aggregation and enables kin-recognition**

333 The results above suggest that the ability to aggregate is dependent on the particular PilA
334 variant carried. To investigate this prediction in detail we analysed PilA variability in 647 *V.*

335 *cholerae* genomes deposited in NCBI. Indeed, BLAST analyses indicated that PilA exhibits
336 extensive variation, whereas the other proteins encoded within its operon, as well as those
337 from neighbouring genes, are all highly conserved (Figure S11). Of the 636 intact *pilA* genes
338 identified, the majority (492/636) encode a PilA identical to that of A1552, which is likely
339 due to the over-representation of patient-derived pandemic strains in the database. Next, in
340 order to build a picture of PilA diversity we extracted the unique PilA coding sequences
341 (56/636) (Figure S12A) and combined them with those of an in-house collection of various
342 environmental and patient isolates. The resulting phylogenetic tree consists of around 12
343 distinct groups and was used to sample PilA diversity (Figure 6A). As expected, the extreme
344 N-terminus, which contains the signal sequence required for membrane trafficking and pre-
345 pilin peptidase recognition, and the N-terminal domain that forms the long structural alpha
346 helix (α1), are both highly conserved (Figure S12A and B). In contrast, apart from a few
347 clusters of key conserved residues, including the C-terminal cysteines that form the
348 characteristic disulphide-bonded loop, the C-terminal domains are highly variable (Figure
349 S12A and B).

350 To avoid the potential problems of working in various strain backgrounds, we
351 inserted new *pilA* alleles at the native *pilA* locus in A1552, and used a short (30 bp)
352 duplication of 3' end of the original *pilA* to maintain any regulation of the downstream
353 genes. We validated this *pilA* replacement (*pilA*rep) approach using A1552 PilA (*i.e.* Tn*tfoX*,
354 *pilA*rep[WT]), which is fully transformable, and in the absence of *pilT* aggregates at levels
355 similar to the unmodified parent (Figure 6B and C). We then tested 16 different PilA
356 sequences from across the tree (Figure 6A). Interestingly, all were equally capable of
357 supporting similar levels of transformation (Figure 6B). In contrast, in the absence of *pilT*
358 only 8 PilAs supported a strong aggregation phenotype, 1 (PilA DRC186-4) was intermediate,
359 and 7 did not detectably aggregate (Figure 6A and C). Consistent with these data, Δ*pilT* cells
360 producing an identical PilA (*i.e.* Tn*tfoX*, *pilA*rep[WT]) formed well-mixed aggregates (Figure

361 6D) when grown together with Tn*tfoX* Δ*pilT* GFP, whereas those producing an aggregation
362 defective PilA were largely excluded. Surprisingly, cells producing pili composed of an
363 aggregation proficient PilA did not intermix with the aggregates formed by the A1552 PilA
364 pili (Figure 6E). Remarkably, however, cells of these strains aggregated in a pilin-specific
365 manner, preferentially forming aggregates with cells producing pili composed of the same
366 PilA. In all cases, as shown by the representative example in Figure 6E, this resulted in
367 aggregates that were either almost exclusively labelled or unlabelled, as well as a variety of
368 composite aggregates that in many cases likely resulted from the fusion of two or more
369 separate aggregates. These data indicate that pili composed of different PilA are able to
370 discriminate between one another and thus, implies that specific pilus-pilus interactions are
371 responsible. Furthermore, these data demonstrate that PilA variability not only determines
372 the ability to aggregate, but also provides a potential mechanism for kin-recognition.
373
374 **The unusual tail of ATCC25872/V52 PilA inhibits aggregation**
375 To investigate why some of the *pilA* alleles are unable to support aggregation, *pilA*rep
376 constructs were made encoding cysteine variants of the WT (*pilA*rep[WT S67C]) and 2 non-
377 aggregating alleles (*i.e. pilA*rep[Sa5Y S67C] and *pilA*rep[V52 N67C]) to allow visualisation and
378 comparison of the various pili. All constructs behaved similarly to the equivalent non-
379 cysteine variant, though the *pilA*rep[Sa5Y S67C] had a modest transformation defect (Figure
380 S13A and B). The *pilA*rep[WT S67C] readily formed pili, as well as large structures composed
381 of detached pili, as described above (Figure 7A and Figure S13C). Both the Sa5Y and V52
382 cysteine variants were piliated at similar levels to the WT control, although the Sa5Y pili
383 were generally very short (Figure 7A and B). Similarly, in the absence of *pilT* cells producing
384 both types of pili were hyper-piliated (Figure 7A and B). This effect was especially clear for
385 the V52 cysteine variant and strongly supports the idea that the inability of some alleles to

386 aggregate is likely not due to a failure to produce sufficient numbers of pili but reflects a
387 specific property of the pilin itself.

388 V52 and ATCC25872 encode an identical PilA with a C-terminal extension or 'tail'
389 composed of an unusual repetitive stretch (SGSGSGSGSGSGSGSGSGSGN). Among the PilA
390 sequences analysed here, there were 9 examples of this type of tail clustered into 2 well-
391 separated phylogenetic groups (Figure S10). Moreover, 3/7 of the *pilA*rep PilAs unable to
392 support aggregation contain a tail (Figure S12B). Thus, to test if the tail affected PilA function
393 we created a truncated variant *i.e. pilA*rep[V52Δtail]. The truncated variant was similarly
394 transformable to the equivalent tailed version (Figure 7C). Remarkably, however, in the
395 absence of *pilT* the *pilA*rep[V52Δtail] strain displayed a strong aggregation phenotype,
396 indistinguishable from that of A1552 PilA control (Figure 7D), and demonstrated a similar
397 pattern of kin-recognition in co-culture experiments (Figure 7E). These data suggest that the
398 tail inhibits the ability of pili to aggregate, possibly by masking the site of pilus-pilus
399 interaction. Indeed, a strain in which this tail was transplanted onto A1552 PilA (*i.e.*
400 *pilA*rep[WT+tail] remained highly transformable but was unable to aggregate (Figure 7C and
401 D).

402

403 **Discussion**

404 **Pilus retraction required for DNA uptake**

405 The demonstration here that the DNA-uptake pili are highly dynamic, that these dynamics
406 are PilT dependent, and that cells lacking *pilT* are minimally transformable, provides direct
407 evidence for the longstanding model, whereby pilus retraction facilitates DNA uptake. The
408 results also argue against other potential mechanisms such as pilus ejection (Balaban *et al.*,
409 2014), which was never observed. However, important questions regarding the precise
410 mechanism of DNA uptake remain. Does DNA bind directly to the pilus? Alternatively, does
411 pilus retraction simply allow promiscuous entry of DNA through the open outer membrane

412 pore? Similarly, how does DNA uptake proceed in bacteria like *Streptococcus pneumoniae*
413 that also use T4P (Laurenceau *et al.*, 2013) but lack an obvious retraction ATPase? The
414 finding that PilT is the primary retraction ATPase, and that cells lacking *pilT* are hyper-
415 piliated with static pili is consistent with the established role of PilT in various species,
416 including those that use T4P for natural competence for transformation (Graupner *et al.*,
417 2001; Seitz and Blokesch, 2013; Wolfgang *et al.*, 1998). Interestingly, PilU seems to provide a
418 level of functional redundancy for both the DNA-uptake pilus and the MSHA pilus. Similar
419 partial redundancy has also been observed in *Pseudomonas* and *Neisseria sp*. (Eriksson *et al.*,
420 2012; Graupner *et al.*, 2001; Park *et al.*, 2002; Whitchurch and Mattick, 1994) and in
421 agreement with our finding that PilU activity requires the presence of PilT, Georgiadou *et al.*
422 also detected an interaction between the two proteins (Georgiadou *et al.*, 2012).
423
424 **DNA-uptake pilus capable of auto-aggregation**
425 Unexpectedly, we discovered that in the absence of retraction DNA-uptake pili are capable
426 of mediating auto-aggregation via specific pilus-pilus interactions. The simplest explanation
427 for the dependence of this phenotype on non-retractile pili is that the strength of pilus
428 retraction is sufficient to disrupt the interactions between pili. Additionally, given the
429 transient interactions between cells expected to occur during growth in liquid culture as
430 mostly used in our experimental setup, interactions between pili are likely rare under these
431 conditions. Still, the idea that pili can interact with one another is further evidenced by the
432 fact that pili sheared into the media accumulate into large structures. Since aggregation en-
433 masse requires ≥2 pili per cells, the increased density and static nature of pili in the absence
434 of retraction likely combine to facilitate auto-aggregation. Indeed, aggregation of *N.*
435 *meningitidis* cells, which typically display around 5 pili, occurs at low levels but is
436 dramatically enhanced in the absence of *pilT* (Hélaine *et al.*, 2005; Imhaus and Duménil,
437 2014).

438 Although co-regulated, the DNA-uptake pilus and the residual components of the
439 DNA uptake machinery (*i.e.* ComEA, ComEC *etc.*) are two discrete systems that likely evolved
440 separately (Seitz and Blokesch, 2013; Seitz *et al.*, 2014). Given our finding that PilA variability
441 does not affect transformation, and the possible functions discussed below, we propose that
442 the primary function of the DNA-uptake pilus is not to mediate natural competence but is to
443 act as an environmental colonisation and kin-discrimination factor. Nevertheless, at this
444 point we do not fully understand the relevance of the auto-aggregation phenotype to the
445 biology of *V. cholerae*, in part because only limited information is available on its natural
446 lifestyle in the aquatic environment. Therefore, one possibility is that aggregation is a
447 vestigial evolutionary feature that is unrelated to the current lifestyle of *V. cholerae*. For the
448 reasons that follow we do not favour this hypothesis.

449 First, we discovered that MO10 – an important pandemic strain of *V. cholerae* –
450 carries a naturally occurring *pilT* mutation that renders it defective for pilus retraction, is
451 hyper-piliated and thus, innately capable of aggregation. Second, despite the diversity seen
452 among environmental isolates, all pandemic strains examined retain the same *pilA* allele
453 (see below) and were equally capable of aggregating when retraction was blocked. Third, its
454 association with chitinous surfaces, which are abundant in aquatic ecosystems and provide
455 both a nutritive surface and potentially a vehicle for dissemination, likely dominates the
456 natural lifestyle of *V. cholerae*. On these colonised chitin surfaces, cells exist as members of
457 dense biofilm communities, held together primarily by a polysaccharide matrix. An attractive
458 hypothesis is that the crowded conditions and gel-like mechanical properties of the matrix
459 might naturally facilitate pilus-pilus interactions by increasing the chances of interactions
460 between cells and act to either inhibit or otherwise retard pilus retraction. If correct, such
461 interactions could have multiple beneficial functions, as outlined below.

462

463 **Potential functions of pilus-pilus interactions on chitinous surfaces**

464 Auto-aggregation is a widespread virulence mechanism employed by a variety of important
465 human pathogens *e.g. E. coli* and *N. meningitidis*, and is typically mediated by T4P (Bieber *et*
466 *al.*, 1998; Chamot-Rooke *et al.*, 2011), though other mechanisms have been reported
467 (Sherlock *et al.*, 2005). By allowing cells to act in concert and to better resist insults either
468 from changing conditions or host defences, aggregation can provide a clear advantage over
469 individual cells.

470 On chitin surfaces, even localised pilus-pilus interactions could serve to supplement
471 the adhesive function of the biofilm by holding cells together and providing a mechanism to
472 resist mechanical stresses, especially shear stress at the biofilm surface (Persat *et al.*, 2015).
473 Such interactions could also help enrich *V. cholerae* on chitin surfaces by actively retaining
474 pilus-producing cells, while excluding possible competitor species, and thus, by increasing
475 the selectivity of the biofilm enhance community fitness. Importantly, since the DNA-uptake
476 pilus is specifically produced on chitin, this could allow it to act as a signal to reinforce the
477 colonisation of nutritious surfaces, as has previously been suggested (Meibom *et al.*, 2004;
478 Shime-Hattori *et al.*, 2006). The ability of pili to hold cells together may also confer distinct
479 advantages during biofilm dispersal, which occurs upon high cell density and nutrient
480 depletion (Hammer and Bassler, 2003; Singh *et al.*, 2017). Interestingly, Singh *et al*., recently
481 showed that *V. cholerae* cells depart from biofilms formed on glass as individuals. By
482 maintaining intercellular contacts formed on chitin surfaces, even between small groups of
483 departing bacteria, these cells would have an increased fitness on arrival at a new niche by
484 arriving in number. Indeed, *V. cholerae* can be isolated from environmental waters as
485 multicellular aggregates and although it was suggested that these may originate from
486 cholera stools, it seems equally plausible that they may have been shed from chitin surfaces
487 (Faruque *et al.*, 2006).

488 Intestinal colonisation by *V. cholerae* requires auto-aggregation on the cell surface,
489 mediated by interactions between bundles of TCP pili (Kirn *et al.*, 2000; Taylor *et al.*, 1987).
490 In addition to protecting cells from immune attack by physical sequestration, cells are
491 surrounded by TCP matrices, which appear to provide resistance to bile acids (Krebs and
492 Taylor, 2011). Interestingly, although the DNA-uptake pilus is dispensable for intestinal
493 colonisation in an *in vitro* animal model (Fullner and Mekalanos, 1999), where the chitin
494 inducer is absent, patients recovering from cholera exhibit a strong immune response to PilA
495 (and the secretin PilQ) (Hang *et al.*, 2003). One explanation for this response is that it results
496 from the ingestion of colonised chitin particles (Blokesch, 2015). If the DNA-uptake pilus
497 would form extensive pili networks on chitin, like those formed by TCP during infection, and
498 like those we observed in liquid culture, it is tempting to speculate that they might protect
499 the bacteria during gastric transit, possibly by preserving the integrity of the biofilm. Indeed,
500 a similar mechanism has been proposed to explain the observation that the TCP-mediated
501 aggregates found in cholera stool are hyper-infectious (Faruque *et al.*, 2006; Krebs and
502 Taylor, 2011; Merrell *et al.*, 2002; Nielsen *et al.*, 2010).
503
504 **Specific pilin interactions provide a mechanism for kin recognition**
505 Kin recognition, the ability to recognise self, has obvious utility in controlling community
506 composition as well as in facilitating communication and cooperation with neighbours,
507 though it remains an emerging field of study (Wall, 2016). Previously, artificially varying the
508 number and post-translational modification state of pili was shown to enable a form of cell
509 sorting in *N. gonorrhoeae* (Oldewurtel *et al.*, 2015). In contrast, the finding here that specific
510 interactions between the major pilin can allow pili to discriminate between one another,
511 together with the natural diversity of PilA, provides a direct mechanism for specific kin
512 recognition. Although further work will be needed to define compatibility groups between
513 the various *pilA* alleles, the existence of such diversity and the finding that it controls the

514 ability of pili to aggregate but does not affect transformation, supports the idea that these
515 pili mediate environmental colonisation and that kin recognition is involved in this process.
516 During growth on chitin *V. cholerae* simultaneously produces a type VI secretion system
517 (Borgeaud *et al.*, 2015), which is a molecular killing device, commonly used against non-kin
518 bacterial neighbours (Ho *et al.*, 2014). Given the results descried here, we speculate that the
519 kin recognition mechanism provided by PilA could be used as an intentional avoidance
520 system to evade attack by non-kin. Likewise, it could also act as a secondary verification
521 mechanism to kill any invading non-kin, though further work will be needed to determine
522 whether there is any interplay between the two systems.

523 A potential limitation of *pilA* as a kin recognition determinant is that by encoding
524 specificity at a single locus, it can easily be shared with other strains by horizontal gene
525 transfer. Indeed, this is evident in toxigenic *V. cholerae* O37 serogroup strains (e.g. V52 and
526 ATCC25872), which carry a completely different *pilA* to the one that would be expected
527 based on their ancestry from toxigenic O1 classical progenitors (Bik *et al.*, 1996).
528 Interestingly, in these strains PilA has acquired a repetitive tail that inhibits the ability of the
529 pilus to mediate aggregation. This might represent adaptation to a particular niche or else
530 might represent an escape mechanism to avoid interactions with another strain. However, it
531 is notable that these strains only caused localised outbreaks of cholera whereas the O139
532 serogroup converted strains (*e.g.* MO10), which retain the pandemic *pilA* allele, have caused
533 devastating outbreaks (Nelson *et al.*, 2009). Given the suggestions above that pili mediated
534 cell-cell interactions may reinforce survival on chitin surfaces, future studies should address
535 any potential link between the *pilA* allele carried and cholera transmission.

536 Finally, in bacteria that lead host-associated lifestyles such as *Neisseria sp.* variability
537 of the major pilin is thought to facilitate immune escape. However, in addition to *V.*
538 *cholerae*, other bacteria with mainly environmental lifestyles also exhibit diversity in their
539 major pilins (Aagesen and Häse, 2012; Giltner *et al.*, 2012). This may represent niche

540 specialisation or a strategy to avoid phage predation. Alternatively, it could represent a
541 widespread mechanism for bacterial kin recognition.
542
543 **Materials and Methods**
544 **Bacterial strains and plasmids**
545 The bacterial strains used in this study are shown in Supplementary Table S1, together with
546 the plasmids used and their construction.
547
548 **General methods**
549 Bacterial cultures were grown aerobically at 30˚C or 37˚C, as required. Liquid medium used
550 for growing bacterial strains was Lysogeny Broth (LB-Miller; 10 g/L NaCl, Carl Roth,
551 Switzerland) and solid medium was LB agar. Where indicated, LB-S contained 20 g/L NaCl.
552 Ampicillin (Amp; 100 µg/mL), gentamicin (Gent; 50 µg/mL), kanamycin (Kan; 50-75 µg/mL),
553 streptomycin (Str; 100 µg/mL) and rifampicin (Rif; 100 µg/mL) were used for selection in *E.*
554 *coli* and *V. cholerae*, as required. To induce expression from the P_{BAD} promoter, cultures
555 were grown in media supplemented with 0.2% L-arabinose. Natural transformation of *V.*
556 *cholerae* on chitin flakes was done in 0.5 x DASW (Defined artificial seawater), supplemented
557 with vitamins (MEM, Gibco) and 50 mM HEPES, as previously described (Meibom *et al.*,
558 2005). Counter-selection of phenylalanyl-tRNA synthetase (*pheS**) insertions (Trans2
559 method; see below) was done on medium supplemented with 20 mM 4-chloro-
560 phenylalanine (cPhe; Sigma-Aldrich, Switzerland). Thiosulfate citrate bile salts sucrose (TCBS;
561 Sigma-Aldrich, Switzerland) agar was used to counter-select for *E. coli* following bacterial
562 mating. SacB-based counter-selection was done on NaCl-free medium containing 10 %
563 sucrose.
564

565 **Strain construction**

566 DNA manipulations and *E. coli* transformations were carried out using standard methods
567 (Sambrook *et al.*, 1989), and all constructs were verified by PCR and DNA sequencing
568 (Microsynth AG, Switzerland). Genetic engineering of *V. cholerae* was done using a
569 combination of natural transformation and FLP-recombination; Trans-FLP (De Souza Silva
570 and Blokesch, 2010; Marvig and Blokesch, 2010), *pheS**-based counter-selection; Trans2
571 (Gurung *et al.*, 2017; Van der Henst *et al.*, 2017), and allelic exchange using bi-parental
572 mating and the counter-selectable plasmid pGP704-Sac28 (Meibom *et al.*, 2004). The mini-
573 Tn7 transposon carrying *araC* and various P_{BAD}-driven genes was integrated into the large
574 chromosome by tri-parental mating, as previously described (Bao *et al.*, 1991).

575

576 **Transformation frequency assay**

577 Diverse strains harbouring an arabinose-inducible *tfoX* gene inside the mini-Tn7 (Tn*tfoX*)
578 were tested for transformation using a chitin-independent transformation frequency assay,
579 as previously described (Lo Scrudato and Blokesch, 2012; Seitz and Blokesch, 2013). Briefly,
580 overnight cultures were back-diluted 1:100 in fresh media with and without arabinose, as
581 indicated, and grown 3h at 30˚C with shaking (180 rpm). 0.5 mL aliquots of the cultures were
582 mixed with 1 µg genomic DNA (GC#135; A1552-lacZ-Kan) in 1.5 mL eppendorf tubes and
583 incubated 5h at 30˚C with shaking (180 rpm), prior to serial dilution in PBS (Phosphate
584 buffered saline) and enumeration after overnight growth on LB media in the absence and
585 presence of kanamycin. Transformation frequency was calculated as the number of
586 transformants divided by the total number of bacteria.

587

588 **Aggregation assay**

589 Overnight cultures were back-diluted 1:100 in the absence and presence of arabinose, as
590 needed, and grown in 14 mL round bottom polystyrene test tubes (Falcon, Corning) on a

591 carousel style rotary wheel (40 rpm) at 30˚C. After 6h growth, aggregates were allowed to
592 settle by standing the tube at RT for 30 min. The optical density at 600 nm ($O.D._{600\ nm}$) of the
593 culture was then measured before and after mechanical disruption (vortex max speed; ~5 s),
594 which served to disperse any settled aggregates and return them to solution. Aggregation is
595 expressed as the ratio of the $O.D._{600\ nm}$ Pre/Post-vortexing. For time-course experiments the
596 standing time was reduced to 5 min. To visualise aggregates by microscopy overnight
597 cultures were back-diluted either 1:100 individually or 1:200 when mixed, as needed, and
598 were grown for 4h, as described above.
599
600 **Microscopy**
601 Cells were mounted on microscope slides coated with a thin agarose pad (1.2% w/v in PBS),
602 covered with a #1 cover-slip, and were observed using a Zeiss Axio Imager M2 epi-
603 fluorescence microscope attached to an AxioCam MRm camera and controlled by Zeiss
604 AxioVision software. Image acquisition was done using a Plan-Apochromat 100×/1.4 oil
605 objective illuminated by an HXP120 lamp. Images were analysed and prepared for
606 publication using ImageJ (http://rsb.info.nih.gov/ij).
607
608 **Pilus staining and quantification**
609 Alexa Fluor™ 488 C_5 Maleimide (AF-488-Mal; Thermo Fisher Scientific; Cat# A10254) was
610 dissolved in DMSO, aliquoted and stored at -20˚C protected from light. Cultures used for
611 staining were grown for 3.5h at 30˚C on the rotary wheel, as above, in the absence and
612 presence of competence induction, as required. To stain cells 100 µL of culture was mixed
613 with dye at a final concentration of 25 µg/mL (Ellison *et al.*, 2017) and incubated at RT for 5
614 min in the dark. Stained cells were harvested by centrifugation (5000 x *g*; 1 min), washed
615 once with LB, re-suspended in 200 µL LB and imaged immediately. For quantification of
616 piliation in snapshot imaging approximately 2000 cells per strain were analysed in each of

617 three independent repeats. A subset of this data set was also analysed for the number of pili
618 per cell and pilus length, as indicated in the text. For time-lapse analysis, images were
619 acquired at RT at 10 s intervals for 1 min (*i.e.* 7 frames). To analyse the number of pili
620 produced per cell, per min, 5 fields of cells were analysed for each of the three independent
621 repeats, yielding an analysis of 1947 cells in total.
622
623 **Western blotting**
624 Cell lysates were prepared by suspending harvested cells in 2x Laemmli buffer (100 µL buffer
625 per O.D. unit) before boiling at 95˚C for 15 min. Proteins were separated by SDS-PAGE using
626 a 15% resolving gel and blotted onto PVDF membranes using a wet-transfer apparatus.
627 Immuno-detection was performed as described previously (Lo Scrudato and Blokesch, 2012).
628 Primary anti-PilA antibodies were raised in rabbits against synthetic peptides of A1552 PilA
629 (Eurogentec, Belgium; #1510525) and used at a dilution of 1:5000. Anti-Rabbit IgG HRP
630 (Sigma; Cat# A9169) diluted 1:5000 was used as a secondary antibody. Sample loading was
631 verified with anti-RNA Sigma70-HRP (BioLegend; Cat# 663205) diluted 1:10,000.
632
633 **Motility assay**
634 To quantity motility phenotypes 2 µL overnight culture was spotted soft LB agar (0.3%)
635 plates (two technical replicates) and incubated at RT for 24h prior to photography. The
636 swarming diameter (cm) was measured and is the mean of three independent biological
637 repeats. A flagellin-deficient (Δ*flaA*) non-motile strain was used as a negative control.
638
639 **Bacterial two-hybrid**
640 To study any potential interaction between PilT and PilU a Bacterial Adenylate Cyclase-Based
641 Two-Hybrid (BACTH) system was employed (Euromedex, Cat# EUK001) (Karimova *et al.*,
642 1998). PCR fragments carrying *pilT* and *pilU* were cloned between the *KpnI*/*BamHI* sites of

643 each of the BACTH vectors, which were routinely maintained in *E. coli* XL-10 Gold. 100 ng of
644 each vector was co-transformed into competent cells of *E. coli* BTH101, in all possible
645 combinations. Empty vectors were used as negative controls and a leucine zipper pair as a
646 positive control. 5 µL of each transformation was spotted onto LB plates containing Kan50,
647 Amp100, 0.5 mM IPTG (isopropyl-β-D-thiogalactopyranoside), 40 µg/mL X-gal (5-Bromo-4-
648 chloro-3-indolyl-β-D-galactopyranoside) and incubated at 30˚C for 40h prior to photography.
649

650 **Bioinformatics of PilA diversity**

651 *Vibrio cholerae* genomes were obtained from NCBI (National Center for Biotechnology
652 Information), and are listed in Supplementary File S1. Geneious software (10.2.3) (Kearse *et*
653 *al.*, 2012) was used to perform custom BLAST analyses and identify *pilA*. Unique PilA
654 sequences were extracted and combined with the PilA sequences from A1552 and a
655 collection of environmental isolates, as deduced by Sanger sequencing (Supplementary File
656 S2), as indicated in the text. PilA sequences were aligned with Muscle and a consensus
657 neighbour-joining tree constructed using the Jukes-Cantor substitution model, resampled
658 with 100 bootstrap replicates. A1552 MshA was used as an outgroup.
659

660 **Reproducibility**

661 All experiments were independently repeated at least three times, with similar results.

662 **Acknowledgements**

663 We thank Ivan Mateus-Gonzalez for assistance with bioinformatics analyses. We further
664 thank A. Boehm, S. Pukatzki, J. Mekalanos, and members of the Institut National de
665 Recherche Biomédicale of the Democratic Republic of the Congo, for providing *V. cholerae*
666 strains and V. Pelicic for advice on *pheS*-mediated counter-selection. Work on this problem
667 was supported by a Marie Skłodowska-Curie Individual Fellowship (703340; CMDNAUP) to
668 D.W.A. and by EPFL intramural funding and a Starting Grant from the European Research
669 Council (ERC; 309064-VIR4ENV) to MB. M.B. is a Howard Hughes Medical Institute (HHMI)
670 International Research Scholar.

671

672 **Author contributions**

673 Conception, design and analysis: D.W.A and M.B. Performed research: D.W.A, S.S, C.S and
674 M.B. Wrote the manuscript: D.W.A and M.B.

675

676 **Declaration of Interests**

677 The authors declare no competing interests

678 **References**

679 Aagesen, A.M., and Häse, C.C. (2012). Sequence analyses of type IV pili from *Vibrio*
680 *cholerae*, *Vibrio parahaemolyticus*, and *Vibrio vulnificus*. Microb Ecol *64*, 509-524.

681 Absalon, C., Van Dellen, K., and Watnick, P.I. (2011). A communal bacterial adhesin
682 anchors biofilm and bystander cells to surfaces. PLoS Pathog *7*, e1002210.

683 Aldova, E., Laznickova, K., Stepankova, E., and Lietava, J. (1968). Isolation of
684 nonagglutinable vibrios from an enteritis outbreak in Czechoslovakia. J Infect Dis
685 *118*, 25-31.

686 Balaban, M., Battig, P., Muschiol, S., Tirier, S.M., Wartha, F., Normark, S., and
687 Henriques-Normark, B. (2014). Secretion of a pneumococcal type II secretion system
688 pilus correlates with DNA uptake during transformation. Proc Natl Acad Sci U S A
689 *111*, E758-765.

690 Bao, Y., Lies, D.P., Fu, H., and Roberts, G.P. (1991). An improved Tn7-based system
691 for the single-copy insertion of cloned genes into chromosomes of gram-negative
692 bacteria. Gene *109*, 167-168.

693 Bartlett, T.M., Bratton, B.P., Duvshani, A., Miguel, A., Sheng, Y., Martin, N.R., Nguyen,
694 J.P., Persat, A., Desmarais, S.M., VanNieuwenhze, M.S.*, et al.* (2017). A Periplasmic
695 Polymer Curves *Vibrio cholerae* and Promotes Pathogenesis. Cell *168*, 172-185 e115.

696 Berk, V., Fong, J.C., Dempsey, G.T., Develioglu, O.N., Zhuang, X., Liphardt, J., Yildiz,
697 F.H., and Chu, S. (2012). Molecular architecture and assembly principles of *Vibrio*
698 *cholerae* biofilms. Science *337*, 236-239.

699 Berry, J.L., and Pelicic, V. (2015). Exceptionally widespread nanomachines composed
700 of type IV pilins: the prokaryotic Swiss Army knives. FEMS Microbiol Rev *39*, 134-154.

701 Biais, N., Ladoux, B., Higashi, D., So, M., and Sheetz, M. (2008). Cooperative
702 retraction of bundled type IV pili enables nanonewton force generation. PLoS Biol *6*,
703 e87.

704 Bieber, D., Ramer, S.W., Wu, C.Y., Murray, W.J., Tobe, T., Fernandez, R., and
705 Schoolnik, G.K. (1998). Type IV pili, transient bacterial aggregates, and virulence of
706 enteropathogenic *Escherichia coli*. Science *280*, 2114-2118.

707 Bik, E.M., Gouw, R.D., and Mooi, F.R. (1996). DNA fingerprinting of *Vibrio cholerae*
708 strains with a novel insertion sequence element: a tool to identify epidemic strains. J
709 Clin Microbiol *34*, 1453-1461.

710 Blair, K.M., Turner, L., Winkelman, J.T., Berg, H.C., and Kearns, D.B. (2008). A
711 molecular clutch disables flagella in the *Bacillus subtilis* biofilm. Science *320*, 1636-
712 1638.

713 Blokesch, M. (2015). Competence-induced type VI secretion might foster intestinal
714 colonization by *Vibrio cholerae*: Intestinal interbacterial killing by competence-
715 induced *V. cholerae*. Bioessays *37*, 1163-1168.

716 Blokesch, M., and Schoolnik, G.K. (2007). Serogroup conversion of *Vibrio cholerae* in
717 aquatic reservoirs. PLoS Pathog *3*, e81.

718 Borgeaud, S., Metzger, L.C., Scrignari, T., and Blokesch, M. (2015). The type VI
719 secretion system of *Vibrio cholerae* fosters horizontal gene transfer. Science *347*, 63-
720 67.

721 Chamot-Rooke, J., Mikaty, G., Malosse, C., Soyer, M., Dumont, A., Gault, J., Imhaus,
722 A.F., Martin, P., Trellet, M., Clary, G.*, et al.* (2011). Posttranslational modification of
723 pili upon cell contact triggers *N. meningitidis* dissemination. Science *331*, 778-782.

724 Chang, Y.W., Kjaer, A., Ortega, D.R., Kovacikova, G., Sutherland, J.A., Rettberg, L.A.,
725 Taylor, R.K., and Jensen, G.J. (2017). Architecture of the *Vibrio cholerae* toxin-
726 coregulated pilus machine revealed by electron cryotomography. Nat Microbiol *2*,
727 16269.

728 Chang, Y.W., Rettberg, L.A., Treuner-Lange, A., Iwasa, J., Sogaard-Andersen, L., and
729 Jensen, G.J. (2016). Architecture of the type IVa pilus machine. Science *351*,
730 aad2001.

731 Chiang, S.L., Taylor, R.K., Koomey, M., and Mekalanos, J.J. (1995). Single amino acid
732 substitutions in the N-terminus of *Vibrio cholerae* TcpA affect colonization,
733 autoagglutination, and serum resistance. Mol Microbiol *17*, 1133-1142.

734 Chiavelli, D.A., Marsh, J.W., and Taylor, R.K. (2001). The mannose-sensitive
735 hemagglutinin of *Vibrio cholerae* promotes adherence to zooplankton. Appl Environ
736 Microbiol *67*, 3220-3225.

737 Chun, J., Grim, C.J., Hasan, N.A., Lee, J.H., Choi, S.Y., Haley, B.J., Taviani, E., Jeon, Y.S.,
738 Kim, D.W., Lee, J.H.*, et al.* (2009). Comparative genomics reveals mechanism for
739 short-term and long-term clonal transitions in pandemic *Vibrio cholerae*. Proc Natl
740 Acad Sci U S A *106*, 15442-15447.

741 Clemens, J.D., Nair, G.B., Ahmed, T., Qadri, F., and Holmgren, J. (2017). Cholera.
742 Lancet *390*, 1539-1549.

743 Colwell, R.R., Huq, A., Islam, M.S., Aziz, K.M., Yunus, M., Khan, N.H., Mahmud, A.,
744 Sack, R.B., Nair, G.B., Chakraborty, J.*, et al.* (2003). Reduction of cholera in
745 Bangladeshi villages by simple filtration. Proc Natl Acad Sci U S A *100*, 1051-1055.

746 Craig, L., Volkmann, N., Arvai, A.S., Pique, M.E., Yeager, M., Egelman, E.H., and
747 Tainer, J.A. (2006). Type IV pilus structure by cryo-electron microscopy and
748 crystallography: implications for pilus assembly and functions. Mol Cell *23*, 651-662.

749 De Souza Silva, O., and Blokesch, M. (2010). Genetic manipulation of *Vibrio cholerae*
750 by combining natural transformation with FLP recombination. Plasmid *64*, 186-195.

751 Ellison, C.K., Kan, J., Dillard, R.S., Kysela, D.T., Ducret, A., Berne, C., Hampton, C.M.,
752 Ke, Z., Wright, E.R., Biais, N.*, et al.* (2017). Obstruction of pilus retraction stimulates
753 bacterial surface sensing. Science *358*, 535-538.

754 Eriksson, J., Eriksson, O.S., and Jonsson, A.B. (2012). Loss of meningococcal PilU
755 delays microcolony formation and attenuates virulence in vivo. Infect Immun *80*,
756 2538-2547.

757 Faruque, S.M., Biswas, K., Udden, S.M., Ahmad, Q.S., Sack, D.A., Nair, G.B., and
758 Mekalanos, J.J. (2006). Transmissibility of cholera: in vivo-formed biofilms and their
759 relationship to infectivity and persistence in the environment. Proc Natl Acad Sci U S
760 A *103*, 6350-6355.

761 Fong, J.C., Syed, K.A., Klose, K.E., and Yildiz, F.H. (2010). Role of Vibrio polysaccharide
762 (vps) genes in VPS production, biofilm formation and *Vibrio cholerae* pathogenesis.
763 Microbiology *156*, 2757-2769.

764 Fullner, K.J., and Mekalanos, J.J. (1999). Genetic characterization of a new type IV-A
765 pilus gene cluster found in both classical and El Tor biotypes of *Vibrio cholerae*. Infect
766 Immun *67*, 1393-1404.

767 Gangel, H., Hepp, C., Muller, S., Oldewurtel, E.R., Aas, F.E., Koomey, M., and Maier,
768 B. (2014). Concerted spatio-temporal dynamics of imported DNA and ComE DNA
769 uptake protein during gonococcal transformation. PLoS Pathog *10*, e1004043.

770 Gebhart, C., Ielmini, M.V., Reiz, B., Price, N.L., Aas, F.E., Koomey, M., and Feldman,
771 M.F. (2012). Characterization of exogenous bacterial oligosaccharyltransferases in
772 *Escherichia coli* reveals the potential for O-linked protein glycosylation in *Vibrio*
773 *cholerae* and *Burkholderia thailandensis*. Glycobiology *22*, 962-974.

774 Georgiadou, M., Castagnini, M., Karimova, G., Ladant, D., and Pelicic, V. (2012).
775 Large-scale study of the interactions between proteins involved in type IV pilus
776 biology in *Neisseria meningitidis*: characterization of a subcomplex involved in pilus
777 assembly. Mol Microbiol *84*, 857-873.

778 Giltner, C.L., Nguyen, Y., and Burrows, L.L. (2012). Type IV pilin proteins: versatile
779 molecular modules. Microbiol Mol Biol Rev *76*, 740-772.

780 Gold, V.A., Salzer, R., Averhoff, B., and Kuhlbrandt, W. (2015). Structure of a type IV
781 pilus machinery in the open and closed state. Elife *4*.

782 Graupner, S., Weger, N., Sohni, M., and Wackernagel, W. (2001). Requirement of
783 novel competence genes *pilT* and *pilU* of *Pseudomonas stutzeri* for natural
784 transformation and suppression of pilT deficiency by a hexahistidine tag on the type
785 IV pilus protein PilAI. J Bacteriol *183*, 4694-4701.

786 Gurung, I., Berry, J.L., Hall, A.M.J., and Pelicic, V. (2017). Cloning-independent
787 markerless gene editing in *Streptococcus sanguinis*: novel insights in type IV pilus
788 biology. Nucleic Acids Res *45*, e40.

789 Hammer, B.K., and Bassler, B.L. (2003). Quorum sensing controls biofilm formation in
790 *Vibrio cholerae*. Mol Microbiol *50*, 101-104.

791 Hang, L., John, M., Asaduzzaman, M., Bridges, E.A., Vanderspurt, C., Kirn, T.J., Taylor,
792 R.K., Hillman, J.D., Progulske-Fox, A., Handfield, M.*, et al.* (2003). Use of in vivo-
793 induced antigen technology (IVIAT) to identify genes uniquely expressed during
794 human infection with *Vibrio cholerae*. Proc Natl Acad Sci U S A *100*, 8508-8513.

795 Hélaine, S., Carbonnelle, E., Prouvensier, L., Beretti, J.L., Nassif, X., and Pelicic, V.
796 (2005). PilX, a pilus-associated protein essential for bacterial aggregation, is a key to
797 pilus-facilitated attachment of *Neisseria meningitidis* to human cells. Mol Microbiol
798 *55*, 65-77.

799 Ho, B.T., Dong, T.G., and Mekalanos, J.J. (2014). A view to a kill: the bacterial type VI
800 secretion system. Cell Host Microbe *15*, 9-21.

801 Huq, A., Xu, B., Chowdhury, M.A., Islam, M.S., Montilla, R., and Colwell, R.R. (1996).
802 A simple filtration method to remove plankton-associated *Vibrio cholerae* in raw
803 water supplies in developing countries. Appl Environ Microbiol *62*, 2508-2512.

804 Imhaus, A.F., and Duménil, G. (2014). The number of *Neisseria meningitidis* type IV
805 pili determines host cell interaction. EMBO J *33*, 1767-1783.

806 Jakovljevic, V., Leonardy, S., Hoppert, M., and Sogaard-Andersen, L. (2008). PilB and
807 PilT are ATPases acting antagonistically in type IV pilus function in *Myxococcus*
808 *xanthus*. J Bacteriol *190*, 2411-2421.

809 Joelsson, A., Liu, Z., and Zhu, J. (2006). Genetic and phenotypic diversity of quorum-
810 sensing systems in clinical and environmental isolates of *Vibrio cholerae*. Infect
811 Immun *74*, 1141-1147.

812 Johnston, C., Martin, B., Fichant, G., Polard, P., and Claverys, J.P. (2014). Bacterial
813 transformation: distribution, shared mechanisms and divergent control. Nat Rev
814 Microbiol *12*, 181-196.

815 Jones, C.J., Utada, A., Davis, K.R., Thongsomboon, W., Zamorano Sanchez, D.,
816 Banakar, V., Cegelski, L., Wong, G.C., and Yildiz, F.H. (2015). C-di-GMP Regulates
817 Motile to Sessile Transition by Modulating MshA Pili Biogenesis and Near-Surface
818 Motility Behavior in *Vibrio cholerae*. PLoS Pathog *11*, e1005068.

819 Karimova, G., Pidoux, J., Ullmann, A., and Ladant, D. (1998). A bacterial two-hybrid
820 system based on a reconstituted signal transduction pathway. Proc Natl Acad Sci U S
821 A *95*, 5752-5756.

822 Kearse, M., Moir, R., Wilson, A., Stones-Havas, S., Cheung, M., Sturrock, S., Buxton,
823 S., Cooper, A., Markowitz, S., Duran, C.*, et al.* (2012). Geneious Basic: an integrated
824 and extendable desktop software platform for the organization and analysis of
825 sequence data. Bioinformatics *28*, 1647-1649.

826 Kirn, T.J., Jude, B.A., and Taylor, R.K. (2005). A colonization factor links *Vibrio*
827 *cholerae* environmental survival and human infection. Nature *438*, 863-866.

828 Kirn, T.J., Lafferty, M.J., Sandoe, C.M., and Taylor, R.K. (2000). Delineation of pilin
829 domains required for bacterial association into microcolonies and intestinal
830 colonization by Vibrio cholerae. Mol Microbiol *35*, 896-910.

831 Kolappan, S., Coureuil, M., Yu, X., Nassif, X., Egelman, E.H., and Craig, L. (2016).
832 Structure of the *Neisseria meningitidis* Type IV pilus. Nat Commun *7*, 13015.

833 Krebs, S.J., and Taylor, R.K. (2011). Protection and attachment of *Vibrio cholerae*
834 mediated by the toxin-coregulated pilus in the infant mouse model. J Bacteriol *193*,
835 5260-5270.

836 Laurenceau, R., Péhau-Arnaudet, G., Baconnais, S., Gault, J., Malosse, C.,
837 Dujeancourt, A., Campo, N., Chamot-Rooke, J., Le Cam, E., Claverys, J.P.*, et al.* (2013).
838 A type IV pilus mediates DNA binding during natural transformation in *Streptococcus*
839 *pneumoniae*. PLoS Pathog *9*, e1003473.

840 Leighton, T.L., Buensuceso, R.N., Howell, P.L., and Burrows, L.L. (2015). Biogenesis of
841 *Pseudomonas aeruginosa* type IV pili and regulation of their function. Environ
842 Microbiol *17*, 4148-4163.

843 Li, M., Shimada, T., Morris, J.G., Jr., Sulakvelidze, A., and Sozhamannan, S. (2002).
844 Evidence for the emergence of non-O1 and non-O139 *Vibrio cholerae* strains with
845 pathogenic potential by exchange of O-antigen biosynthesis regions. Infect Immun
846 *70*, 2441-2453.

847 Lo Scrudato, M., and Blokesch, M. (2012). The regulatory network of natural
848 competence and transformation of *Vibrio cholerae*. PLoS Genet *8*, e1002778.

849 Maier, B., and Wong, G.C.L. (2015). How Bacteria Use Type IV Pili Machinery on
850 Surfaces. Trends Microbiol *23*, 775-788.

851 Marvig, R.L., and Blokesch, M. (2010). Natural transformation of *Vibrio cholerae* as a
852 tool - optimizing the procedure. BMC Microbiol *10*, 155.

853 Matthey, N., and Blokesch, M. (2016). The DNA-Uptake Process of Naturally
854 Competent *Vibrio cholerae*. Trends Microbiol *24*, 98-110.

855 McCallum, M., Tammam, S., Khan, A., Burrows, L.L., and Howell, P.L. (2017). The
856 molecular mechanism of the type IVa pilus motors. Nat Commun *8*, 15091.

857 Meibom, K.L., Blokesch, M., Dolganov, N.A., Wu, C.Y., and Schoolnik, G.K. (2005).
858 Chitin induces natural competence in *Vibrio cholerae*. Science *310*, 1824-1827.

859 Meibom, K.L., Li, X.B., Nielsen, A.T., Wu, C.Y., Roseman, S., and Schoolnik, G.K.
860 (2004). The *Vibrio cholerae* chitin utilization program. Proc Natl Acad Sci U S A *101*,
861 2524-2529.

862 Merrell, D.S., Butler, S.M., Qadri, F., Dolganov, N.A., Alam, A., Cohen, M.B.,
863 Calderwood, S.B., Schoolnik, G.K., and Camilli, A. (2002). Host-induced epidemic
864 spread of the cholera bacterium. Nature *417*, 642-645.

865 Merz, A.J., So, M., and Sheetz, M.P. (2000). Pilus retraction powers bacterial
866 twitching motility. Nature *407*, 98-102.

867 Moorthy, S., and Watnick, P.I. (2004). Genetic evidence that the *Vibrio cholerae*
868 monolayer is a distinct stage in biofilm development. Mol Microbiol *52*, 573-587.

869 Nelson, E.J., Harris, J.B., Morris, J.G., Jr., Calderwood, S.B., and Camilli, A. (2009).
870 Cholera transmission: the host, pathogen and bacteriophage dynamic. Nat Rev
871 Microbiol *7*, 693-702.

872 Nielsen, A.T., Dolganov, N.A., Rasmussen, T., Otto, G., Miller, M.C., Felt, S.A.,
873 Torreilles, S., and Schoolnik, G.K. (2010). A bistable switch and anatomical site
874 control *Vibrio cholerae* virulence gene expression in the intestine. PLoS Pathog *6*,
875 e1001102.

876 Oldewurtel, E.R., Kouzel, N., Dewenter, L., Henseler, K., and Maier, B. (2015).
877 Differential interaction forces govern bacterial sorting in early biofilms. Elife *4*.

878 Park, H.S., Wolfgang, M., and Koomey, M. (2002). Modification of type IV pilus-
879 associated epithelial cell adherence and multicellular behavior by the PilU protein of
880 *Neisseria gonorrhoeae*. Infect Immun *70*, 3891-3903.

881 Persat, A., Nadell, C.D., Kim, M.K., Ingremeau, F., Siryaporn, A., Drescher, K.,
882 Wingreen, N.S., Bassler, B.L., Gitai, Z., and Stone, H.A. (2015). The mechanical world
883 of bacteria. Cell *161*, 988-997.

884 Sambrook, J., Fritsch, E.F., and Maniatis, T. (1989). Molecular Cloning: A Laboratory
885 Manual. Cold Spring Harbor: Cold Spring Harbor Laboratory Press.

886 Seitz, P., and Blokesch, M. (2013). DNA-uptake machinery of naturally competent
887 *Vibrio cholerae*. Proc Natl Acad Sci U S A *110*, 17987-17992.

888 Seitz, P., and Blokesch, M. (2014). DNA transport across the outer and inner
889 membranes of naturally transformable *Vibrio cholerae* is spatially but not temporally
890 coupled. MBio *5*.

891 Seitz, P., Pezeshgi Modarres, H., Borgeaud, S., Bulushev, R.D., Steinbock, L.J.,
892 Radenovic, A., Dal Peraro, M., and Blokesch, M. (2014). ComEA is essential for the
893 transfer of external DNA into the periplasm in naturally transformable *Vibrio*
894 *cholerae* cells. PLoS Genet *10*, e1004066.

895 Sherlock, O., Vejborg, R.M., and Klemm, P. (2005). The TibA adhesin/invasin from
896 enterotoxigenic *Escherichia coli* is self recognizing and induces bacterial aggregation
897 and biofilm formation. Infect Immun *73*, 1954-1963.

898 Shime-Hattori, A., Iida, T., Arita, M., Park, K.S., Kodama, T., and Honda, T. (2006).
899 Two type IV pili of *Vibrio parahaemolyticus* play different roles in biofilm formation.
900 FEMS Microbiol Lett *264*, 89-97.

901 Singh, P.K., Bartalomej, S., Hartmann, R., Jeckel, H., Vidakovic, L., Nadell, C.D., and
902 Drescher, K. (2017). *Vibrio cholerae* Combines Individual and Collective Sensing to
903 Trigger Biofilm Dispersal. Curr Biol *27*, 3359-3366 e3357.

904 Skerker, J.M., and Berg, H.C. (2001). Direct observation of extension and retraction
905 of type IV pili. Proc Natl Acad Sci U S A *98*, 6901-6904.

906 Tamplin, M.L., Gauzens, A.L., Huq, A., Sack, D.A., and Colwell, R.R. (1990).
907 Attachment of *Vibrio cholerae* serogroup O1 to zooplankton and phytoplankton of
908 Bangladesh waters. Appl Environ Microbiol *56*, 1977-1980.

909 Taylor, R.K., Miller, V.L., Furlong, D.B., and Mekalanos, J.J. (1987). Use of *phoA* gene
910 fusions to identify a pilus colonization factor coordinately regulated with cholera
911 toxin. Proc Natl Acad Sci U S A *84*, 2833-2837.

912 Teschler, J.K., Zamorano-Sanchez, D., Utada, A.S., Warner, C.J., Wong, G.C.,
913 Linington, R.G., and Yildiz, F.H. (2015). Living in the matrix: assembly and control of
914 *Vibrio cholerae* biofilms. Nat Rev Microbiol *13*, 255-268.

915 Utada, A.S., Bennett, R.R., Fong, J.C.N., Gibiansky, M.L., Yildiz, F.H., Golestanian, R.,
916 and Wong, G.C.L. (2014). *Vibrio cholerae* use pili and flagella synergistically to effect
917 motility switching and conditional surface attachment. Nat Commun *5*, 4913.

918 Van der Henst, C., Clerc, S., Stutzmann, S., Stoudmann, C., Scrignari, T., Maclachlan,
919 C., Knott, G., and Blokesch, M. (2017). Molecular insights into *Vibrio cholerae*'s intra-
920 amoebal host-pathogen interactions. bioRxiv.

921 Waldor, M.K., and Mekalanos, J.J. (1996). Lysogenic conversion by a filamentous
922 phage encoding cholera toxin. Science *272*, 1910-1914.

923 Wall, D. (2016). Kin Recognition in Bacteria. Annu Rev Microbiol *70*, 143-160.

924 Watnick, P.I., Fullner, K.J., and Kolter, R. (1999). A role for the mannose-sensitive
925 hemagglutinin in biofilm formation by Vibrio cholerae El Tor. J Bacteriol *181*, 3606-
926 3609.

927 Watnick, P.I., and Kolter, R. (1999). Steps in the development of a *Vibrio cholerae* El
928 Tor biofilm. Mol Microbiol *34*, 586-595.

929 Whitchurch, C.B., and Mattick, J.S. (1994). Characterization of a gene, *pilU*, required
930 for twitching motility but not phage sensitivity in *Pseudomonas aeruginosa*. Mol
931 Microbiol *13*, 1079-1091.

Wolfgang, M., Lauer, P., Park, H.S., Brossay, L., Hebert, J., and Koomey, M. (1998). PilT mutations lead to simultaneous defects in competence for natural transformation and twitching motility in piliated *Neisseria gonorrhoeae*. Mol Microbiol *29*, 321-330.

Figure 1

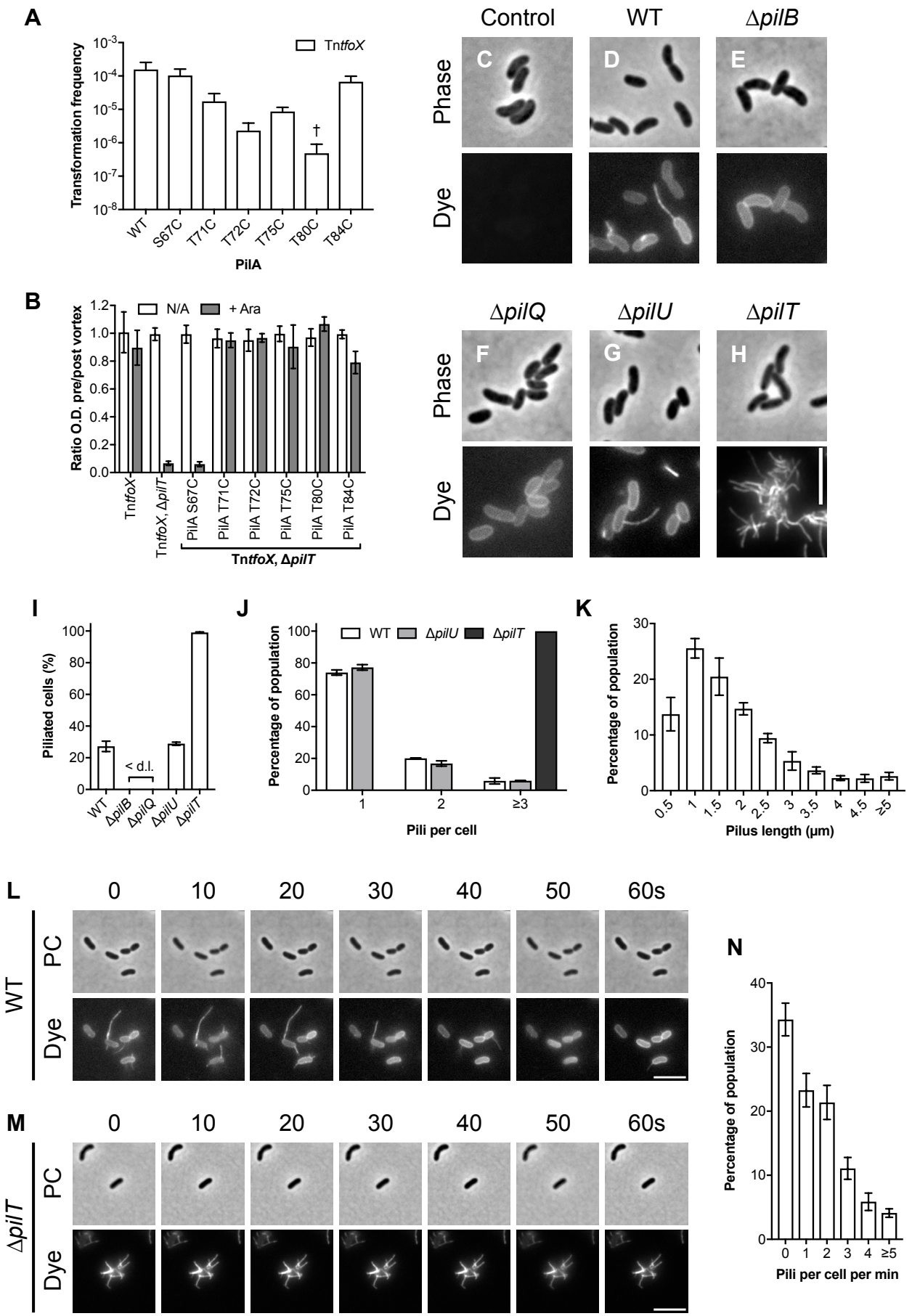
A
Transformation frequency
TntfoX
WT
S67C
T71C
T72C
T75C
T80C
T84C
PilA
Control
WT
ΔpilB
Phase
Dye
C
D
E
B
Ratio O.D. pre/post vortex
N/A
+ Ara
TntfoX
TntfoX, ΔpilT
PilA S67C
PilA T71C
PilA T72C
PilA T75C
PilA T80C
PilA T84C
TntfoX, ΔpilT
ΔpilQ
ΔpilU
ΔpilT
F
G
H
I
Piliated cells (%)
< d.l.
WT
ΔpilB
ΔpilQ
ΔpilU
ΔpilT
J
Percentage of population
WT
ΔpilU
ΔpilT
Pili per cell
K
Percentage of population
Pilus length (μm)
L
0
10
20
30
40
50
60s
PC
Dye
M
ΔpilT
N
Percentage of population
Pili per cell per min

Figure 1. Direct observation of dynamic DNA-uptake pili.

(**A**) Functionality of PilA cysteine variants in chitin-independent transformation assay. Transformation frequencies are the mean of three independent biological repeats (±S.D). < d.l., below detection limit. †, < d.l. in one repeat.

(**B**) Effect of PilA cysteine variants on the ability of retraction deficient cells to aggregate. Aggregation is shown as the ratio of the culture optical density (O.D. $_{600\ nm}$) before and after vortexing, in the absence (N/A; no addition) and presence (+Ara) of *tfoX* induction, as indicated. Values are the mean of three repeats (±S.D.).

(**C**-**H**) Snapshot imaging of pili in cells (A1552-Tn*tfoX*, PilA[S67C]) producing PilA[S67C] stained with AF-488-Mal. (**C**) Uninduced WT control. (**D**-**H**) Induced cells producing PilA[S67C] in (**D**) WT, (**E**) Δ*pilB*, (**F**) Δ*pilQ*, (**G**) Δ*pilU* and (**H**) Δ*pilT* backgrounds. Scale bar = 5 µm.

(**I**-**K**) Quantification of piliation in snapshot imaging. Bars represent mean of three repeats (±S.D.). (**I**) Percentage of piliated cells in the indicated backgrounds. *n* = *c.a.* 2000 cells per strain per repeat. (**J**) Histogram of number of pili per cell in piliated cells in WT, Δ*pilU* and Δ*pilT* backgrounds, as indicated. *n* = *c.a.* 300 cells per strain per repeat. (**K**) Histogram of pilus length in WT cells. *n* = *c.a.* 500-600 cells per repeat.

(**L**-**M**) Time-lapse series of pilus dynamics in (**L**) WT (A1552-Tn*tfoX*, PilA[S67C]) and (**M**) Δ*pilT* (A1552-Tn*tfoX*, PilA[S67C], Δ*pilT*) backgrounds. Cells were stained with AF-488-Mal and imaged at 10s intervals for 1 minute. Upper panels show phase-contrast (PC), lower panels show fluorescence (dye). Time (s), as indicated. Bars = 5 µm.

(**N**) Histogram showing quantification of pili produced per cell per min in the WT (A1552-Tn*tfoX*, PilA[S67C]). Bars represent mean of three repeats (±S.D.). *n* = *c.a.* 500-700 cells per repeat.

Figure 2

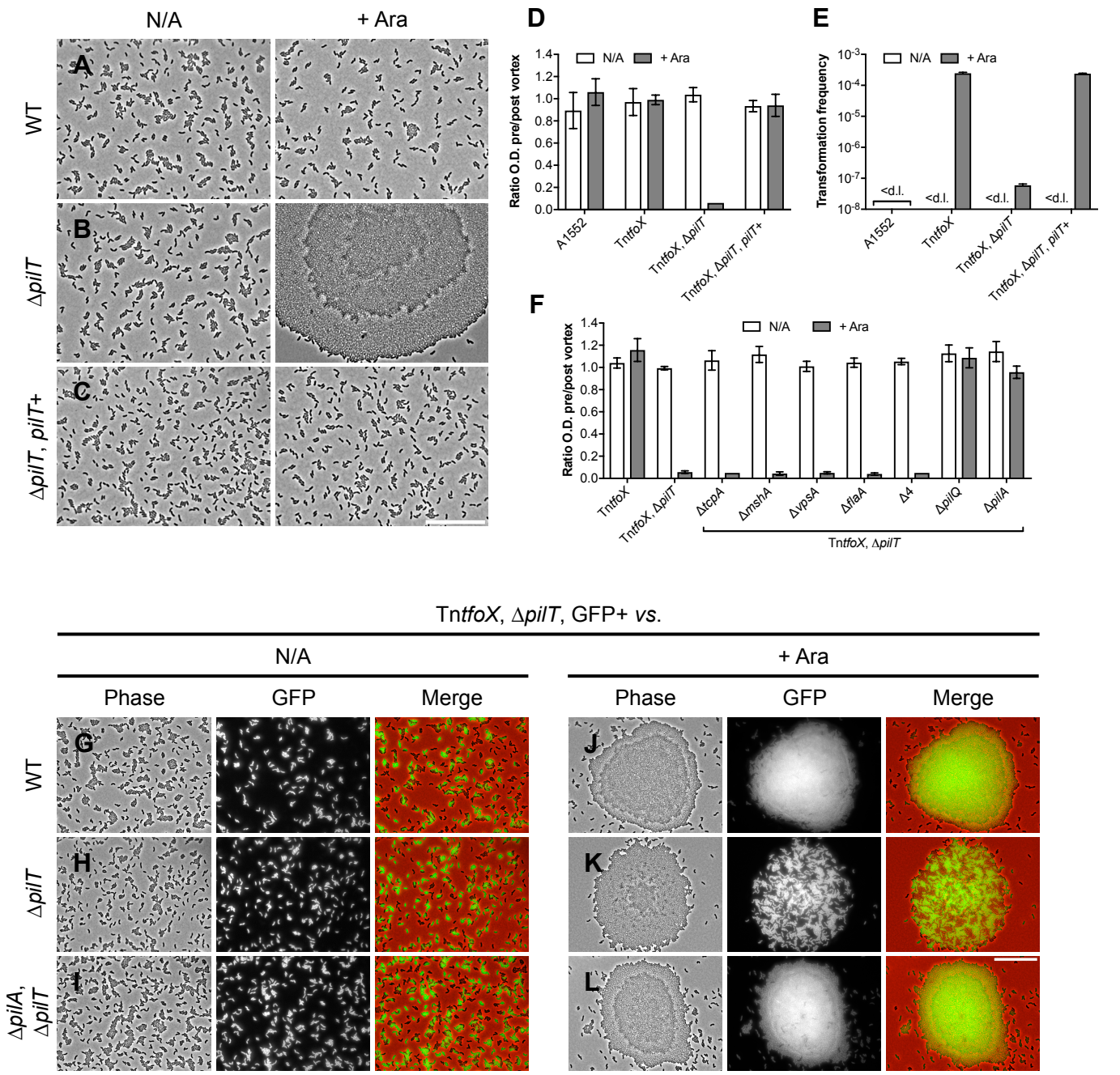
N/A
+ Ara
A
B
C
WT
ΔpilT
ΔpilT, pilT+
D
Ratio O.D. pre/post vortex
N/A
+ Ara
A1552
TntfoX
TntfoX, ΔpilT
TntfoX, ΔpilT, pilT+
E
Transformation frequency
<d.l.
F
TntfoX, ΔpilT
ΔtcpA
ΔmshA
ΔvpsA
ΔflaA
Δ4
ΔpilQ
ΔpilA
TntfoX, ΔpilT, GFP+ vs.
Phase
GFP
Merge
G
H
I
J
K
L
ΔpilA, ΔpilT

Figure 2. Competent cells auto-aggregate in the absence of pilus retraction.

(**A**-**C**) Phase-contrast microscopy of Tn*tfoX* cells grown in the absence (N/A; no addition) and presence (+ Ara) of *tfoX* induction, in a (**A**) WT, (**B**) Δ*pilT* and (**C**) Δ*pilT*, *pilT*+ background, as indicated. Scale bar = 25 µm.

(**D**-**E**) Aggregation and transformation frequency of cells grown in the absence (N/A; no addition) and presence (+Ara) of *tfoX* induction, as indicated. A1552 (without inducible *tfoX*) was used as a negative control. Values are the mean of three repeats (±S.D.). (**D**) Aggregation is shown as the ratio of the culture optical density (O.D. $_{600\ nm}$) before and after vortexing. (**E**) Chitin-independent transformation frequency assay. < d.l., below detection limit.

(**F**) Effect of various deletion backgrounds on the ability of retraction deficient cells to aggregate. Aggregation is shown as the ratio of the culture optical density (O.D. $_{600\ nm}$) before and after vortexing, in the absence (N/A; no addition) and presence (+Ara) of *tfoX* induction, as indicated. Δ4 = Δ*tcpA*, Δ*mshA*, Δ*vpsA*, Δ*flaA* quadruple mutant. Values are the mean of three repeats (±S.D.).

(**G**-**L**) Co-culture of fluorescent Δ*pilT* cells (A1552-Tn*tfoX*, Δ*pilT*, GFP+) producing GFP and non-fluorescent cells of the (**G**, **J**) WT (A1552-Tn*tfoX*), (**H**, **K**) Δ*pilT* (A1552-Tn*tfoX*, Δ*pilT*) and (**I**, **L**) Δ*pilA*, Δ*pilT* (A1552-Tn*tfoX*, Δ*pilA*, Δ*pilT*), grown in the absence (N/A; no addition) and presence of *tfoX* induction, as indicated. Merged images show GFP in green and phase-contrast in red. Bar = 25 µm.

Figure 3

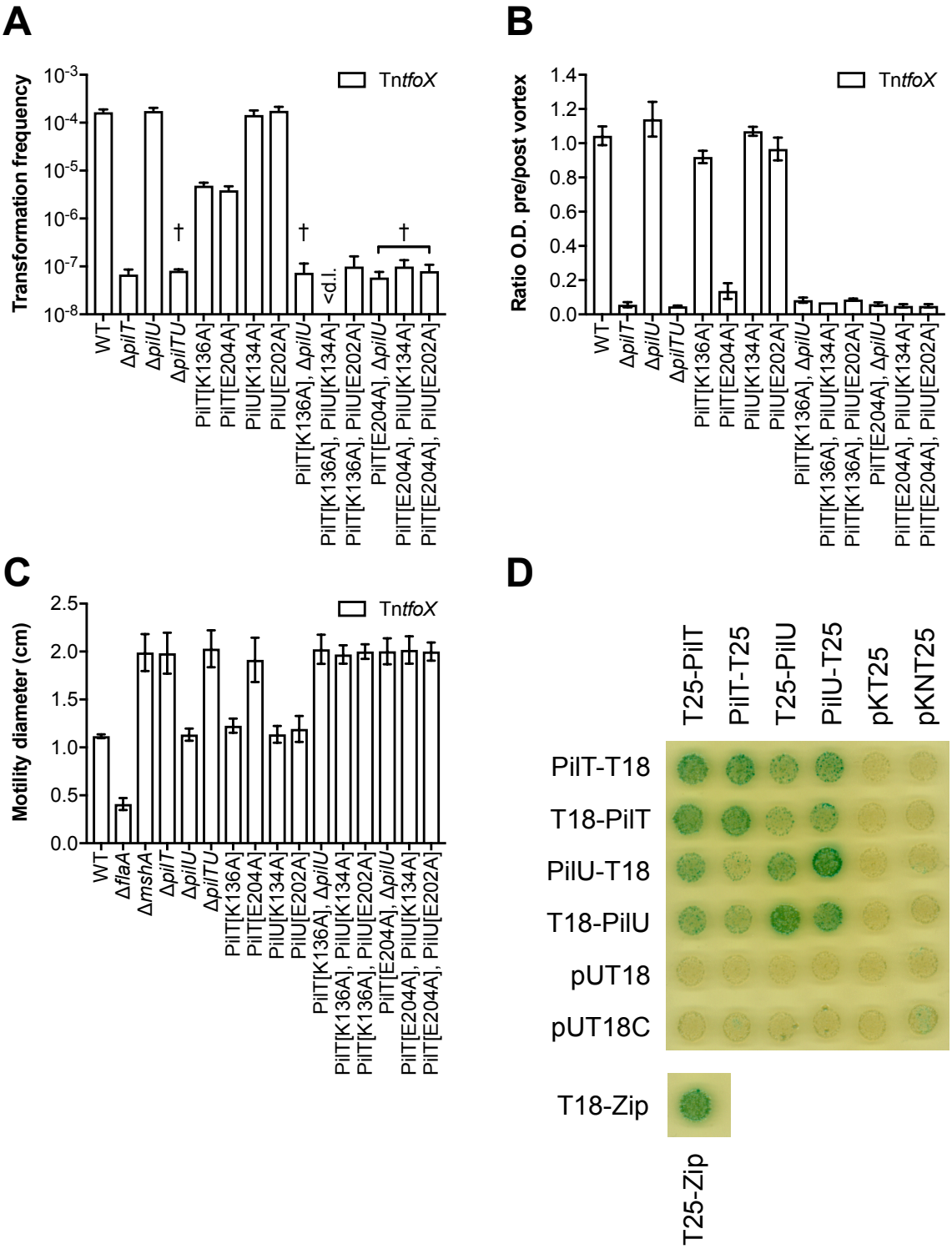
A
Transformation frequency
TntfoX
WT
ΔpilT
ΔpilU
ΔpilTU
PilT[K136A]
PilT[E204A]
PilU[K134A]
PilU[E202A]
PilT[K136A], ΔpilU
PilT[K136A], PilU[K134A]
PilT[K136A], PilU[E202A]
PilT[E204A], ΔpilU
PilT[E204A], PilU[K134A]
PilT[E204A], PilU[E202A]
<d.l.
B
Ratio O.D. pre/post vortex
C
Motility diameter (cm)
ΔflaA
ΔmshA
D
T25-PilT
PilT-T25
T25-PilU
PilU-T25
pKT25
pKNT25
PilT-T18
T18-PilT
PilU-T18
T18-PilU
pUT18
pUT18C
T18-Zip
T25-Zip

Figure 3. ATPase activity of PilT and PilU controls pilus retraction.

(**A**-**C**) Functionality of PilT and PilU Walker A and Walker B variants assessed by transformation frequency, aggregation and motility. (**A**) Chitin-independent transformation assay. Transformation frequencies are the mean of three repeats (±S.D). < d.l., below detection limit. †, < d.l. in one repeat. (**B**) Aggregation is shown as the ratio of the culture optical density (O.D. $_{600\ nm}$) before and after vortexing in the presence of *tfoX* induction. Values are the mean of three repeats (±S.D.). (**C**) Surface motility was determined on soft LB agar plates. The swarming diameter (cm) is the mean of three repeats (±S.D.). A flagellin-deficient (Δ*flaA*) non-motile strain was used as a negative control.

(**D**) Bacterial Two-hybrid interactions between PilT and PilU. Representative image of *E. coli* strain BTH101 producing combinations of N and C-terminal fusions of PilT and PilU to the T18 and T25 domains of adenylate cyclase, as indicated. Negative controls are empty vectors, positive control is the leucine zipper fusion.

Figure 4

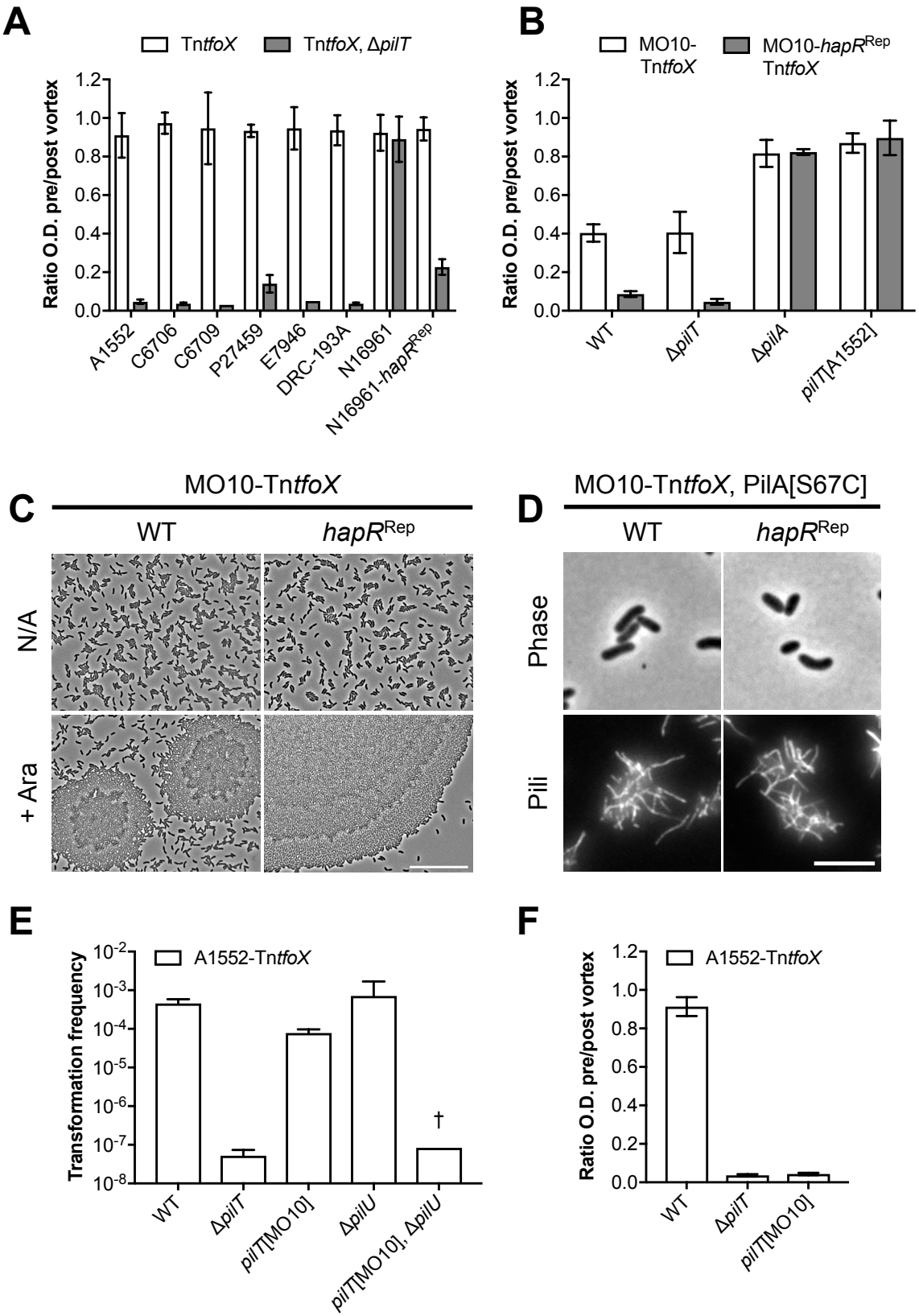
A
TntfoX
TntfoX, ΔpilT
Ratio O.D. pre/post vortex
1.2
1.0
0.8
0.6
0.4
0.2
0.0
A1552
C6706
C6709
P27459
E7946
DRC-193A
N16961
N16961-hapRRep
B
MO10-TntfoX
MO10-hapRRep TntfoX
Ratio O.D. pre/post vortex
WT
ΔpilT
ΔpilA
pilT[A1552]
C
MO10-TntfoX
WT
hapRRep
N/A
+ Ara
D
MO10-TntfoX, PilA[S67C]
WT
hapRRep
Phase
Pili
E
A1552-TntfoX
Transformation frequency
10-2
10-3
10-4
10-5
10-6
10-7
10-8
†
WT
ΔpilT
pilT[MO10]
ΔpilU
pilT[MO10], ΔpilU
F
A1552-TntfoX
Ratio O.D. pre/post vortex
WT
ΔpilT
pilT[MO10]

Figure 4. Pandemic strain MO10 contains a naturally occurring *pilT* mutation.

(**A**-**B**) Aggregation of pandemic strains of *V. cholerae*. Aggregation is shown as the ratio of the culture optical density (O.D. $_{600\ nm}$) before and after vortexing. Strains were cultured in the presence of *tfoX* induction. Values are the mean of three repeats (±S.D.). (**A**) Aggregation of pandemic strains, including the effect of *hapR*^{Rep} on N16961, in a Tn*tfoX* and a Tn*tfoX*, Δ*pilT* background, as indicated. (**B**) Aggregation of pandemic strain MO10 in a MO10-Tn*tfoX* and a MO10-*hapR*^{Rep}, Tn*tfoX* background, as indicated.

(**C**) Phase-contrast microscopy of MO10 cells in the WT (MO10-Tn*tfoX*) and *hapR*^{Rep} (MO10-*hapR*^{Rep}, Tn*tfoX*) backgrounds, grown in the absence (N/A; no addition) and presence (+ Ara) of *tfoX* induction, as indicated. Bar = 25 µm.

(**D**) The pili of WT (MO10-Tn*tfoX*) and *hapR*^{Rep} (MO10-*hapR*^{Rep}, Tn*tfoX*) cells producing PilA[S67C] were stained with AF-488-Mal. Bar = 5 µm.

(**E**-**F**) Functionality of MO10 PilT (*i.e. pilT*[MO10]) assessed by transformation frequency and aggregation in an A1552-Tn*tfoX* background. (**E**) Chitin-independent transformation assay. Transformation frequencies are the mean of three repeats (±S.D). < d.l., below detection limit. †, < d.l. in two repeats. (**F**) Aggregation is shown as the ratio of the culture optical density (O.D. $_{600\ nm}$) before and after vortexing. Strains were cultured in the presence of *tfoX* induction. Values are the mean of three repeats (±S.D.).

Figure 5

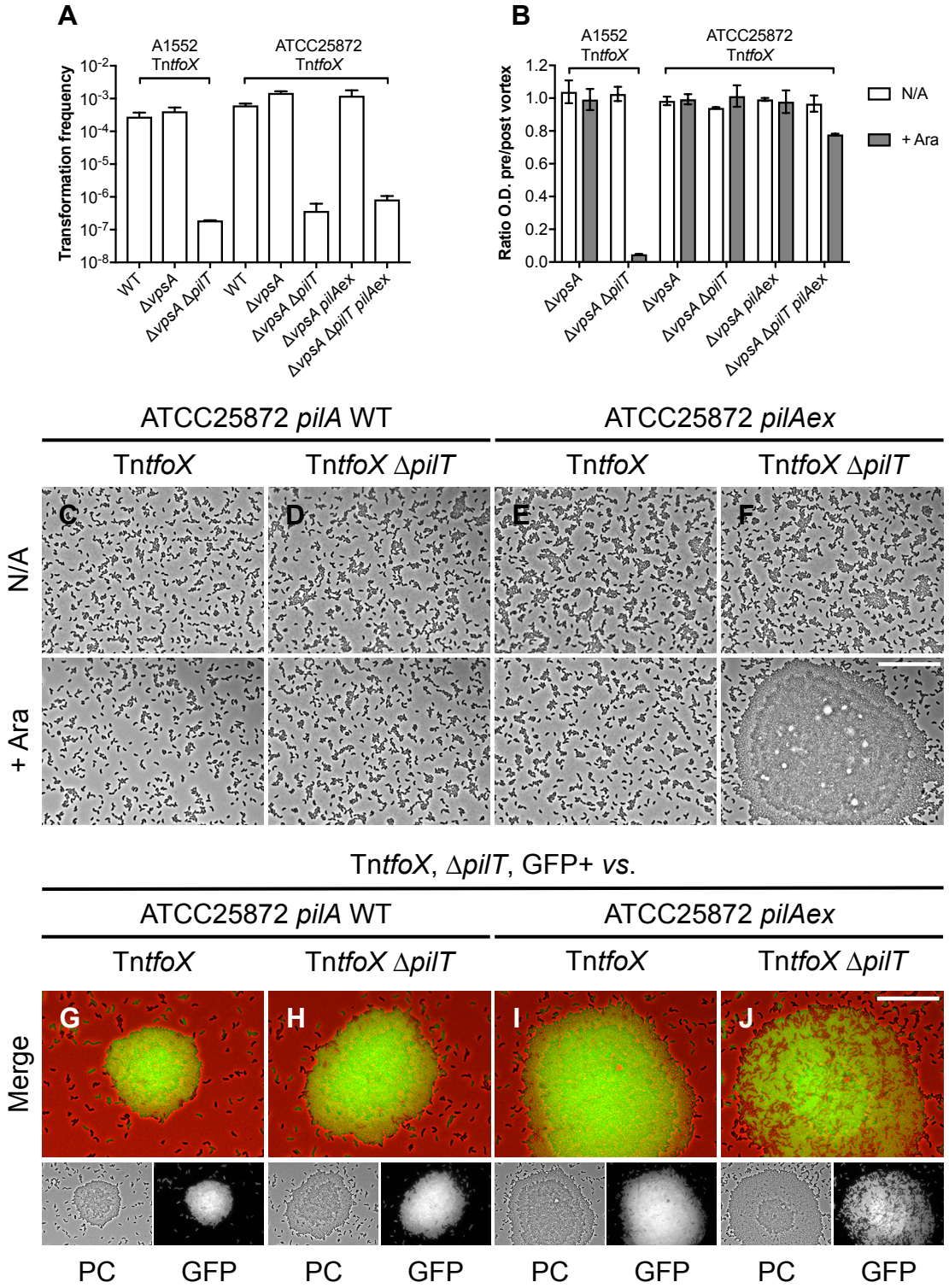
A
A1552
TntfoX
ATCC25872
TntfoX
Transformation frequency
10-2
10-3
10-4
10-5
10-6
10-7
10-8
WT
ΔvpsA
ΔvpsA ΔpilT
WT
ΔvpsA
ΔvpsA ΔpilT
ΔvpsA pilAex
ΔvpsA ΔpilT pilAex
B
A1552
TntfoX
ATCC25872
TntfoX
Ratio O.D. pre/post vortex
1.2
1.0
0.8
0.6
0.4
0.2
0.0
N/A
+ Ara
ΔvpsA
ΔvpsA ΔpilT
ΔvpsA
ΔvpsA ΔpilT
ΔvpsA pilAex
ΔvpsA ΔpilT pilAex
ATCC25872 pilA WT
ATCC25872 pilAex
TntfoX
TntfoX ΔpilT
TntfoX
TntfoX ΔpilT
N/A
+ Ara
C
D
E
F
TntfoX, ΔpilT, GFP+ vs.
ATCC25872 pilA WT
ATCC25872 pilAex
TntfoX
TntfoX ΔpilT
TntfoX
TntfoX ΔpilT
Merge
G
H
I
J
PC
GFP
PC
GFP
PC
GFP
PC
GFP

Figure 5. A1552 PilA is sufficient for aggregation in a pathogenic non-O1/O139 strain.

(**A**-**B**) Transformation frequency and aggregation of *V. cholerae* strain ATCC25872 compared to that of A1552. (**A**) Chitin-independent transformation assay. Transformation frequencies are the mean of three repeats (±S.D). (**B**) Aggregation is shown as the ratio of the culture optical density (O.D. $_{600\ nm}$) before and after vortexing, in the absence (N/A; no addition) and presence (+Ara) of *tfoX* induction, as indicated. Values are the mean of three repeats (±S.D.).

(**C**-**F**) Phase-contrast microscopy of ATCC25872-Tn*tfoX*, Δ*vpsA* cells carrying (**C** and **D**) their native *pilA* (*pilA* WT) and (**E** and **F**) A1552 *pilA* (*pilA*ex), in a (**C** and **E**) *pilT*+ and (**D** and **F**) Δ*pilT* background, as indicated. Strains were cultured in the absence (N/A; no addition) and presence (+ Ara), as indicated. Bar = 25 µm. Note that ATCC25872 derivatives were co-deleted for *vpsA* to rule out any compounding effects of biofilm formation.

(**G**-**J**) Co-culture of fluorescent A1552-Tn*tfoX*, Δ*pilT*, GFP+, producing GFP, and non-fluorescent cells of ATCC25872-Tn*tfoX*, Δ*vpsA* carrying (**G** and **H**) *pilA* WT and (**I** and **J**) *pilA*ex, in a (**G** and **I**) *pilT*+ and (**H** and **J**) Δ*pilT* background, as indicated. Cells were grown in the presence of *tfoX* induction. Merged images show GFP in green and phase-contrast (PC) in red. Bar = 25 µm.

Figure 6

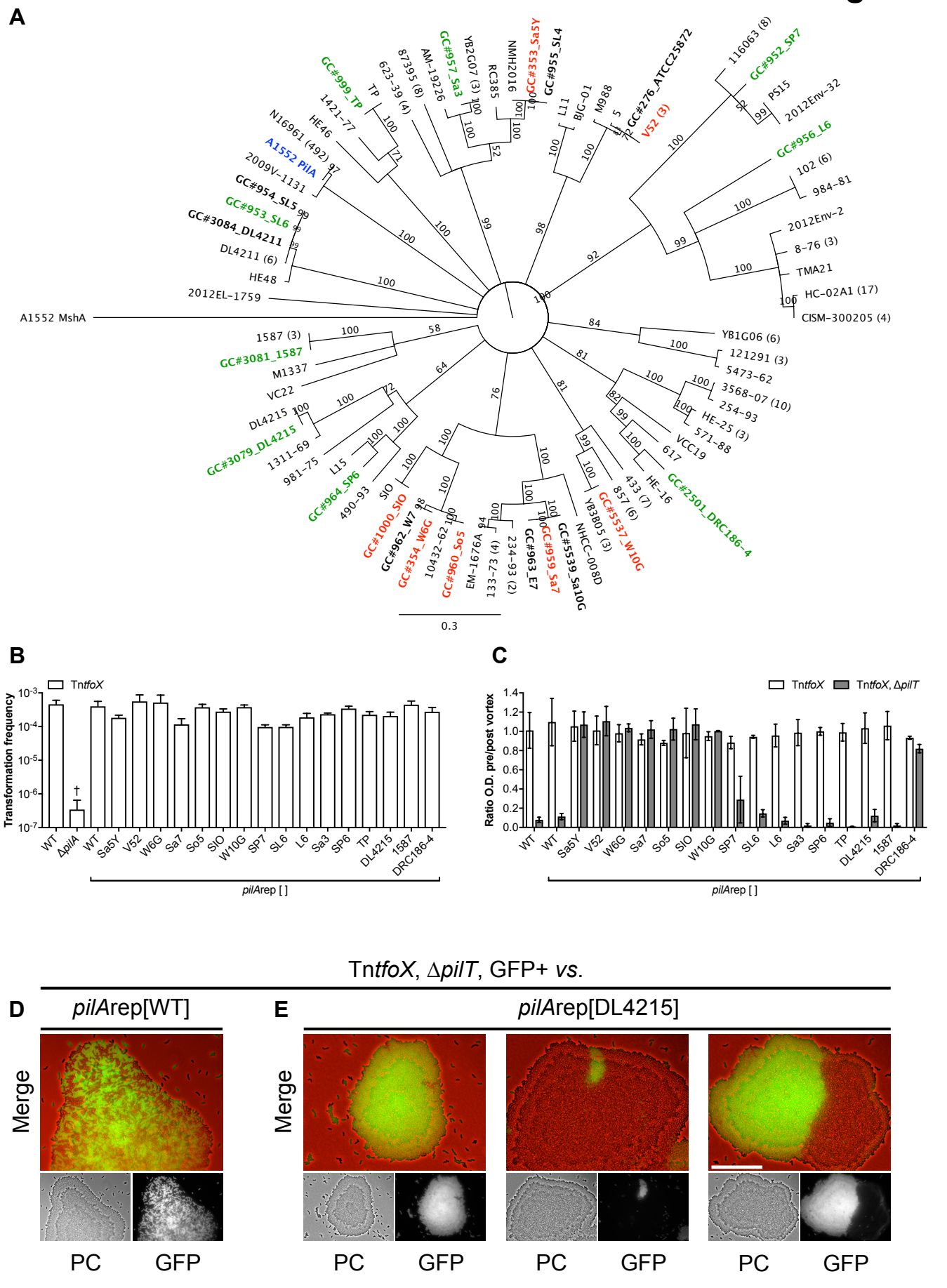

A
GC#999_TP
TP
1421-77
HE46
N16961 (492)
A1552 PilA
2009V-1131
GC#954_SL5
GC#953_SL6
GC#3084_DL4211
DL4211 (6)
HE48
2012EL-1759
A1552 MshA
GC#957_Sa3
AM-19226
87395 (8)
623-39 (4)
YB2G07 (3)
RC385
NMH2016
GC#353_Sa5Y
GC#955_SL4
L11
BJG-01
M988
GC#276_ATCC25872
V52 (3)
116063 (8)
GC#952_SP7
PS15
2012Env-32
GC#956_L6
102 (6)
984-81
2012Env-2
8-76 (3)
TMA21
HC-02A1 (17)
CISM-300205 (4)
YB1G06 (6)
121291 (3)
5473-62
3568-07 (10)
254-93
HE-25 (3)
571-88
VCC19
617
GC#2501_DRC186-4
HE-16
433 (7)
857 (6)
GC#5537_W10G
YB3B05 (3)
NHCC-008D
GC#5539_Sa10G
GC#959_Sa7
GC#963_E7
234-93 (2)
133-73 (4)
EM-1676A
GC#960_So5
10432-62
GC#354_W6G
GC#962_W7
GC#1000_SlO
SlO
490-93
GC#964_SP6
L15
981-75
1311-69
GC#3079_DL4215
DL4215
VC22
M1337
GC#3081_1587
1587 (3)
0.3
B
TntfoX
Transformation frequency
WT
ΔpilA
WT
Sa5Y
V52
W6G
Sa7
So5
SlO
W10G
SP7
SL6
L6
Sa3
SP6
TP
DL4215
1587
DRC186-4
pilArep [ ]
C
TntfoX
TntfoX, ΔpilT
Ratio O.D. pre/post vortex
WT
WT
Sa5Y
V52
W6G
Sa7
So5
SlO
W10G
SP7
SL6
L6
Sa3
SP6
TP
DL4215
1587
DRC186-4
pilArep [ ]
TntfoX, ΔpilT, GFP+ vs.
D
pilArep[WT]
Merge
PC
GFP
E
pilArep[DL4215]
Merge
PC
GFP
PC
GFP
PC
GFP

Figure 6. PilA variability governs auto-aggregation and enables kin-recognition.

(**A**) Consensus neighbour-joining phylogenetic tree of PilA. The tree consists of the 56 unique PilA sequences identified from NCBI, 22 sequences from an in-house collection of various environmental and patient isolates (bold), and A1552 PilA (blue) and MshA (outgroup). Values shown are consensus support values (%). Aggregation capable (green) and incapable (red) PilAs tested in the *pilA*rep experiments are highlighted. Note that ATCC25872 and V52 PilA are identical.

(**B**-**C**) Functionality of A1552-Tn*tfoX*, *pilA*rep[WT] and 16 different PilAs assessed by transformation frequency and aggregation. (**B**) Chitin-independent transformation frequency assay. WT (A1552-Tn*tfoX*) and Δ*pilA* (A1552-Tn*tfoX*, Δ*pilA*) served as positive and negative controls. Transformation frequencies are the mean of three repeats (±S.D). †, <d.l. in one repeat. (**C**) Aggregation was determined for the WT and each *pilA*rep strain in a *pilT*+ (A1552-Tn*tfoX*) and Δ*pilT* (A1552-Tn*tfoX*, Δ*pilT*) background, as indicated. Aggregation is shown as the ratio of the culture optical density (O.D. $_{600\ nm}$) before and after vortexing, in the presence of *tfoX* induction. Values are the mean of three repeats (±S.D.).

(**D**-**E**) Co-culture of fluorescent A1552-Tn*tfoX*, Δ*pilT*, GFP+, producing GFP, and non-fluorescent cells of (**D**) *pilA*rep[WT] (A1552-Tn*tfoX*, Δ*pilT*, *pilA*rep[WT]) and (**E**) *pilA*rep[DL4215] (A1552-Tn*tfoX*, Δ*pilT*, *pilA*rep[DL4215]), as indicated. Cells were grown in the presence of *tfoX* induction. Merged images show GFP in green and phase-contrast (PC) in red. Bar = 25 µm.

Figure 7

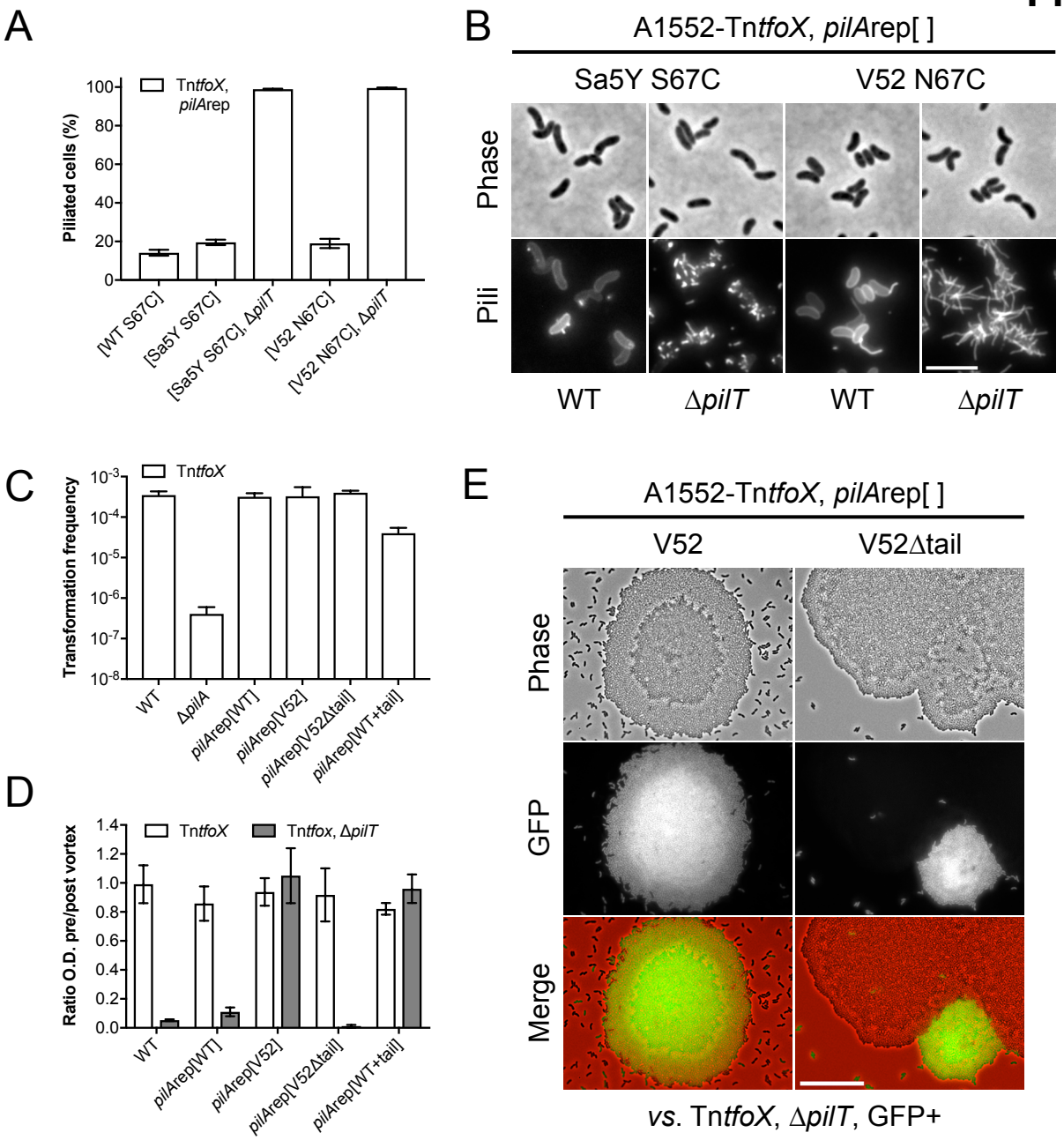
A
Piliated cells (%)
TntfoX, pilArep
100
80
60
40
20
0
[WT S67C]
[Sa5Y S67C]
[Sa5Y S67C], ΔpilT
[V52 N67C]
[V52 N67C], ΔpilT
B
A1552-TntfoX, pilArep[ ]
Sa5Y S67C
V52 N67C
Phase
Pili
WT
ΔpilT
WT
ΔpilT
C
Transformation frequency
TntfoX
10-3
10-4
10-5
10-6
10-7
10-8
WT
ΔpilA
pilArep[WT]
pilArep[V52]
pilArep[V52Δtail]
pilArep[WT+tail]
D
Ratio O.D. pre/post vortex
TntfoX
Tntfox, ΔpilT
1.4
1.2
1.0
0.8
0.6
0.4
0.2
0.0
WT
pilArep[WT]
pilArep[V52]
pilArep[V52Δtail]
pilArep[WT+tail]
E
A1552-TntfoX, pilArep[ ]
V52
V52Δtail
Phase
GFP
Merge
vs. TntfoX, ΔpilT, GFP+

Figure 7. The unusual tail of ATCC25872/V52 PilA inhibits aggregation.

(**A**-**B**) Labelling of pili in *pilA*rep cysteine variants of A1552, Sa5Y and V52 PilA. (**A**) Quantification of piliation in snapshot imaging. Bars represent mean of three repeats (±S.D.). *n* = *c.a.* 2000 cells per strain per repeat. (**B**) Direct observation of pili stained with AF-488-Mal in *pilA*rep[Sa5Y PilA S67C] and *pilA*rep[V52 PilA N67C], in a WT (A1552-Tn*tfoX*) and Δ*pilT* (A1552-Tn*tfoX*, Δ*pilT*) background, as indicated. Bar = 5 µm.

(**C**-**D**) Functionality of *pilA*rep tail variants assessed by natural transformation and aggregation. (**C**) Chitin-independent transformation assay. WT (A1552-Tn*tfoX*) and *pilA* (A1552-Tn*tfoX*, Δ*pilA*) served as positive and negative controls. Transformation frequencies are the mean of three repeats (±S.D). (**D**) Aggregation was determined for the WT and each *pilA*rep strain in a *pilT*+ (A1552-Tn*tfoX*) and Δ*pilT* (A1552-Tn*tfoX*, Δ*pilT*) background, as indicated. Aggregation is shown as the ratio of the culture optical density (O.D. $_{600\ nm}$) before and after vortexing, in the presence of *tfoX* induction. Values are the mean of three repeats (±S.D.).

(**E**) Co-culture of fluorescent A1552-Tn*tfoX*, Δ*pilT*, GFP+*,* producing GFP, and non-fluorescent cells of *pilA*rep[V52] (A1552-Tn*tfoX*, Δ*pilT*, *pilA*rep[V52]) and *pilA*rep[V52Δtail] (A1552-Tn*tfoX*, Δ*pilT*, *pilA*rep[V52Δtail]), as indicated. Note that ATCC25872 and V52 PilA are identical. Cells were grown in the presence of *tfoX* induction. Merged images show GFP in green and phase-contrast in red. Bar = 25 µm.

Supplemental information:

Supplemental Table S1 – Bacterial strains and plasmids

Strain name	Strain #	Genotype[1, 2, 3, 4]	Source
V. cholerae			
A1552 (WT)	GC#1	A1552 Wild type, O1 El Tor Inaba; Rif^R	(Yildiz and Schoolnik, 1998)
A1552-*lacZ*-kan	GC#135	A1552 Ω*lacZ*::*aph*; Kan^R	(Marvig and Blokesch, 2010)
A1552-Tn*tfoX*	GC#1626	Tn*tfoX*	(Lo Scrudato and Blokesch, 2012)
A1552-Tn*tfoX*, Δ*pilT*	GC#2349	Tn*tfoX*, Δ*pilT*::FRT	(Seitz and Blokesch, 2013)
A1552-Tn*tfoX*, Δ*pilA*	GC#3140	Tn*tfoX*, Δ*pilA*	(Seitz and Blokesch, 2013)
A1552-Tn*tfoX*, Δ*pilA*, Δ*pilT*	GC#5699	Tn*tfoX*, Δ*pilT*::FRT, Δ*pilA*	This work
A1552-Tn*tfoX*, PilA[S67C]	GC#5811	Tn*tfoX*, *pilA*[S67C]	This work
A1552-Tn*tfoX*, PilA[T71C]	GC#6173	Tn*tfoX*, *pilA*[T71C]	This work
A1552-Tn*tfoX*, PilA[T72C]	GC#6174	Tn*tfoX*, *pilA*[T72C]	This work
A1552-Tn*tfoX*, PilA[T75C]	GC#6175	Tn*tfoX*, *pilA*[T75C]	This work
A1552-Tn*tfoX*, PilA[T80C]	GC#6176	Tn*tfoX*, *pilA*[T80C]	This work
A1552-Tn*tfoX*, PilA[T84C]	GC#6177	Tn*tfoX*, *pilA*[T84C]	This work
A1552-Tn*tfoX*, PilA[S67C], Δ*pilT*	GC#6178	Tn*tfoX*, *pilA*[S67C], Δ*pilT*::FRT	This work
A1552-Tn*tfoX*, PilA[T71C], Δ*pilT*	GC#6179	Tn*tfoX*, *pilA*[T71C], Δ*pilT*::FRT	This work
A1552-Tn*tfoX*, PilA[T72C], Δ*pilT*	GC#6180	Tn*tfoX*, *pilA*[T72C], Δ*pilT*::FRT	This work
A1552-Tn*tfoX*, PilA[T75C], Δ*pilT*	GC#6181	Tn*tfoX*, *pilA*[T75C], Δ*pilT*::FRT	This work
A1552-Tn*tfoX*, PilA[T80C], Δ*pilT*	GC#6182	Tn*tfoX*, *pilA*[T80C], Δ*pilT*::FRT	This work
A1552-Tn*tfoX*, PilA[T84C], Δ*pilT*	GC#6183	Tn*tfoX*, *pilA*[T84C], Δ*pilT*::FRT	This work

A1552-Tn*tfoX*, PilA[S67C], Δ*pilQ*	GC#6184	Tn*tfoX*, *pilA*[S67C], Δ*pilQ*	This work
A1552-Tn*tfoX*, PilA[S67C], Δ*pilB*	GC#6185	Tn*tfoX*, *pilA*[S67C], Δ*pilB*	This work
A1552-Tn*tfoX*, Δ*pilA*, *comEA-mCherry*	GC#2492	Tn*tfoX*, Δ*pilA*, *comEA-mCherry*::FRT	(Seitz *et al.*, 2014)
A1552-Tn*tfoX*, PilA[S67C], *comEA-mCherry*	GC#5848	Tn*tfoX*, *pilA*[S67C], *comEA-mCherry*::FRT	This work
A1552-Tn*tfoX*, PilA[S67C], Δ*pilU*	GC#6187	Tn*tfoX*, *pilA*[S67C], Δ*pilU*::FRT	This work
A1552-Tn*pilA*	GC#5714	Tn*pilA* (= *araC*, P_{BAD}-*pilA*)	This work
A1552-Tn*pilA*, Δ*mshA*	GC#5715	Tn*pilA*, Δ*mshA*::FRT	This work
A1552-Tn*pilA*, Δ*ompA*	GC#5716	Tn*pilA*, Δ*ompA*::FRT	This work
A1552-Tn*pilA*[S67C]	GC#5717	Tn*pilA*[S67C] (= *araC*, P_{BAD}-*pilA*[S67C])	This work
A1552-Tn*pilA*[S67C], Δ*mshA*	GC#5718	Tn*pilA*[S67C], Δ*mshA*::FRT	This work
A1552-Tn*pilA*[S67C], Δ*ompA*	GC#5719	Tn*pilA*[S67C], Δ*ompA*::FRT	This work
A1552-Tn*tfoX*, Δ*pilT*, *pilT*+	GC#5889	Tn*tfoX*, Δ*pilT*::FRT, Ω*lacZ*::(P_{pilT}-*pilT*)	This work
A1552-*lacZ*-*pheS**	GC#4609	Ω*lacZ*::(FRT-*aph*-*pheS**-FRT); Kan^R	(Van der Henst *et al.*, 2017)
A1552-GFP+	GC#4625	Ω*lacZ*::($P_{A1/O4/O3}$-*gfp*)	This work
A1552-Tn*tfoX*, GFP+	GC#6153	Tn*tfoX*, Ω*lacZ*::($P_{A1/O4/O3}$-*gfp*)	This work
A1552-Tn*tfoX*, Δ*pilT*, GFP+	GC#6154	Tn*tfoX*, Δ*pilT*::FRT, Ω*lacZ*::($P_{A1/O4/O3}$-*gfp*)	This work
A1552-Tn*tfoX*, Δ*pilT*, Δ*pilQ*	GC#6150	Tn*tfoX*, Δ*pilT*::FRT, Δ*pilQ*	This work
A1552-Tn*tfoX*, Δ*pilT*, Δ*mshA*	GC#6151	Tn*tfoX*, Δ*pilT*::FRT, Δ*mshA*	This work
A1552Δ*flaA*	GC#1996	Δ*flaA*::FRT	(Van der Henst *et al.*, 2017)
A1552-Tn*tfoX*, Δ*flaA*	GC#2000	Tn*tfoX*, Δ*flaA*::FRT	This work
A1552-Tn*tfoX*, Δ*pilT*, Δ*flaA*	GC#6158	Tn*tfoX*, Δ*pilT*::FRT, Δ*flaA*::FRT	This work
A1552Δ*vpsA*	GC#1965	Δ*vpsA*::FRT	(Van der Henst *et al.*, 2016)
A1552-Tn*tfoX*, Δ*vpsA*	GC#2848	Tn*tfoX*, Δ*vpsA*::FRT	This work

A1552-Tn*tfoX*, Δ*pilT*, Δ*vpsA*	GC#5873	Tn*tfoX*, Δ*pilT*::FRT, Δ*vpsA*::FRT	This work
A1552Δ*tcpA*	GC#2210	Δ*tcpA*::FRT	(Seitz and Blokesch, 2013)
A1552-Tn*tfoX*, Δ*tcpA*	GC#3746	Tn*tfoX*, Δ*tcpA*::FRT	This work
A1552-Tn*tfoX*, Δ*pilT*, Δ*tcpA*	GC#6159	Tn*tfoX*, Δ*pilT*::FRT, Δ*tcpA*::FRT	This work
A1552Δ*mshA*	GC#2200	Δ*mshA*::FRT	(Seitz and Blokesch, 2013)
A1552-Tn*tfoX*, Δ*mshA*	GC#2822	Tn*tfoX*, Δ*mshA*::FRT	This work
A1552Δ*mshA*, Δ*tcpA*, Δ*flaA*, Δ*vpsA*	GC#6161	Δ*mshA*::FRT, Δ*tcpA*::FRT, Δ*flaA*::FRT, Δ*vpsA*::FRT	This work
A1552Δ*mshA*, Δ*tcpA*, Δ*flaA*, Δ*vpsA*, Δ*pilT*	GC#6163	Δ*mshA*::FRT, Δ*tcpA*::FRT, Δ*flaA*::FRT, Δ*vpsA*::FRT, Δ*pilT*::FRT	This work
A1552-Tn*tfoX*, Δ*mshA*, Δ*tcpA*, Δ*flaA*, Δ*vpsA*	GC#6166	Tn*tfoX*, Δ*mshA*::FRT, Δ*tcpA*::FRT, Δ*flaA*::FRT, Δ*vpsA*::FRT	This work
A1552-Tn*tfoX*, Δ*mshA*, Δ*tcpA*, Δ*flaA*, Δ*vpsA*, Δ*pilT*	GC#6167	Tn*tfoX*, Δ*mshA*::FRT, Δ*tcpA*::FRT, Δ*flaA*::FRT, Δ*vpsA*::FRT, Δ*pilT*::FRT	This work
A1552Δ*pglL*	GC#826	Δ*pglL* (*VC0393*)	This work
A1552-Tn*tfoX*, Δ*pglL*	GC#2871	Tn*tfoX*, Δ*pglL* (*VC0393*)	This work
A1552-Tn*tfoX*, Δ*pglL*, Δ*pilT*	GC#5827	Tn*tfoX*, Δ*pglL* (*VC0393*), Δ*pilT*::FRT	This work
A1552Δ*rbmEF*	GC#3619	Δ*rbmEF*::FRT	This work
A1552-Tn*tfoX*, Δ*rbmEF*	GC#5785	Tn*tfoX*, Δ*rbmEF*::FRT	This work
A1552-Tn*tfoX*, Δ*rbmEF*, Δ*pilT*	GC#5842	Tn*tfoX*, Δ*rbmEF*::FRT, Δ*pilT*::FRT	This work
A1552Δ*vpsT*	GC#3620	Δ*vpsT*::FRT	This work
A1552-Tn*tfoX*, Δ*vpsT*	GC#5786	Tn*tfoX*, Δ*vpsT*::FRT	This work
A1552-Tn*tfoX*, Δ*vpsT*, Δ*pilT*	GC#5843	Tn*tfoX*, Δ*vpsT*::FRT, Δ*pilT*::FRT	This work
A1552Δ*bap1*	GC#3621	Δ*bap1*::FRT	This work
A1552-Tn*tfoX*, Δ*bap1*	GC#5787	Tn*tfoX*, Δ*bap1*::FRT	This work
A1552-Tn*tfoX*, Δ*bap1*, Δ*pilT*	GC#5844	Tn*tfoX*, Δ*bap1*::FRT, Δ*pilT*::FRT	This work
A1552-Δ*rbmA*	GC#3907	Δ*rbmA*::FRT	This work
A1552-Tn*tfoX*, Δ*rbmA*	GC#5788	Tn*tfoX*, Δ*rbmA*::FRT	This work
A1552-Tn*tfoX*, Δ*rbmA*, Δ*pilT*	GC#5845	Tn*tfoX*, Δ*rbmA*::FRT, Δ*pilT*::FRT	This work

A1552Δ*gbpA*	GC#348	Δ*gbpA*	This work
A1552-Tn*tfoX*, Δ*gbpA*	GC#2026	Tn*tfoX*, Δ*gbpA*	This work
A1552-Tn*tfoX*, Δ*gbpA*, Δ*pilT*	GC#5846	Tn*tfoX*, Δ*gbpA*, Δ*pilT*::FRT	This work
A1552Δ*crvA*	GC#4581	Δ*cvrA*::FRT	This work
A1552-Tn*tfoX*, Δ*crvA*	GC#5871	Tn*tfoX*, Δ*cvrA*::FRT	This work
A1552-Tn*tfoX*, Δ*crvA*, Δ*pilT*	GC#5874	Tn*tfoX*, Δ*cvrA*::FRT, Δ*pilT*::FRT	This work
A1552-Tn*tfoX*, Δ*VC0502*	GC#6171	Tn*tfoX*, Δ*VC0502*::FRT	This work
A1552-Tn*tfoX*, Δ*VC0502*, Δ*pilT*	GC#6172	Tn*tfoX*, Δ*VC0502*::FRT, Δ*pilT*::FRT	This work
A1552-Tn*toxT*	GC#5955	Tn*toxT*	This work
A1552Δ*ctx*	GC#1434	Δ*ctx*::FRT	(Blokesch, 2012)
A1552-Tn*toxT*, Δ*ctx*	GC#5956	Tn*toxT*, Δ*ctx*::FRT	This work
A1552-Tn*toxT*, Δ*tcpA*	GC#6027	Tn*toxT*, Δ*tcpA*::FRT	This work
A1552-Tn*vdcA*	GC#2947	Tn*vdcA*	(Metzger *et al.*, 2016)
A1552-Tn*cdpA*	GC#2948	Tn*cdpA*	(Metzger *et al.*, 2016)
A1552-Tn*vdcA*, Δ*pilT*	GC#6155	Tn*vdcA*, Δ*pilT*::FRT	This work
A1552-Tn*cdpA*, Δ*pilT*	GC#6156	Tn*cdpA*, Δ*pilT*::FRT	This work
A1552-Tn*vdcA*, Δ*mshA*	GC#6168	Tn*vdcA*, Δ*mshA*::FRT	This work
A1552-Tn*vdcA*, Δ*pilA*	GC#6169	Tn*vdcA*, Δ*pilA*	This work
A1552-Tn*vdcA*, Δ*vpsA*	GC#6170	Tn*vdcA*, Δ*vpsA*::FRT	This work
A1552-Tn*tfoX*, Δ*pilU*	GC#6152	Tn*tfoX*, Δ*pilU*::FRT	This work
A1552-Tn*tfoX*, Δ*pilTU*	GC#6164	Tn*tfoX*, Δ*pilTU*::FRT	This work
A1552-Tn*tfoX*, PilT[K136A]	GC#6189	Tn*tfoX*, *pilT*[K136A]	This work
A1552-Tn*tfoX*, PilT[E204A]	GC#6157	Tn*tfoX*, *pilT*[E204A]	This work
A1552-Tn*tfoX*, PilU[K134A]	GC#6190	Tn*tfoX*, *pilU*[K134A]	This work
A1552-Tn*tfoX*, PilU[E202A]	GC#6192	Tn*tfoX*, *pilU*[E202A]	This work
A1552-Tn*tfoX*, PilT[K136A], Δ*pilU*	GC#6194	Tn*tfoX*, *pilT*[K136A], Δ*pilU*::FRT	This work

A1552-Tn*tfoX*, PilT[K136A], PilU[K134A]	GC#6195	Tn*tfoX*, *pilT*[K136A], *pilU*[K134A]	This work
A1552-Tn*tfoX*, PilT[K136A], PilU[E202A]	GC#6196	Tn*tfoX*, *pilT*[K136A], *pilU*[E202A]	This work
A1552-Tn*tfoX*, PilT[E204A], Δ*pilU*	GC#6165	Tn*tfoX*, *pilT*[E204A], Δ*pilU*::FRT	This work
A1552-Tn*tfoX*, PilT[E204A], PilU[K134A]	GC#6191	Tn*tfoX*, *pilT*[E204A], *pilU*[K134A]	This work
A1552-Tn*tfoX*, PilT[E204A], PilU[E202A]	GC#6193	Tn*tfoX*, *pilT*[E204A], *pilU*[E202A]	This work
C6706-original	GC#4522	C6706-original; O1 El Tor Inaba; isolated in 1991, Peru; Str^{S} (original isolate before introduction of streptomycin resistance-causing mutation; non-mutated *luxO*).	Gift from J. Mekalanos (Harvard); (Van der Henst *et al.*, 2017)
C6709	GC#1503	C6709; O1 El Tor Inaba; isolated in 1991, Peru; Str^{R}	(Nesper *et al.*, 2002; Wachsmuth *et al.*, 1993)
P27459	GC#1504	P27459; O1 El Tor Inaba; isolated in 1976, Bangladesh; Str^{R}	(Nesper *et al.*, 2002; Wachsmuth *et al.*, 1993)
E7946	GC#2600	E7946; El Tor Ogawa; isolated in 1978, Bahrain; Str^{R}	(Lazinski and Camilli, 2013; Miller *et al.*, 1989)
DRC-193A	GC#1954	DRC-193A; O1 patient isolate from 2011 (isolated at the Institut National de Recherche Biomédicale; Democratic Republic of the Congo); *ctxAB*+ *tcp*+ *hapR*+; Str^{R}	(Borgeaud *et al.*, 2015)
N16961	GC#2	N16961; O1 El Tor Inaba; isolated in 1971, Bangladesh; *hapR* frame-shift, Str^{R}	(Heidelberg *et al.*, 2000)
N16961-$hapR^{Rep}$	GC#5663	N16961-$hapR^{Rep}$ (*hapR* frame-shift repaired)	(Van der Henst *et al.*, 2017)
C6706-original-Tn*tfoX*	GC#5655	C6706-original Tn*tfoX*	This work
C6706-original-Tn*tfoX*, Δ*pilT*	GC#5975	C6706-original Tn*tfoX*, Δ*pilT*	This work
C6709-Tn*tfoX*	GC#1958	C6709 Tn*tfoX*	This work
C6709-Tn*tfoX*, Δ*pilT*	GC#5972	C6709 Tn*tfoX*, Δ*pilT*	This work
P27459-Tn*tfoX*	GC#1959	P27459 Tn*tfoX*	(Borgeaud *et al.*, 2015)
P27459-Tn*tfoX*, Δ*pilT*	GC#5973	P27459 Tn*tfoX*, Δ*pilT*	This work
DRC-193A-Tn*tfoX*	GC#1964	DRC-193A Tn*tfoX*	(Borgeaud *et al.*, 2015)

DRC-193A-Tn*tfoX*, Δ*pilT*	GC#5974	DRC-193A Tn*tfoX*, Δ*pilT*	This work
E7946-Tn*tfoX*	GC#2606	E7946 Tn*tfoX*	(Borgeaud *et al.*, 2015)
E7946-Tn*tfoX*, Δ*pilT*	GC#5976	E7946 Tn*tfoX*, Δ*pilT*	This work
N16961-Tn*tfoX*	GC#6013	N16961 Tn*tfoX*	This work
N16961-Tn*tfoX*, Δ*pilT*	GC#6014	N16961 Tn*tfoX*, Δ*pilT*	This work
N16961-*hapR*^{Rep}-Tn*tfoX*	GC#5696	N16961-*hapR*^{Rep} Tn*tfoX*	This work
N16961-*hapR*^{Rep}- Tn*tfoX*, Δ*pilT*	GC#5978	N16961-*hapR*^{Rep} Tn*tfoX*, Δ*pilT*	This work
MO10	GC#5	MO10; O139 strain; isolated in 1992, India; *hapR* mutated (HapR[R12L]), Str^{R}	(Waldor and Mekalanos, 1994a, b)
MO10-*hapR*^{Rep}	GC#5661	MO10-*hapR*^{Rep} (HapR[R12L] variant repaired)	This work
MO10-Tn*tfoX*	GC#5924	MO10 Tn*tfoX*	This work
MO10-*hapR*^{Rep}-Tn*tfoX*	GC#5690	MO10-*hapR*^{Rep} Tn*tfoX*	This work
MO10-Tn*tfoX*, Δ*pilA*	GC#6002	MO10 Tn*tfoX*, Δ*pilA*	This work
MO10-*hapR*^{Rep}-Tn*tfoX*, Δ*pilA*	GC#5940	MO10-*hapR*^{Rep} Tn*tfoX*, Δ*pilA*	This work
MO10-Tn*tfoX*, Δ*pilT*	GC#5970	MO10 Tn*tfoX*, Δ*pilT*	This work
MO10-*hapR*^{Rep}-Tn*tfoX*, Δ*pilT*	GC#5971	MO10-*hapR*^{Rep} Tn*tfoX*, Δ*pilT*	This work
MO10-Tn*tfoX*, PilA[S67C]	GC#6029	MO10 Tn*tfoX*, *pilA*[PilA S67C]	This work
MO10-*hapR*^{Rep}-Tn*tfoX*, PilA[S67C]	GC#5964	MO10-*hapR*^{Rep} Tn*tfoX*, *pilA*[PilA S67C]	This work
MO10-Tn*tfoX*, PilT[A1552]	GC#6018	MO10 Tn*tfoX*, *pilT*[PilT A1552]	This work
MO10-*hapR*^{Rep}-Tn*tfoX*, PilT[A1552]	GC#6019	MO10-*hapR*^{Rep} Tn*tfoX*, *pilT*[PilT A1552]	This work
A1552-Tn*tfoX*, Δ*pilT*	GC#5969	Tn*tfoX*, Δ*pilT*	This work
A1552-Tn*tfoX*, PilT[MO10]	GC#5968	Tn*tfoX*, *pilT*[MO10]	This work
A1552- Tn*tfoX*, PilT[MO10], Δ*pilU*	GC#6197	Tn*tfoX*, *pilT*[MO10], Δ*pilU*::FRT	This work
ATCC25872	GC#276	ATCC25872; non-O1 (O37); isolated in 1965, Czechoslovakia; Str^{R}	(Aldova *et al.*, 1968; Felsenfeld *et al.*, 1970)
ATCC25872-Tn*tfoX*	GC#2932	ATCC25872 Tn*tfoX*	This work

ATCC25872-Tn*tfoX*, Δ*vpsA*	GC#6160	ATCC25872 Tn*tfoX*, Δ*vpsA*::FRT	This work
ATCC25872-Tn*tfoX*, Δ*vpsA*, Δ*pilT*	GC#6162	ATCC25872 Tn*tfoX*, Δ*vpsA*::FRT, Δ*pilT*::FRT	This work
ATCC25872-Tn*tfoX*, Δ*vpsA*, *pilA*ex	GC#6188	ATCC25872 Tn*tfoX*, Δ*vpsA*::FRT, *pilA*ex[A1552]	This work
ATCC25872-Tn*tfoX*, Δ*vpsA*, Δ*pilT pilA*ex	GC#6186	ATCC25872 Tn*tfoX*, Δ*vpsA*::FRT, *pilA*ex[A1552], Δ*pilT*::FRT	This work
Sa5Y	GC#353	Sa5Y; non-O1/O139 Environmental isolate Ca, USA	(Keymer *et al.*, 2007)
W6G	GC#354	W6G; non-O1/O139 Environmental isolate Ca, USA	(Keymer *et al.*, 2007)
SP7	GC#952	SP7; non-O1/O139 Environmental isolate Ca, USA	(Keymer *et al.*, 2007)
SL6	GC#953	SL6; non-O1/O139 Environmental isolate Ca, USA	(Keymer *et al.*, 2007)
SL5	GC#954	SL5; non-O1/O139 Environmental isolate Ca, USA	(Keymer *et al.*, 2007)
SL4	GC#955	SL4; non-O1/O139 Environmental isolate Ca, USA	(Keymer *et al.*, 2007)
L6	GC#956	L6; non-O1/O139 Environmental isolate Ca, USA	(Keymer *et al.*, 2007)
Sa3	GC#957	Sa3; non-O1/O139 Environmental isolate Ca, USA	(Keymer *et al.*, 2007)
Sa7	GC#959	Sa7; non-O1/O139 Environmental isolate Ca, USA	(Keymer *et al.*, 2007)
So5	GC#960	So5; non-O1/O139 Environmental isolate Ca, USA	(Keymer *et al.*, 2007)
W7	GC#962	W7; non-O1/O139 Environmental isolate Ca, USA	(Keymer *et al.*, 2007)
E7	GC#963	E7; non-O1/O139 Environmental isolate Ca, USA	(Keymer *et al.*, 2007)
SP6	GC#964	SP6; non-O1/O139 Environmental isolate Ca, USA	(Keymer *et al.*, 2007)
W10G	GC#5537	W10G; non-O1/O139 Environmental isolate Ca, USA	(Keymer *et al.*, 2007)
Sa10G	GC#5539	Sa10G; non-O1/O139 Environmental isolate Ca, USA	(Keymer *et al.*, 2007)
TP	GC#999	TP; non-O1/O139 Environmental isolate Ca, USA	(Purdy *et al.*, 2005)
SIO	GC#1000	SIO; non-O1/O139 Environmental isolate Ca, USA	(Purdy *et al.*, 2005)
V52	GC#1510	V52; non-O1 (O37); Isolated in 1968, Sudan; Str^R	(Bik *et al.*, 1996; Nesper *et al.*, 2002)
DRC186-4	GC#2501	DRC186-4; non-O1 patient isolate from 2011 (isolated at the Institut National de Recherche Biomédicale; Democratic Republic of the Congo) Str^S, Amp^R	Blokesch lab collection, unpublished

DL4215	GC#3079	DL4215; non-O1 (O113) Environmental isolate 2008, Rio Grande, USA	(Unterweger *et al.*, 2014)
1587	GC#3081	1587; non-O1 (O12) Clinical isolate 1994, Peru	(Unterweger *et al.*, 2014)
DL4211	GC#3084	DL4211; non-O1 (O123) Environmental isolate 2008, Rio Grande, USA	(Unterweger *et al.*, 2014)
A1552-Tn*tfoX*, *pilA*rep[WT]	GC#5814	Tn*tfoX*, *pilA*rep[WT; A1552]	This work
A1552-Tn*tfoX*, *pilA*rep[Sa5Y]	GC#5815	Tn*tfoX*, *pilA*rep[353; Sa5Y]	This work
A1552-Tn*tfoX*, *pilA*rep[W6G]	GC#5746	Tn*tfoX*, *pilA*rep[354; W6G]	This work
A1552-Tn*tfoX*, *pilA*rep[SP7]	GC#5758	Tn*tfoX*, *pilA*rep[952; SP7]	This work
A1552-Tn*tfoX*, *pilA*rep[SL6]	GC#5750	Tn*tfoX*, *pilA*rep[953; SL6]	This work
A1552-Tn*tfoX*, *pilA*rep[L6]	GC#5747	Tn*tfoX*, *pilA*rep[956; L6]	This work
A1552-Tn*tfoX*, *pilA*rep[Sa3]	GC#5748	Tn*tfoX*, *pilA*rep[957; Sa3]	This work
A1552-Tn*tfoX*, *pilA*rep[Sa7]	GC#5749	Tn*tfoX*, *pilA*rep[959; Sa7]	This work
A1552-Tn*tfoX*, *pilA*rep[So5]	GC#5759	Tn*tfoX*, *pilA*rep[960; So5]	This work
A1552-Tn*tfoX*, *pilA*rep[SP6]	GC#5725	Tn*tfoX*, *pilA*rep[964; SP6]	This work
A1552-Tn*tfoX*, *pilA*rep[W10G]	GC#5751	Tn*tfoX*, *pilA*rep[5537; W10G]	This work
A1552-Tn*tfoX*, *pilA*rep[TP]	GC#5722	Tn*tfoX*, *pilA*rep[999; TP]	This work
A1552-Tn*tfoX*, *pilA*rep[SIO]	GC#5726	Tn*tfoX*, *pilA*rep[1000; SIO]	This work
A1552-Tn*tfoX*, *pilA*rep[V52]	GC#5816	Tn*tfoX*, *pilA*rep[1510; V52]	This work
A1552-Tn*tfoX*, *pilA*rep[DRC186-4]	GC#5727	Tn*tfoX*, *pilA*rep[2501; DRC186-4]	This work
A1552-Tn*tfoX*, *pilA*rep[DL4215]	GC#5723	Tn*tfoX*, *pilA*rep[3079; DL4215]	This work
A1552-Tn*tfoX*, *pilA*rep[1587]	GC#5724	Tn*tfoX*, *pilA*rep[3081; 1587]	This work
A1552-Tn*tfoX*, *pilA*rep[WT], Δ*pilT*	GC#5828	Tn*tfoX*, *pilA*rep[WT; A1552], Δ*pilT*::FRT	This work
A1552-Tn*tfoX*, *pilA*rep[Sa5Y], Δ*pilT*	GC#5829	Tn*tfoX*, *pilA*rep[353; Sa5Y], Δ*pilT*::FRT	This work
A1552-Tn*tfoX*, *pilA*rep[W6G], Δ*pilT*	GC#5752	Tn*tfoX*, *pilA*rep[354; W6G], Δ*pilT*::FRT	This work

A1552-Tn*tfoX*, *pilA*rep[SP7], Δ*pilT*	GC#5760	Tn*tfoX*, *pilA*rep[952; SP7], Δ*pilT*::FRT	This work
A1552-Tn*tfoX*, *pilA*rep[SL6], Δ*pilT*	GC#5756	Tn*tfoX*, *pilA*rep[953; SL6], Δ*pilT*::FRT	This work
A1552-Tn*tfoX*, *pilA*rep[L6], Δ*pilT*	GC#5753	Tn*tfoX*, *pilA*rep[956; L6], Δ*pilT*::FRT	This work
A1552-Tn*tfoX*, *pilA*rep[Sa3], Δ*pilT*	GC#5754	Tn*tfoX*, *pilA*rep[957; Sa3], Δ*pilT*::FRT	This work
A1552-Tn*tfoX*, *pilA*rep[Sa7], Δ*pilT*	GC#5755	Tn*tfoX*, *pilA*rep[959; Sa7], Δ*pilT*::FRT	This work
A1552-Tn*tfoX*, *pilA*rep[So5], Δ*pilT*	GC#5761	Tn*tfoX*, *pilA*rep[960; So5], Δ*pilT*::FRT	This work
A1552-Tn*tfoX*, *pilA*rep[SP6], Δ*pilT*	GC#5736	Tn*tfoX*, *pilA*rep[964; SP6], Δ*pilT*::FRT	This work
A1552-Tn*tfoX*, *pilA*rep[W10G], Δ*pilT*	GC#5757	Tn*tfoX*, *pilA*rep[5537; W10G], Δ*pilT*::FRT	This work
A1552-Tn*tfoX*, *pilA*rep[TP], Δ*pilT*	GC#5733	Tn*tfoX*, *pilA*rep[999; TP], Δ*pilT*::FRT	This work
A1552-Tn*tfoX*, *pilA*rep[SIO], Δ*pilT*	GC#5737	Tn*tfoX*, *pilA*rep[1000; SIO], Δ*pilT*::FRT	This work
A1552-Tn*tfoX*, *pilA*rep[V52], Δ*pilT*	GC#5830	Tn*tfoX*, *pilA*rep[1510; V52], Δ*pilT*::FRT	This work
A1552-Tn*tfoX*, *pilA*rep[DRC186-4], Δ*pilT*	GC#5738	Tn*tfoX*, *pilA*rep[2501; DRC186-4], Δ*pilT*::FRT	This work
A1552-Tn*tfoX*, *pilA*rep[DL4215], Δ*pilT*	GC#5734	Tn*tfoX*, *pilA*rep[3079; DL4215], Δ*pilT*::FRT	This work
A1552-Tn*tfoX*, *pilA*rep[1587], Δ*pilT*	GC#5735	Tn*tfoX*, *pilA*rep[3081; 1587], Δ*pilT*::FRT	This work
A1552-Tn*tfoX*, *pilA*rep[WT PilA S67C]	GC#5745	Tn*tfoX*, *pilA*rep[WT A1552 PilA S67C]	This work
A1552-Tn*tfoX*, *pilA*rep[WT PilA S67C], Δ*pilT*	GC#5739	Tn*tfoX*, *pilA*rep[WT A1552 PilA S67C], Δ*pilT*::FRT	This work
A1552-Tn*tfoX*, *pilA*rep[Sa5Y PilA S67C]	GC#5728	Tn*tfoX*, *pilA*rep[Sa5Y PilA S67C]	This work

A1552-Tn*tfoX*, *pilA*rep[Sa5Y PilA S67C], Δ*pilT*	GC#5740	Tn*tfoX*, *pilA*rep[Sa5Y PilA S67C], Δ*pilT*::FRT	This work
A1552-Tn*tfoX*, *pilA*rep[V52 PilA N67C]	GC#5729	Tn*tfoX*, *pilA*rep[V52 PilA N67C]	This work
A1552-Tn*tfoX*, *pilA*rep[V52 PilA N67C], Δ*pilT*	GC#5741	Tn*tfoX*, *pilA*rep[V52 PilA N67C], Δ*pilT*::FRT	This work
A1552-Tn*tfoX*, *pilA*rep[V52 Δtail]	GC#5732	Tn*tfoX*, *pilA*rep[V52Δtail]	This work
A1552-Tn*tfoX*, *pilA*rep[V52 Δtail], Δ*pilT*	GC#5744	Tn*tfoX*, *pilA*rep[V52Δtail], Δ*pilT*::FRT	This work
A1552-Tn*tfoX*, *pilA*rep[WT+tail]	GC#6093	Tn*tfoX*, *pilA*rep[A1552 PilA-tail]	This work
A1552-Tn*tfoX*, *pilA*rep[WT+tail], Δ*pilT*	GC#6094	Tn*tfoX*, *pilA*rep[A1552 PilA-tail], Δ*pilT*::FRT	This work
E. coli			
S17 λpir	GC#648	Tp^r Sm^r *recA thi pro hsdR-M+ RP4:2-Tc:Mu:* Km^r Tn*7* (λ*pir*)	(Simon *et al.*, 1983)
XL10 gold	GC#734	Tet^rΔ(*mcrA*)*183* Δ(*mcrCB-hsdSMR-mrr*)*173 endA1 supE44 thi-1 recA1 gyrA96 relA1 lac* Hte [F′ *proAB* $lacI^q$*ZΔM15* Tn*10* (Tet^r) Amy Cam^r].	Stratagene; Cat# 200315.
BTH101	GC#6221	F-, *cya-99*, *araD139, galE15, galK16, rpsL1* (Str^r), *hsdR2, mcrA1, mcrB1.*	Euromedex; EUB001
Plasmids			
pBR-FRT-Kan-FRT2	GC#3782	pBR322 derivative containing improved FRT-*aph*-FRT cassette, used as template for TransFLP; Amp^R, Kan^R	(Metzger *et al.*, 2016)
pBR-FLP	GC#1203	pBR322 derivative containing FLP+, λ cI857+, λ pR from pCP20 integrated into the *EcoRV* site of pBR322, used for FLP recombination; Amp^R	(De Souza Silva and Blokesch, 2010)
pFRT-aph-pheS*	GC#4591	pBR322 derivative containing improved FRT-*aph*-FRT cassette, as well as *pheS**[A294G/T251A], used as template for Trans2; Amp^R, Kan^R	(Van der Henst *et al.*, 2017)
pUX-BF13	GC#457	pUX-BF13 - oriR6K, helper plasmid with Tn7 transposition function; Amp^R	(Bao *et al.*, 1991)
pGP704-mTn*tfoX*	GC#1624	pGP704 with mini-Tn7 carrying *araC* and P_{BAD}-*tfoX*; Amp^R, $Gent^R$ (Tn*tfoX*)	(Lo Scrudato and Blokesch, 2012)
pGP704-mTn*cdpA*	GC#2944	pGP704 with mini-Tn7 carrying *araC* and P_{BAD}-*cdpA*; Amp^R, $Gent^R$ (Tn*cdpA*)	(Metzger *et al.*, 2016)
pGP704-mTn*vdcA*	GC#2943	pGP704 with mini-Tn7 carrying *araC* and P_{BAD}-*vdcA*; Amp^R, $Gent^R$ (Tn*vdcA*)	(Metzger *et al.*, 2016)
pGP704-mTn7	GC#5513	pGP704 with mini-Tn7 carrying *araC* and P_{BAD}; Amp^R, $Gent^R$	This work
pGP704-mTn*pilA*	GC#5702	pGP704 with mini-Tn7 carrying *araC* and P_{BAD}-*pilA*; Amp^R, $Gent^R$ (Tn*pilA*)	This work

pGP704-mTn*pilA*[S67C]	GC#5703	pGP704 with mini-Tn7 carrying *araC* and P_{BAD}-*pilA*[S67C]; Amp^R, $Gent^R$ (Tn*pilA*[S67C])	This work
pGP704-mTn*toxT*	GC#5934	pGP704 with mini-Tn7 carrying *araC* and P_{BAD}-*toxT*; Amp^R, $Gent^R$ (Tn*toxT*)	This work
pGP704-Sac28 (p28)	GC#649	pGP704-Sac28 suicide vector, *ori*R6K, *sacB*; Amp^R	(Meibom *et al.*, 2004)
p28-*pilA*	GC#1050	pGP704-Sac28-Δ*pilA*	(Meibom *et al.*, 2004)
p28-*pilB*	GC#1035	pGP704-Sac28-Δ*pilB*	(Meibom *et al.*, 2005)
p28-*pilQ*	GC#1034	pGP704-Sac28-Δ*pilQ*	(Meibom *et al.*, 2005)
p28-*mshA*	GC#1051	pGP704-Sac28-Δ*mshA*	(Meibom *et al.*, 2004)
p28-ΔVC0393	GC#1132	pGP704-Sac28-Δ*VC0393* (Δ*pglL*)	This work
p28-Δ*gbpA*	GC#1005	pGP704-Sac28-Δ*gbpA*	(Meibom *et al.*, 2004)
p28-PilA[S67C]	GC#6202	pGP704-Sac28-*pilA*[S67C]	This work
p28-PilA[T71C]	GC#6203	pGP704-Sac28-*pilA*[T71C]	This work
p28-PilA[T72C]	GC#6204	pGP704-Sac28-*pilA*[T72C]	This work
p28-PilA[T75C]	GC#6205	pGP704-Sac28-*pilA*[T75C]	This work
p28-PilA[T80C]	GC#6206	pGP704-Sac28-*pilA*[T80C]	This work
p28-PilA[T84C]	GC#6207	pGP704-Sac28-*pilA*[T84C]	This work
p28-*pilT*+	GC#6212	pGP704-Sac28-Ω*lacZ*::(P_{pilT}-*pilT*)	This work
p28-PilT[K136A]	GC#6209	pGP704-Sac28-*pilT*[K136A]	This work
p28-PilT[E204A]	GC#6198	pGP704-Sac28-*pilT*[E204A]	This work
p28-PilU[K134A]	GC#6210	pGP704-Sac28-*pilU*[K134A]	This work
p28-PilU[E202A]	GC#6211	pGP704-Sac28-*pilU*[E202A]	This work
p28-$hapR^{Rep}$	GC#5648	pGP704-Sac28-$hapR^{Rep}$ (repairs *hapR* to A1552 sequence)	This work
p28-Δ*pilT*	GC#5959	pGP704-Sac28-Δ*pilT*	This work
p28-PilT[A1552]	GC#5960	pGP704-Sac28-*pilT*[A1552]	This work
p28-PilT[MO10]	GC#5961	pGP704-Sac28-*pilT*[MO10]	This work
p28-*pilA*ex	GC#6208	pGP704-Sac28-*pilA*ex[A1552]	This work
p28-*pilA*rep[WT]	GC#6199	pGP704-Sac28-*pilA*rep[WT; A1552]	This work
p28-*pilA*rep[Sa5Y]	GC#6200	pGP704-Sac28-*pilA*rep[353; Sa5Y]	This work
p28-*pilA*rep[W6G]	GC#5664	pGP704-Sac28-*pilA*rep[354; W6G]	This work
p28-*pilA*rep[SP7]	GC#5665	pGP704-Sac28-*pilA*rep[952; SP7]	This work
p28-*pilA*rep[SL6]	GC#5673	pGP704-Sac28-*pilA*rep[953; SL6]	This work
p28-*pilA*rep[L6]	GC#5666	pGP704-Sac28-*pilA*rep[956; L6]	This work
p28-*pilA*rep[Sa3]	GC#5667	pGP704-Sac28-*pilA*rep[957; Sa3]	This work

p28-*pilA*rep[Sa7]	GC#5668	pGP704-Sac28-*pilA*rep[959; Sa7]	This work
p28-*pilA*rep[So5]	GC#5669	pGP704-Sac28-*pilA*rep[960; So5]	This work
p28-*pilA*rep[SP6]	GC#5674	pGP704-Sac28-*pilA*rep[964; SP6]	This work
p28-*pilA*rep[W10G]	GC#5677	pGP704-Sac28-*pilA*rep[5537; W10G]	This work
p28-*pilA*rep[TP]	GC#5670	pGP704-Sac28-*pilA*rep[999; TP]	This work
p28-*pilA*rep[SIO]	GC#5675	pGP704-Sac28-*pilA*rep[1000; SIO]	This work
p28-*pilA*rep[V52]	GC#6201	pGP704-Sac28-*pilA*rep[1510; V52]	This work
p28-*pilA*rep[DRC186-4]	GC#5676	pGP704-Sac28-*pilA*rep[2501; DRC186-4]	This work
p28-*pilA*rep[DL4215]	GC#5671	pGP704-Sac28-*pilA*rep[3079; DL4215]	This work
p28-*pilA*rep[1587]	GC#5672	pGP704-Sac28-*pilA*rep[3081; 1587]	This work
p28-*pilA*rep[WT PilA S67C]	GC#5678	pGP704-Sac28-*pilA*rep[WT A1552 PilA S67C]	This work
p28-*pilA*rep[Sa5Y PilA S67C]	GC#5679	pGP704-Sac28-*pilA*rep[Sa5Y PilA S67C]	This work
p28-*pilA*rep[V52 PilA N67C]	GC#5680	pGP704-Sac28-*pilA*rep[V52 PilA N67C]	This work
p28-*pilA*rep[V52Δtail]	GC#5683	pGP704-Sac28-*pilA*rep[V52Δtail]	This work
p28-*pilA*rep[WT+tail]	GC#6039	pGP704-Sac28-*pilA*rep[A1552 PilA-tail]	This work
pUT18	GC#6222	pUT18; BACTH C-terminal T18 fusions, Amp^R	Euromedex; EUP-18N
pUT18C	GC#6223	pUT18C; BACTH N-terminal T18 fusions, Amp^R	Euromedex; EUP-18C
pUT18C-zip	GC#6224	T18-leucine zipper from yeast GCN4; Amp^R	Euromedex; EUP-18Z
pKT25	GC#6225	pKT25; BACTH N-terminal T25 fusions, Kan^R	Euromedex; EUP-25C
pKNT25	GC#6226	pKNT25; BACTH C-terminal T25 fusions, Kan^R	Euromedex; EUP-25N
pKT25-zip	GC#6227	T25-leucine zipper from yeast GCN4; Kan^R	Euromedex; EUP-25Z
pUT18-*pilT*	GC#6213	pUT18-*pilT*; (PilT-T18) Amp^R	This work
pUT18C-*pilT*	GC#6214	pUT18C-*pilT*; (T18-PilT) Amp^R	This work
pKT25-*pilT*	GC#6215	pKT25-*pilT*; (T25-PilT) Kan^R	This work
pKNT25-*pilT*	GC#6216	pKNT25-*pilT*; (PilT-T25) Kan^R	This work

pUT18-*pilU*	GC#6217	pUT18-*pilU*; (PilU-T18) Amp^R	This work
pUT18C-*pilU*	GC#6218	pUT18C-*pilU*; (T18-PilU) Amp^R	This work
pKT25-*pilU*	GC#6219	pKT25-*pilU*; (T25-PilU) Kan^R	This work
pKNT25-*pilU*	GC#6220	pKNT25-*pilU*; (PilU-T25) Kan^R	This work

[1] Unless stated otherwise, all *V. cholerae* strains are Rif^R derivatives of A1552 (GC#1).

[2] Strains containing mini-Tn7 insertions (*e.g.* Tn*tfoX*) are $Gent^R$.

[3] Derivatives of C6709, P27459, E7946, DRC-193A, N16961, MO10 and ATCC25872 are Str^R.

[4] FRT; flippase recognition target (FRT) scar left behind by TransFLP method.

Supplementary references

Aldova, E., Laznickova, K., Stepankova, E., and Lietava, J. (1968). Isolation of nonagglutinable vibrios from an enteritis outbreak in Czechoslovakia. J Infect Dis *118*, 25-31.

Bao, Y., Lies, D.P., Fu, H., and Roberts, G.P. (1991). An improved Tn7-based system for the single-copy insertion of cloned genes into chromosomes of gram-negative bacteria. Gene *109*, 167-168.

Bik, E.M., Gouw, R.D., and Mooi, F.R. (1996). DNA fingerprinting of *Vibrio cholerae* strains with a novel insertion sequence element: a tool to identify epidemic strains. J Clin Microbiol *34*, 1453-1461.

Blokesch, M. (2012). TransFLP--a method to genetically modify *Vibrio cholerae* based on natural transformation and FLP-recombination. J Vis Exp.

Borgeaud, S., Metzger, L.C., Scrignari, T., and Blokesch, M. (2015). The type VI secretion system of *Vibrio cholerae* fosters horizontal gene transfer. Science *347*, 63-67.

De Souza Silva, O., and Blokesch, M. (2010). Genetic manipulation of *Vibrio cholerae* by combining natural transformation with FLP recombination. Plasmid *64*, 186-195.

Felsenfeld, O., Stegherr-Barrios, A., Aldova, E., Holmes, J., and Parrott, M.W. (1970). In vitro and in vivo studies of streptomycin-dependent cholera vibrios. Appl Microbiol *19*, 463-469.

Heidelberg, J.F., Eisen, J.A., Nelson, W.C., Clayton, R.A., Gwinn, M.L., Dodson, R.J., Haft, D.H., Hickey, E.K., Peterson, J.D., Umayam, L.*, et al.* (2000). DNA sequence of both chromosomes of the cholera pathogen *Vibrio cholerae*. Nature *406*, 477-483.

Keymer, D.P., Miller, M.C., Schoolnik, G.K., and Boehm, A.B. (2007). Genomic and phenotypic diversity of coastal *Vibrio cholerae* strains is linked to environmental factors. Appl Environ Microbiol *73*, 3705-3714.

Lazinski, D.W., and Camilli, A. (2013). Homopolymer tail-mediated ligation PCR: a streamlined and highly efficient method for DNA cloning and library construction. Biotechniques *54*, 25-34.

Lo Scrudato, M., and Blokesch, M. (2012). The regulatory network of natural competence and transformation of *Vibrio cholerae*. PLoS Genet *8*, e1002778.

Marvig, R.L., and Blokesch, M. (2010). Natural transformation of *Vibrio cholerae* as a tool - optimizing the procedure. BMC Microbiol *10*, 155.

Meibom, K.L., Blokesch, M., Dolganov, N.A., Wu, C.Y., and Schoolnik, G.K. (2005). Chitin induces natural competence in *Vibrio cholerae*. Science *310*, 1824-1827.

Meibom, K.L., Li, X.B., Nielsen, A.T., Wu, C.Y., Roseman, S., and Schoolnik, G.K. (2004). The *Vibrio cholerae* chitin utilization program. Proc Natl Acad Sci U S A *101*, 2524-2529.

Metzger, L.C., Stutzmann, S., Scrignari, T., Van der Henst, C., Matthey, N., and Blokesch, M. (2016). Independent Regulation of Type VI Secretion in *Vibrio cholerae* by TfoX and TfoY. Cell Rep *15*, 951-958.

Miller, V.L., DiRita, V.J., and Mekalanos, J.J. (1989). Identification of *toxS*, a regulatory gene whose product enhances *toxR*-mediated activation of the cholera toxin promoter. J Bacteriol *171*, 1288-1293.

Nesper, J., Kraiss, A., Schild, S., Blass, J., Klose, K.E., Bockemuhl, J., and Reidl, J. (2002). Comparative and genetic analyses of the putative *Vibrio cholerae* lipopolysaccharide core oligosaccharide biosynthesis (*wav*) gene cluster. Infect Immun *70*, 2419-2433.

Purdy, A., Rohwer, F., Edwards, R., Azam, F., and Bartlett, D.H. (2005). A glimpse into the expanded genome content of *Vibrio cholerae* through identification of genes present in environmental strains. J Bacteriol *187*, 2992-3001.

Seitz, P., and Blokesch, M. (2013). DNA-uptake machinery of naturally competent *Vibrio cholerae*. Proc Natl Acad Sci U S A *110*, 17987-17992.

Seitz, P., Pezeshgi Modarres, H., Borgeaud, S., Bulushev, R.D., Steinbock, L.J., Radenovic, A., Dal Peraro, M., and Blokesch, M. (2014). ComEA is essential for the transfer of external DNA into the periplasm in naturally transformable *Vibrio cholerae* cells. PLoS Genet *10*, e1004066.

Simon, R., Priefer, U., and Pühler, A. (1983). A Broad Host Range Mobilization System for In Vivo Genetic Engineering: Transposon Mutagenesis in Gram Negative Bacteria. Bio/Technology *1*, 784.

Unterweger, D., Miyata, S.T., Bachmann, V., Brooks, T.M., Mullins, T., Kostiuk, B., Provenzano, D., and Pukatzki, S. (2014). The *Vibrio cholerae* type VI secretion system employs diverse effector modules for intraspecific competition. Nat Commun *5*, 3549.

Van der Henst, C., Clerc, S., Stutzmann, S., Stoudmann, C., Scrignari, T., Maclachlan, C., Knott, G., and Blokesch, M. (2017). Molecular insights into *Vibrio cholerae*'s intra-amoebal host-pathogen interactions. bioRxiv.

Van der Henst, C., Scrignari, T., Maclachlan, C., and Blokesch, M. (2016). An intracellular replication niche for *Vibrio cholerae* in the amoeba *Acanthamoeba castellanii*. ISME J *10*, 897-910.

Wachsmuth, I.K., Evins, G.M., Fields, P.I., Olsvik, O., Popovic, T., Bopp, C.A., Wells, J.G., Carrillo, C., and Blake, P.A. (1993). The molecular epidemiology of cholera in Latin America. J Infect Dis *167*, 621-626.

Waldor, M.K., and Mekalanos, J.J. (1994a). Emergence of a new cholera pandemic: molecular analysis of virulence determinants in *Vibrio cholerae* O139 and development of a live vaccine prototype. J Infect Dis *170*, 278-283.

Waldor, M.K., and Mekalanos, J.J. (1994b). ToxR regulates virulence gene expression in non-O1 strains of *Vibrio cholerae* that cause epidemic cholera. Infect Immun *62*, 72-78.

Yildiz, F.H., and Schoolnik, G.K. (1998). Role of *rpoS* in stress survival and virulence of *Vibrio cholerae*. J Bacteriol *180*, 773-784.

Figure S1

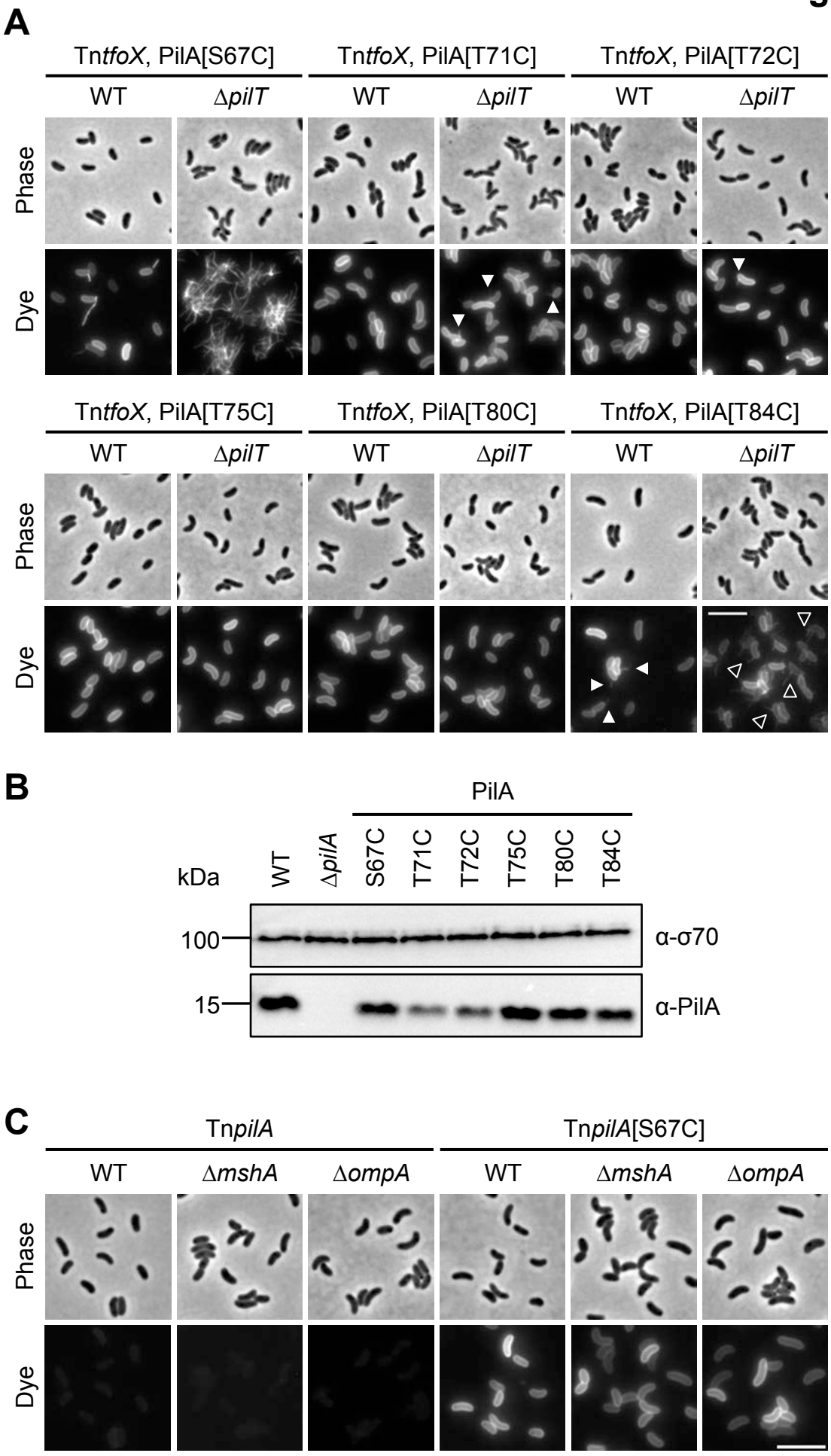
A
TntfoX, PilA[S67C]
TntfoX, PilA[T71C]
TntfoX, PilA[T72C]
WT
ΔpilT
Phase
Dye
TntfoX, PilA[T75C]
TntfoX, PilA[T80C]
TntfoX, PilA[T84C]
B
PilA
kDa
WT
ΔpilA
S67C
T71C
T72C
T75C
T80C
T84C
100
15
α-σ70
α-PilA
C
TnpilA
TnpilA[S67C]
ΔmshA
ΔompA

Figure S1. Controls for PilA cysteine labelling strategy, related to Figure 1.

(**A**) Cells producing PilA[S67C], [T71C], [T72C], [T75C], [T80C] and [T84C] in WT (A1552-Tn*tfoX*) and Δ*pilT* (A1552-Tn*tfoX*, Δ*pilT*) backgrounds, as indicated, were stained with AF-488-Mal. Closed arrowheads indicate strains producing only occasional pili. Open arrowheads indicate multiple weakly stained pili observed in Δ*pilT* cells producing PilA[T84C]. Scale bar = 5 µm.

(**B**) Western blot of PilA levels in cells producing WT PilA or the PilA cysteine variants. Sample loading was verified using σ70 levels and the specificity of the anti-PilA antibody verified using a Δ*pilA* strain as a negative control.

(**C**) Cells producing either inducible PilA (Tn*pilA*) or PilA[S67C] (Tn*pilA*[S67C]) independently of the machinery required for pilus assembly were stained with AF-488-Mal in a WT, Δ*mshA* and Δ*ompA* background, as indicated. Bar = 5 µm.

Figure S2

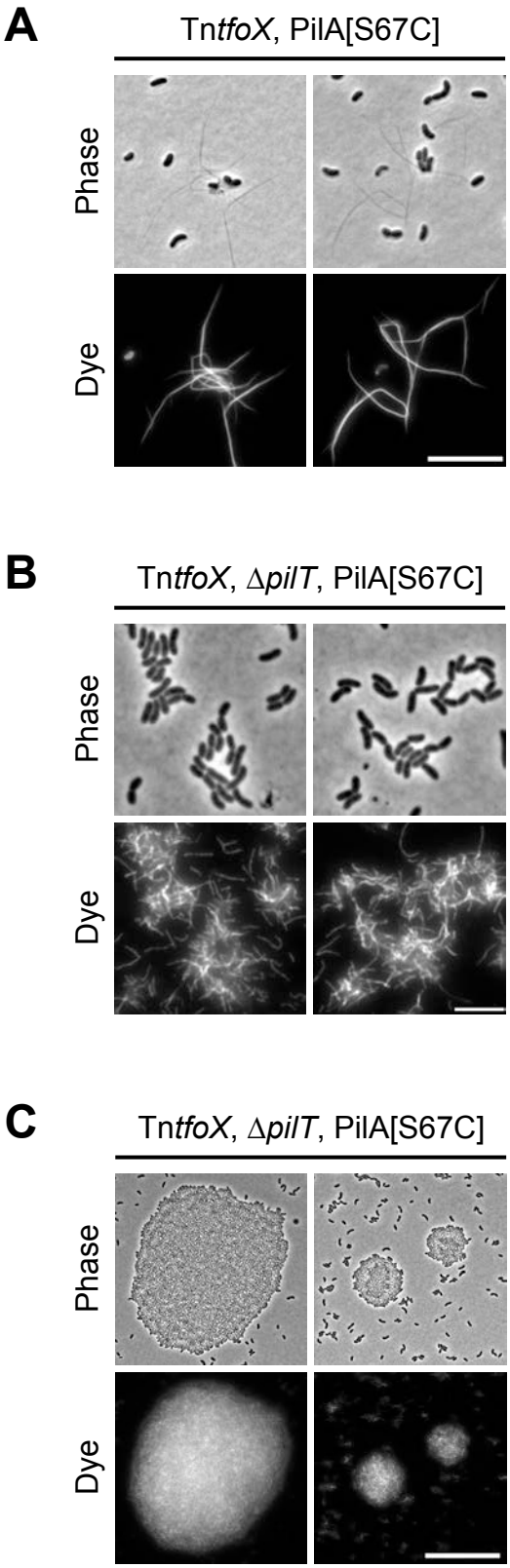
A
Tn*tfoX*, PilA[S67C]
Phase
Dye
B
Tn*tfoX*, Δ*pilT*, PilA[S67C]
Phase
Dye
C
Tn*tfoX*, Δ*pilT*, PilA[S67C]
Phase
Dye

Figure S2. Pili self-interact to form large structures, related to Figure 1.

(**A**) Examples of large structures formed by sheared pili in samples of cells producing PilA[S67C] (A1552-Tn*tfoX*, PilA[S67C]) and stained with AF-488-Mal. Bar = 10 µm.

(**B-C**) Retraction deficient cells producing PilA[S67C] (A1552-Tn*tfoX*, PilA[S67C], Δ*pilT*) were stained with AF-488-Mal. (**B**) Examples of dense 'mesh-like' networks of pili and small clusters formed by hyperpiliated cells. Bar = 5 µm. (**C**) Examples of pilus staining in large aggregates of tightly associated cells. Bar = 25 µm.

Figure S3

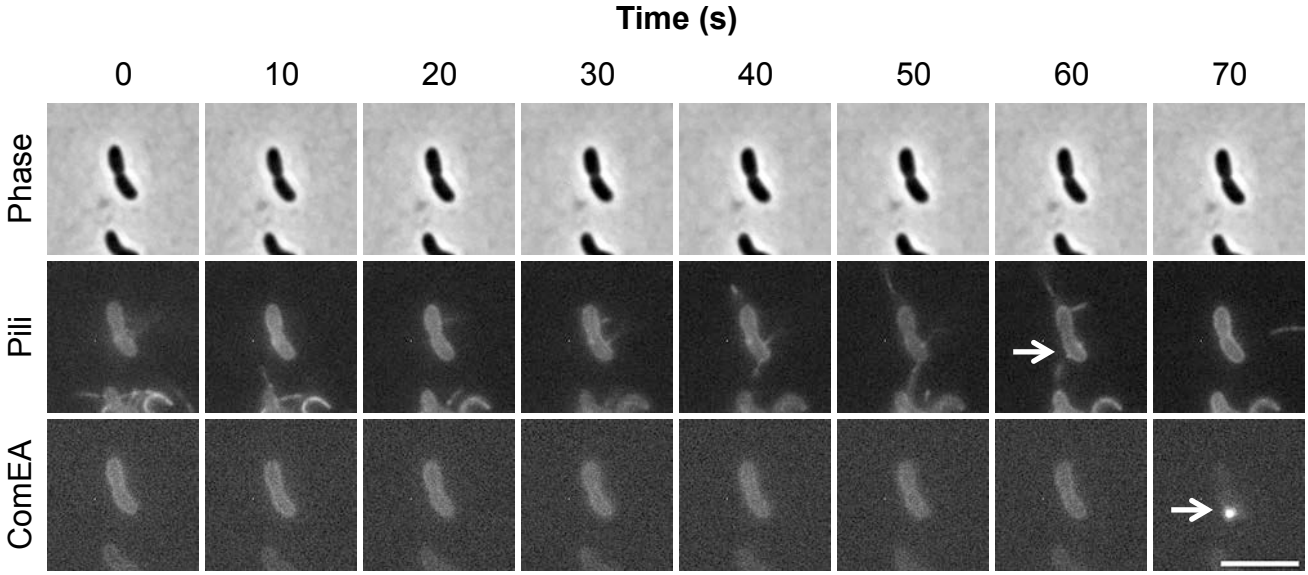

Figure S3. Pilus retraction followed by DNA uptake, related to Figure 1.

Cells producing PilA[S67C] and ComEA-mCherry (A1552-Tn*tfoX*, PilA[S67C], *comEA-mCherry*) were stained with AF-488-Mal, mixed with genomic DNA (20 µg/mL final) and imaged by time-lapse microscopy at 10s intervals. Top panels shows phase-contrast, middle panels show labelled pili and bottom panels show ComEA-mCherry localisation. The switch of ComEA from a peripheral localisation to a focus represents a DNA-uptake event. A pair of arrows indicates the spatial co-localisation between the pilus retraction event at T=60s and the DNA-uptake event at T=70s. Time (s), as indicated. Bar = 5 µm.

Figure S4

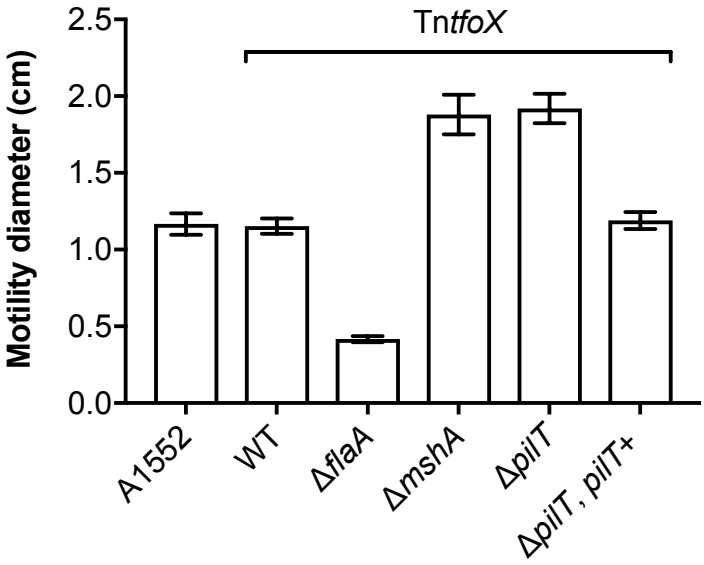
Tn*tfoX*
Motility diameter (cm)
2.5
2.0
1.5
1.0
0.5
0.0
A1552
WT
Δ*flaA*
Δ*mshA*
Δ*pilT*
Δ*pilT*, *pilT*+

Figure S4. Complementation of Δ*pilT* abolishes enhanced motility, related to Figure 2. Surface motility was determined on soft LB agar plates. The swarming diameter (cm) is the mean of three independent biological repeats (±S.D.). A flagellin-deficient (Δ*flaA*) non-motile strain was used as a negative control.

Figure S5

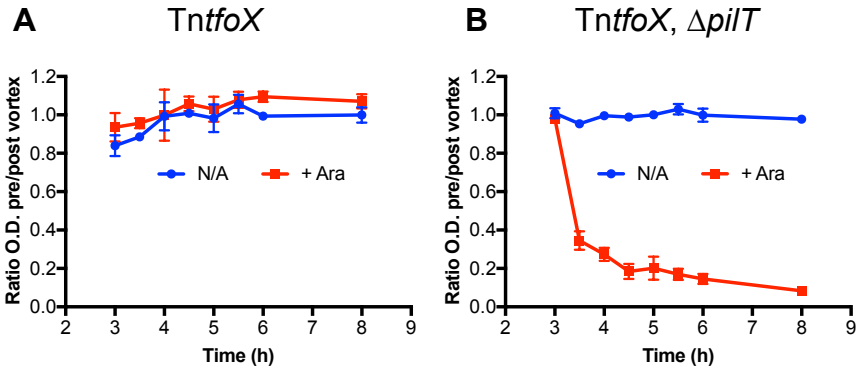
A
TntfoX
B
TntfoX, ΔpilT
Ratio O.D. pre/post vortex
1.2
1.0
0.8
0.6
0.4
0.2
0.0
N/A
+ Ara
2
3
4
5
6
7
8
9
Time (h)

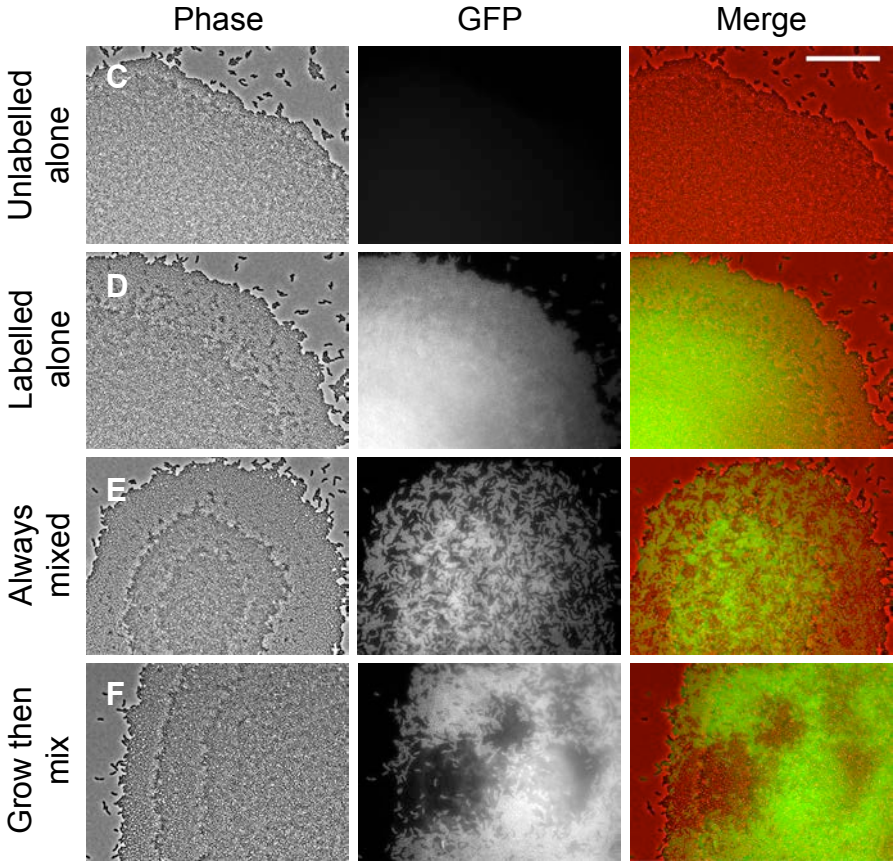
Phase
GFP
Merge
Unlabelled alone
Labelled alone
Always mixed
Grow then mix
C
D
E
F

Figure S5. Aggregation occurs rapidly by accretion, related to Figure 2.

(**A**-**B**) Aggregation of cultures of the (**A**) WT (A1552-Tn*tfoX*) and (**B**) Δ*pilT* (A1552-Tn*tfoX*, Δ*pilT*) was determined at 30 min intervals in the absence (N/A; no addition) and presence (+Ara) of *tfoX* induction, as indicated. Aggregation is shown as the ratio of the culture optical density (O.D. $_{600\ nm}$) before and after vortexing. Values are the mean of three repeats (±S.D.).

(**C**-**F**) Cells of the non-fluorescent (**C**) Δ*pilT* (A1552-Tn*tfoX*, Δ*pilT*) and (**D**) fluorescent Δ*pilT* (A1552-Tn*tfoX*, Δ*pilT*, GFP+) producing GFP were grown separately, or (**E**) mixed 1:1 and grown together from the start or (**F**) grown separately for 3.5h before being mixed 1:1 and grown an additional 30 min. Cultures were grown in the presence of *tfoX* induction. Bar = 25 μm.

Figure S6

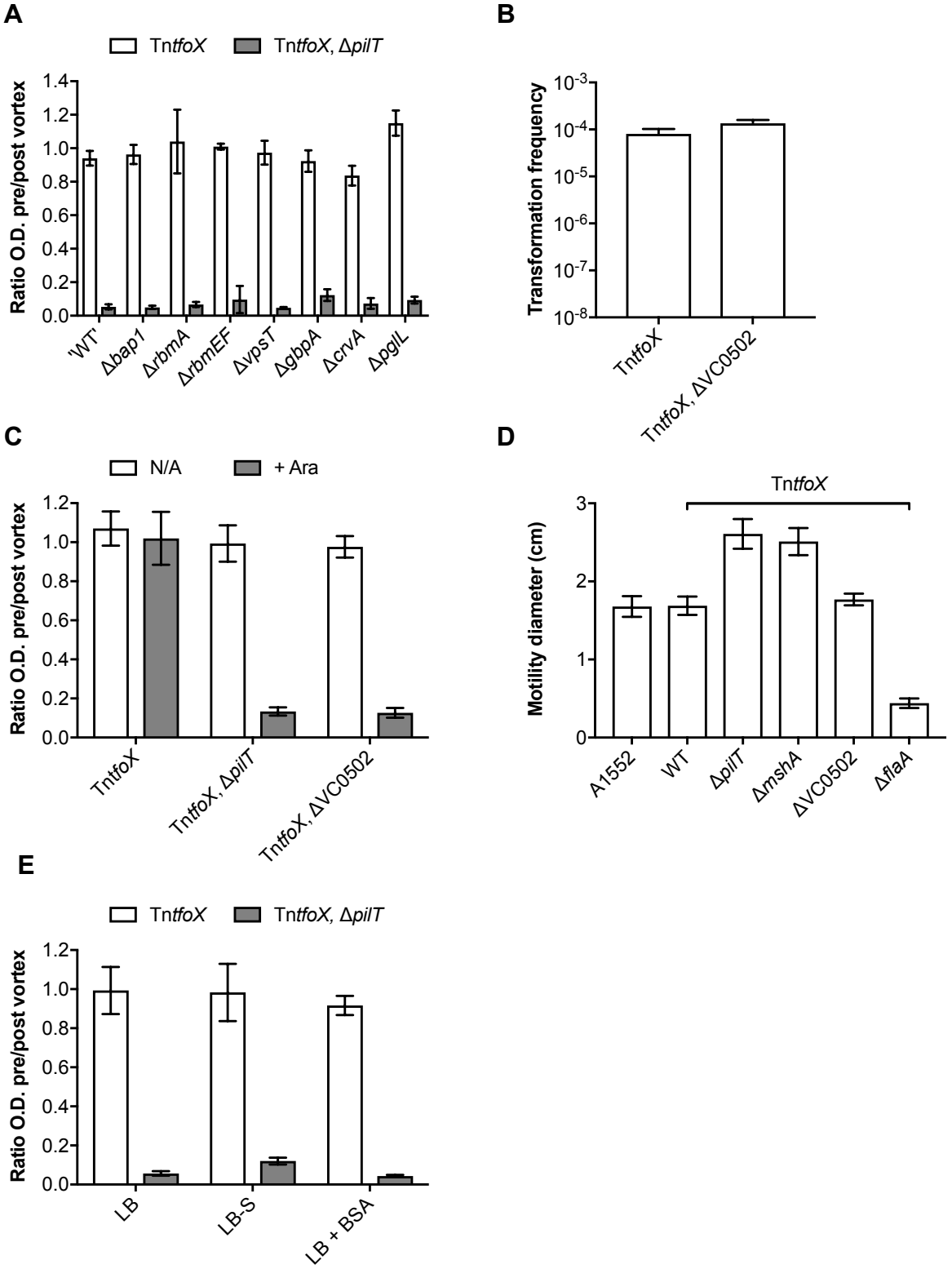
A
TntfoX
TntfoX, ΔpilT
Ratio O.D. pre/post vortex
1.4
1.2
1.0
0.8
0.6
0.4
0.2
0.0
'WT'
Δbap1
ΔrbmA
ΔrbmEF
ΔvpsT
ΔgbpA
ΔcrvA
ΔpglL
B
Transformation frequency
10-3
10-4
10-5
10-6
10-7
10-8
TntfoX
TntfoX, ΔVC0502
C
N/A
+ Ara
Ratio O.D. pre/post vortex
1.2
1.0
0.8
0.6
0.4
0.2
0.0
TntfoX
TntfoX, ΔpilT
TntfoX, ΔVC0502
D
TntfoX
Motility diameter (cm)
3
2
1
0
A1552
WT
ΔpilT
ΔmshA
ΔVC0502
ΔflaA
E
TntfoX
TntfoX, ΔpilT
Ratio O.D. pre/post vortex
1.2
1.0
0.8
0.6
0.4
0.2
0.0
LB
LB-S
LB + BSA

Figure S6. Potential regulators of aggregation, related to Figure 2.

(**A**) Aggregation of cells in WT (A1552-Tn*tfoX*) and Δ*pilT* (A1552-Tn*tfoX*, Δ*pilT*) backgrounds, as indicated, was examined in cells co-deleted for various genes involved in biofilm formation (*bap1*, *rbmA*, *rbmEF*, *vpsT*), adhesion (*gbpA*), cell shape (*crvA*) and a putatative O-linked glycosylase (*VC0393; pglL*). Aggregation is shown as the ratio of the culture optical density (O.D. $_{600\,nm}$) before and after vortexing. Cultures were grown in the presence of *tfoX* induction. Values are the mean of three repeats (±S.D.).

(**B**-**D**) The type IV pilin VC0502 encoded on the *Vibrio* seventh pandemic island II is not required for natural transformation, aggregation or normal surface motility. (**B**) Chitin-independent transformation assay comparing WT (A1552-Tn*tfoX*) and Δ*VC0502* (A1552-Tn*tfoX*, Δ*VC0502*). Transformation frequencies are the mean of three repeats (±S.D). (**C**) Aggregation is shown as the ratio of the culture optical density (O.D. $_{600\,nm}$) before and after vortexing, in the absence (N/A; no addition) and presence (+Ara) of *tfoX* induction, as indicated. Values are the mean of three repeats (±S.D.). (**D**) Surface motility was determined on soft LB agar plates. The swarming diameter (cm) is the mean of three repeats (±S.D.). A flagellin-deficient (Δ*flaA*) non-motile strain was used as a negative control.

(**E**) Growth in media with high salt or Bovine Serum Albumin (BSA) does not affect aggregation. Cells of the WT (A1552-Tn*tfoX*) and Δ*pilT* (A1552-Tn*tfoX*, Δ*pilT*), were grown in LB and in either LB-S (high salt) or LB + BSA (1 mg/mL), as indicated. Aggregation is shown as the ratio of the culture optical density (O.D. $_{600\,nm}$) before and after vortexing. Values are the mean of three repeats (±S.D.).

Figure S7

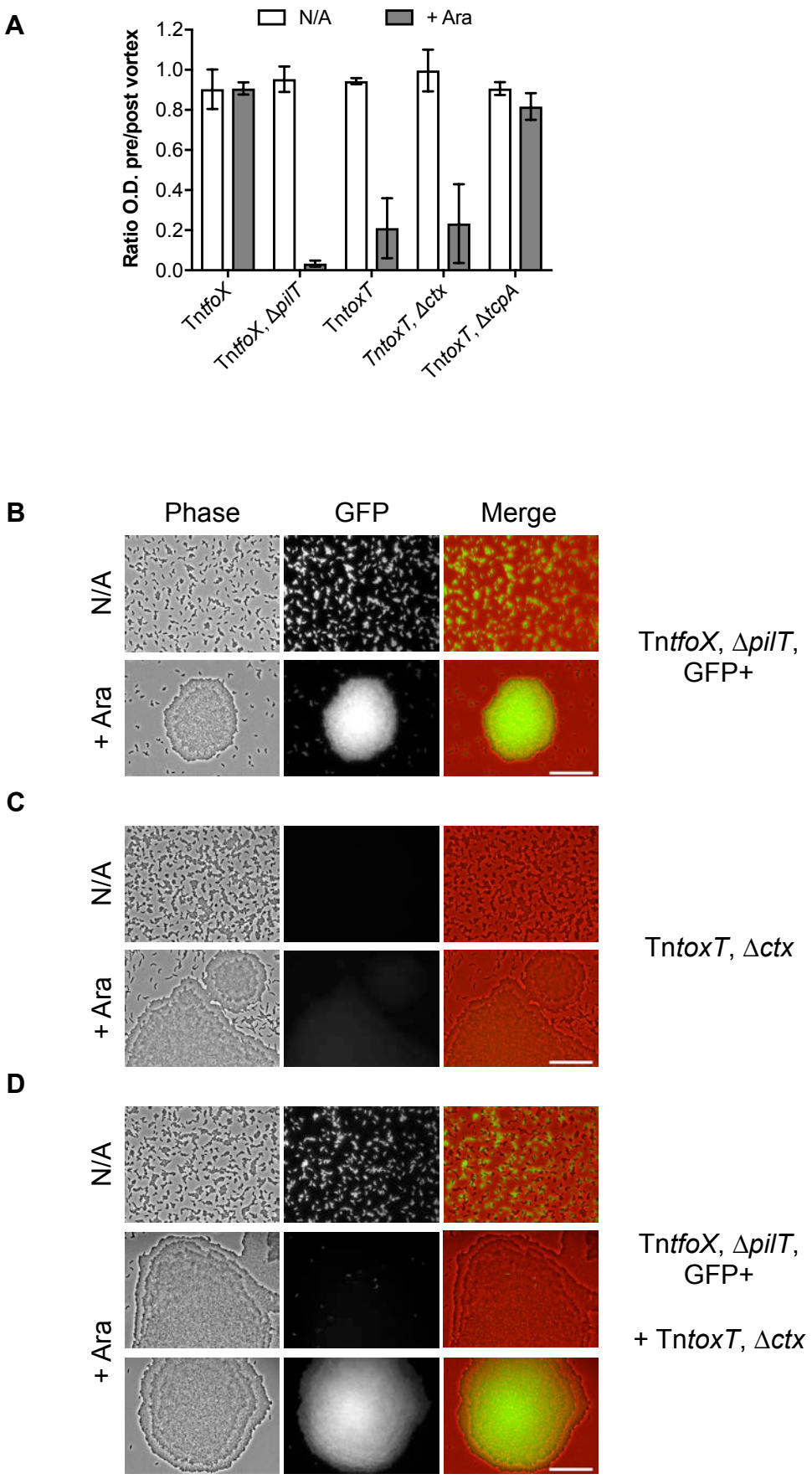
A
N/A
+ Ara
Ratio O.D. pre/post vortex
1.2
1.0
0.8
0.6
0.4
0.2
0.0
TntfoX
TntfoX, ΔpilT
TntoxT
TntoxT, Δctx
TntoxT, ΔtcpA
B
Phase
GFP
Merge
N/A
+ Ara
TntfoX, ΔpilT, GFP+
C
N/A
+ Ara
TntoxT, Δctx
D
N/A
+ Ara
TntfoX, ΔpilT, GFP+
+ TntoxT, Δctx

Figure S7. Comparison of aggregates formed by DNA-uptake pili and TCP, related to Figure 2.

(**A**) Aggregation assay comparing the sedimentation of competence inducible cells (Tn*tfoX*) to cells engineered to produce Toxin co-regulated pili (TCP) (Tn*toxT*). Aggregation is shown as the ratio of the culture optical density (O.D. $_{600\ nm}$) before and after vortexing, in the absence (N/A; no addition) and presence (+Ara) of induction, as indicated. Values are the mean of three repeats (±S.D.).

(**B**-**D**) Cells of the fluorescent (**B**) Δ*pilT* (A1552-Tn*tfoX*, Δ*pilT*, GFP+) producing GFP and (**C**) a non-fluorescent Tn*toxT* (A1552-Tn*toxT*, Δ*ctx*) were grown separately or (**D**) mixed 1:1 and co-cultured in the absence (N/A; no addition) and presence (+ Ara) of inducer, as indicated. Bars = 25 µm.

Figure S8

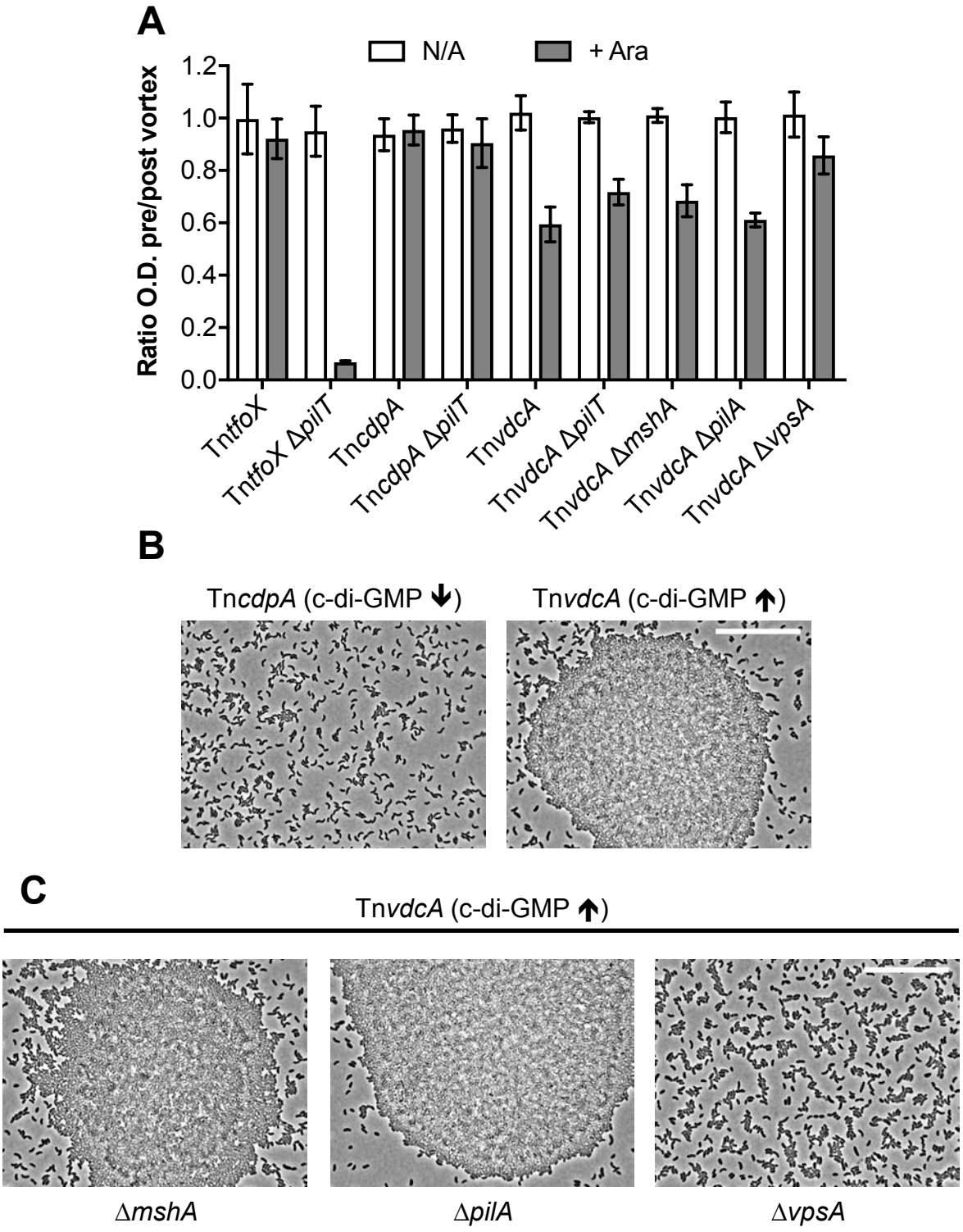
A
N/A
+ Ara
Ratio O.D. pre/post vortex
1.2
1.0
0.8
0.6
0.4
0.2
0.0
TntfoX
TntfoX ΔpilT
TncdpA
TncdpA ΔpilT
TnvdcA
TnvdcA ΔpilT
TnvdcA ΔmshA
TnvdcA ΔpilA
TnvdcA ΔvpsA
B
TncdpA (c-di-GMP ↓)
TnvdcA (c-di-GMP ↑)
C
TnvdcA (c-di-GMP ↑)
ΔmshA
ΔpilA
ΔvpsA

Figure S8. MSHA pili do not support aggregation, related to Figure 2.

(**A**) Aggregation assay comparing the sedimentation of competence inducible cells (Tn*tfoX*) to cells engineered to artificially lower (Tn*cdpA*) or increase (Tn*vdcA*) c-di-GMP levels. Aggregation is shown as the ratio of the culture optical density (O.D. $_{600\ nm}$) before and after vortexing, in the absence (N/A; no addition) and presence (+Ara) of induction, as indicated. Values are the mean of three repeats (±S.D.).

(**B**) Phase-contrast microscopy of cells of strains induced to lower (A1552-Tn*cdpA*) or increase (A1552-Tn*vdcA*) c-di-GMP levels, as indicated. Bar = 25 µm.

(**C**) Phase-contrast microscopy of cells of strains induced to increase c-di-GMP levels in Δ*mshA* (A1552-Tn*vdcA*, Δ*mshA*), Δ*pilA* (A1552-Tn*vdcA*, Δ*pilA*) and Δ*vpsA* (A1552-Tn*vdcA*, Δ*vpsA*) backgrounds, as indicated. Bar = 25 µm.

Figure S9

A

```
                                  Walker A
PilT_Vc          124 G L V L V T G P T G S G K S T T L A A M  143
PilU_Vc          122 G L V L V V G A T G S G K S T T M A A M  141
PilT_Vc[MO10]    124 G L V L V T G P T G S G K S T T L A A M  143
PilT_Pa          124 G L V L V T G P T G S G K S T T L A A M  143
PilT_Mx          125 G L I L V T G P T G S G K S T T L A S M  144
PilT_Ng          124 G M V L V T G P T G S G K S T T L A A M  143
PilT_Nm          124 G M V L V T G P T G S G K S T T L A A M  143
```

B

```
                                  Walker B
PilT_Vc          192 A L R E D P D V I L V G E L R D Q E T I  211
PilU_Vc          190 S L R Q A P D M I L I G E I R S R E T M  209
PilT_Vc[MO10]    192 A L R E D P D V I L V G E L S D Q E T I  211
PilT_Pa          192 A L R E D P D I I L V G E M R D L E T I  211
PilT_Mx          193 I L R Q D P D V V L V G E L R D L E T I  212
PilT_Ng          192 A L R E D P D V I L V G E M R D P E T I  211
PilT_Nm          192 A L R E D P D V I L V G E M R D P E T I  211
```

Figure S9. Alignment of PilT and PilU, related to Figure 3.

Alignment of the (**A**) Walker A and (**B**) atypical Walker B motifs of PilT and PilU from *V. cholerae* (Vc) strain A1552 against PilT from diverse species: Pa, *Pseudomonas aeruginosa*; Mx, *Myxococcus xanthus*; Ng, *Neisseria gonorrhoeae*; Nm, *Neisseria meningitidis*. Sequences were aligned using Muscle and figures prepared using Jalview. Identical residues are shaded in blue. Residues targeted for mutagenesis in the Walker A motif (*i.e.* PilT K134 and PilU K136) and atypical Walker B motif (*i.e.* PilT E204 and PilU E202) are boxed in red. The widely conserved arginine (*i.e.* PilT R206) that is substituted in the pandemic *V. cholerae* strain MO10 is highlighted in green.

Figure S10

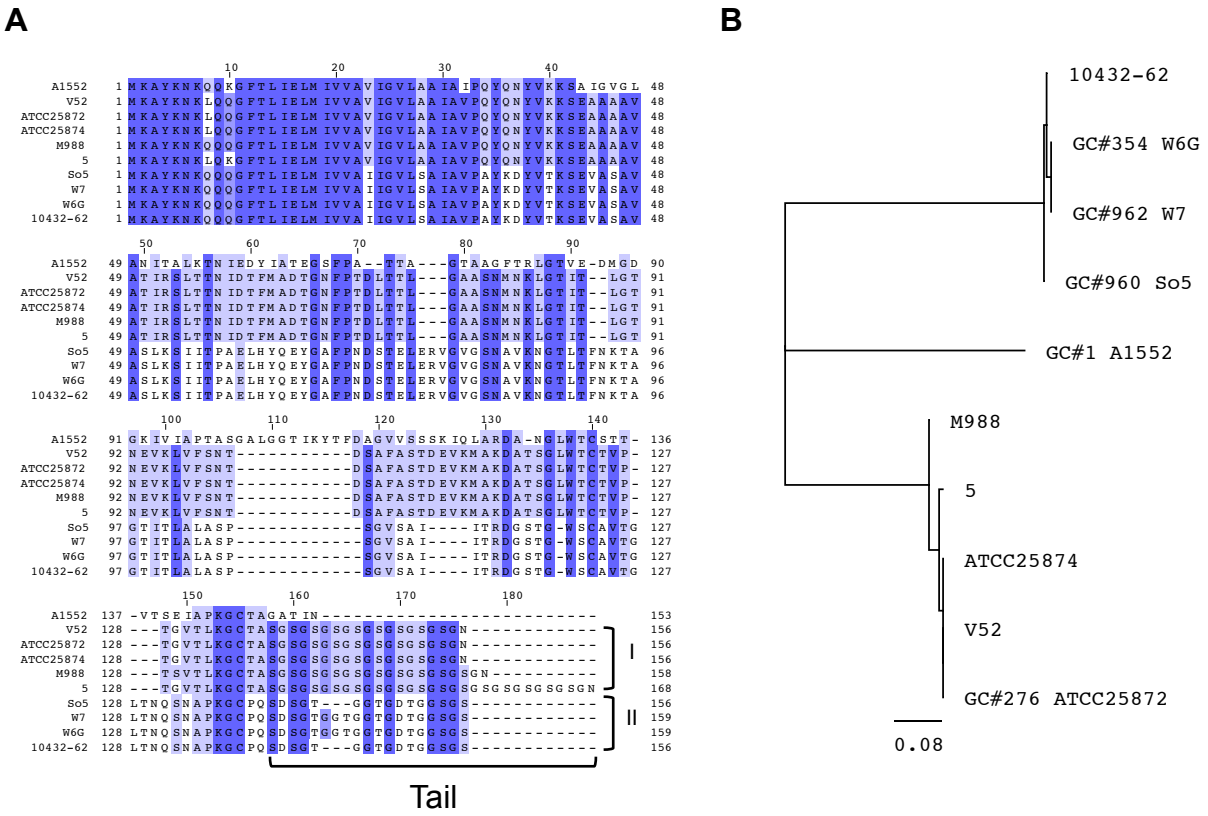
A
B
A1552
V52
ATCC25872
ATCC25874
M988
5
So5
W7
W6G
10432-62
I
II
Tail
10432-62
GC#354 W6G
GC#962 W7
GC#960 So5
GC#1 A1552
M988
5
ATCC25874
V52
GC#276 ATCC25872
0.08

Figure S10. Alignment of PilA with C-terminal extensions, related to Figure 5.

(**A**) Alignment of PilA from *V. cholerae* strain A1552 against PilA from strains V52, ATCC25872, ATCC25874, M988 and 5 (Group I), and So5, W7, W6G and 10432-62 (Group II) that contain a C-terminal extension. Sequences were aligned using Muscle and figures prepared using Jalview. Residues are shaded in graduations of blue according to sequence identity.

(**B**) Neighbour-joining tree of PilA sequences shown in (**A**).

Figure S11

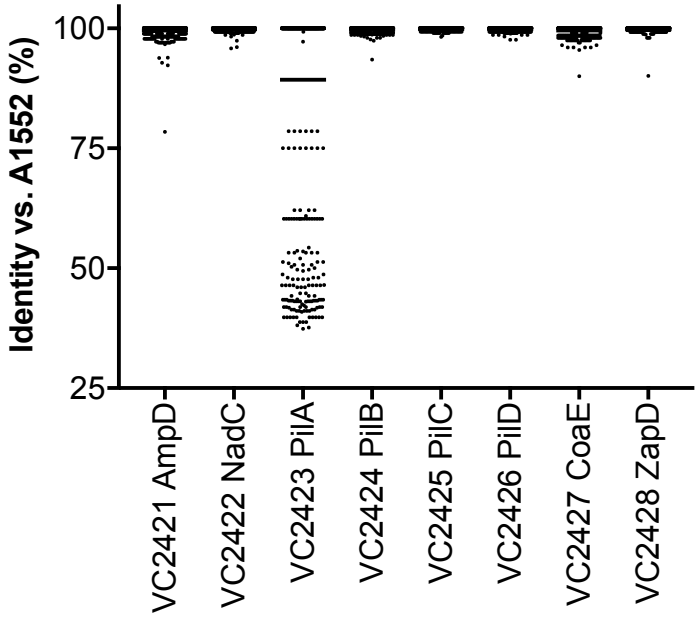
Identity vs. A1552 (%)
100
75
50
25
VC2421 AmpD
VC2422 NadC
VC2423 PilA
VC2424 PilB
VC2425 PilC
VC2426 PilD
VC2427 CoaE
VC2428 ZapD

Figure S11. PilA exhibits strain-to-strain variability, related to Figure 6.

Variability of the proteins encoded by the *pilABCD-coaE* locus and the surrounding genes. Protein sequences from A1552/N16961 were used as the query sequences in BLAST analyses against a custom database of 647 *V. cholerae* genomes.

Figure S12

A

N-terminal domain α-1

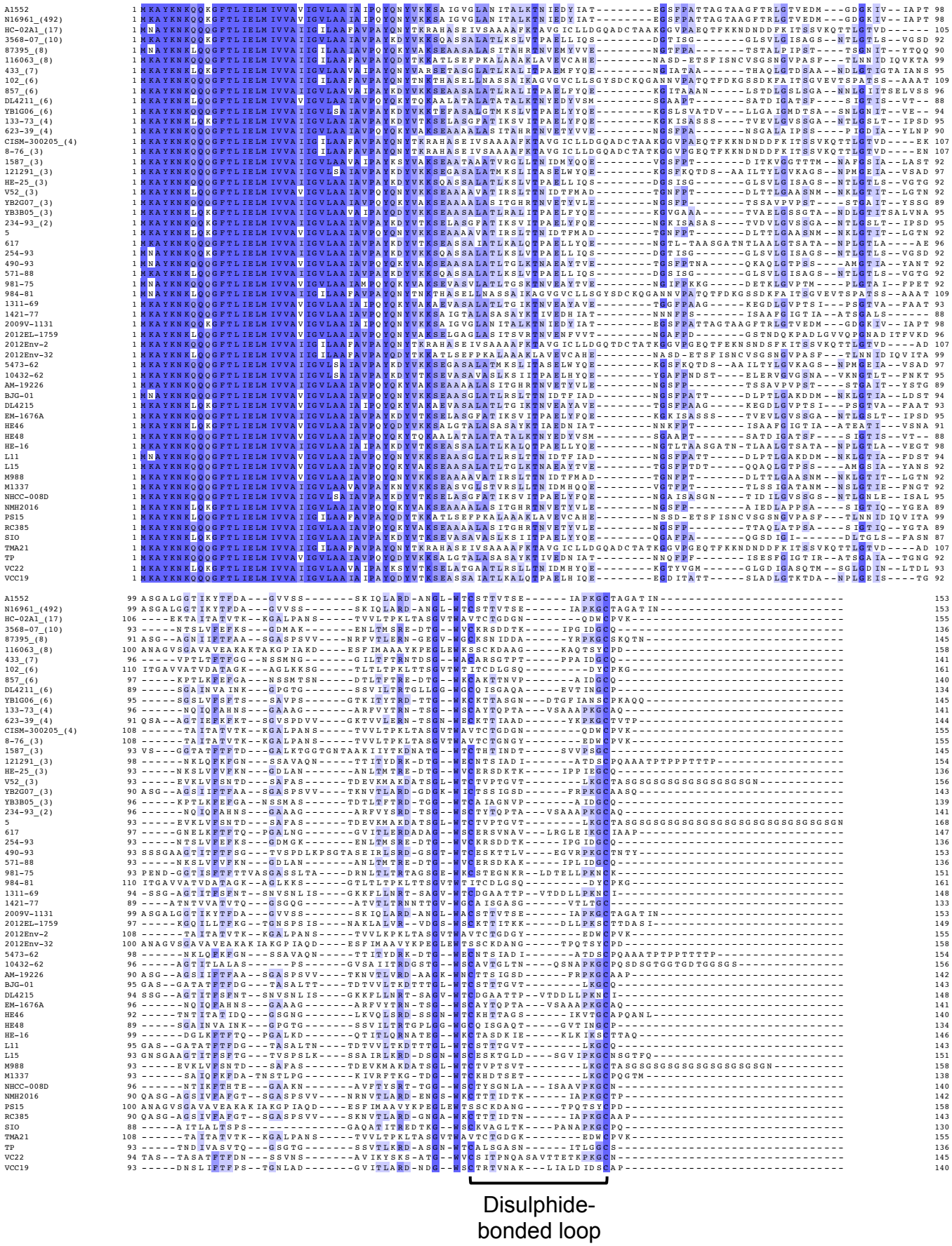

B

N-terminal domain α-1

```
                    10        20        30        40        50        60        70        80        90
A1552      1 MKAYKNKQQKGFTLIELMIVVAVIGVLAAIAIPQYQNYVKKSAIGVGLANITALKTNIEDYIATEG----SFPATTA-----GTAAGFTRLGTVEDMGDG 91
TP         1 MKAYKNKQQQGFTLIELMIVVAVIGVLAAIAVPQYQDYVKKSALGTALASASAYKTIVEDNIATNN----QFPFISESF---GIGTIRATSGAIA----- 88
DL4215     1 MKAYKNKLQKGFTLIELMIVVAVIGVLAAIAIPQYQKYVAKAEVASALATLTGIKTNVEAYAVETG----SFPAAGKEGD--LGVPTSIPSGTVA----- 89
1587       1 MKAYKNKQQQGFTLIELMIVVAIIGVLAAVAIPAYKSYVAKSEAATAAATVRGLLTNIDMYQQEVG----SFPTDITKV---GGTTTMNAFGSIA----- 88
SP6        1 MKAYKNKLQKGFTLIELMIVVAVIGVLAAIAVPQYQKYVAKSEAASALATLTGLKTNAEAYTVETG----SFPTDTQQA---QLGTPSSAMGTIA----- 88
DRC186-4   1 MNAYKNKQQQGFTLIELMIVVAIIGVLAAIAVPAYKDYVTKSEASSAIATLKALQTPAELLYQENG----NL-TVSNALAALGTSENANPLGKLE----- 90
L6         1 MKAYKNKQQQGFTLIELMIVVAIVGILAAFAVPAYQNYTMRAHASEMLSASSAMKTAVGICLISGN-------TNCSSGN---GGVPAKQDLGAFS----- 86
Sa3        1 MKAYKNKQQQGFTLIELMIVVAIIGVLAAIAVPQYQKYVAKSEAAAALASITGHRTNVETYVLENG----SFPTSS------AVPVPSTSTGAIT----- 85
SL6        1 MKAYKNKLQQGFTLIELMIVVAVIGVLAAIAVPQYQKYTQKAALATALATATALKTNYEDYVSMSG----AAPTSAT-----DIGATSFSIGTIS----- 86
SP7        1 MKAYKNKLQQGFTLIELMIVVAIIGILAAFAVPAYQNYTKKATLSEFPKALAAAKLAVEVCAHENASNETTFISNCVSGN--NGVPASFTLNNID----- 93
Sa5Y       1 MKAYKNKLQKGFTLIELMIVVAIIGVLAAIAVPQYQKYVAKSEAAAALASITGHRTNVETYVLENG----SFPAIE------DLAPPSASIGTIQ----- 85
V52        1 MKAYKNKLQQGFTLIELMIVVAVIGVLAAIAVPQYQNYVKKSEAAAAVATIRSLTTNIDTFMADTG----NFPTDLTTL---GAASNMNKLGTIT----- 88
SIO        1 MKAYKNKLQKGFTLIELMIVVAIIGVLAAIAVPAYKDYVTKSEVASAVASLKSIITPAELYYQEQG----AFPA--------QGSDIGIDLTGLS----- 83
W6G        1 MKAYKNKQQQGFTLIELMIVVAIIGVLSAIAVPAYKDYVTKSEVASAVASLKSIITPAELHYQEYG----AFPNDSTELERVGVGSNAVKNGTLT----- 91
Sa7        1 MKAYKNKQQQGFTLIELMIVVAIIGVLAAIAVPAYKDYVTKSELASGFATIKSVITPAELYFQENG----KISASASTVDVLGVSSGANTLGELT----- 91
W10G       1 MKAYKNKLQKGFTLIELMIVVAIIGVLAAVAIPAYQDYVKKSEAASALATLRALITPAELFYQEKG------VGAAATVAELGSSGTANDLGTIT----- 89
So5        1 MKAYKNKQQQGFTLIELMIVVAIIGVLSAIAVPAYKDYVTKSEVASAVASLKSIITPAELHYQEYG----AFPNDSTELERVGVGSNAVKNGTLT----- 91

                   110       120       130       140       150       160       170       180
A1552     92 KIVIAPTASGALGGTIKYTFDAGV-------VSSSKIQLARDA-NGL--WTC----STTVTSEIAPKGCTAGATIN---------------- 153
TP        89 --------TGNGTNDIVASVTQGS-------GTGSSVTLKRDA-SGN--WTC----ALSGASNITLGGCS--------------------- 136
DL4215    90 ---FAAT--SSGAGTITFSFNTSNV---SNLISGKKFLLNRTS-AGV--WTCDGAATTPVTDDLLPKNCI-------------------- 148
1587      89 ---LAST---VSGGTATFTFTDGALKTGGTGNTAAKIIYTKDNATG---WTCT---HTINDTSVVPSGC--------------------- 145
SP6       89 ---YANTGSSGAAGTITFTFSGTVS----PSLKSSAIRLKRDD-SGN--WSCES--NKDATSGIIPKGCNSGTF---------------- 150
DRC186-4  91 ---------VEGTDGLKFTFTQSGA------LKDQTITLQRSGTDG---WKCN---ASDKIEKLKIKSCTTAQ----------------- 142
L6        87 --IESLAGASGASPTVQASVDSGQT--KGKLVAGDTIKLTPTLNTAGVTWQVECV-KAANQQSSIDDWCPVK------------------ 153
Sa3       86 ---YSSG--ASGAGSIIFTFAASGA---SPSVVTKNVTLARDG-DGK--WIC----TSSIGSDFRPKGCAASQ----------------- 143
SL6       87 ----------VTSGAINVAINKGP-------GTGSSVILTRTGLLGG--WGCQ---ISGAQAEVTINGCP--------------------- 134
SP7       94 -IQVITAANAGVSGAVAVEAKAKIA--KGPIAQDESFIMAAVYKPEGLEWKSS---CKDAAGKAQTSYCPD------------------- 158
Sa5Y      86 ---YGEA-QASGAGSIVFAFGTSGA---SPSVVNRNVTLARDE-NGS--WKC----TTTIDTKIAPKGCTP-------------------- 142
V52       89 ----------LGTNEVKLVFSNTDS----AFASTDEVKMAKDATSGL--WTC------TVPTGVTLKGCTASGSGSGSGSGSGSGSGSGN 156
SIO       84 ----------FASNAITLALTS---------PSGAQATITREDTKG---WSCKV--AGLTKPANAPKGCPQ-------------------- 130
W6G       92 --------FNKTAGTITLALAS---------PSGVSAIITRDGSTG---WSCAV--TGLTNQSNAPKGCPQSDSGTGGTGGTGDTGGSGS 159
Sa7       92 ---------ITADNTIQFAHDAGA-------ALGAKFVYTRS--SGG--WSCTYT-QPSAVSAAAPKGCTP-------------------- 141
W10G      90 ------SALVNAKPTLKFEFGANSS-----MASTDTLTFTRD--TGG--WTC-----AIAGNVPAIDGCQ--------------------- 139
So5       92 --------FNKTAGTITLALAS---------PSGVSAIITRDGSTG---WSCAV--TGLTNQSNAPKGCPQSDS---GTGGTGDTGGSGS 156
```

Disulphide-bonded loop

Figure S12. Alignments of unique PilA and PilA used for *pilA*rep, related to Figure 6.

(**A**-**B**) PilA sequences were aligned using Muscle and figures prepared using Jalview. Residues are shaded in graduations of blue according to sequence identity. The regions corresponding to the N-terminal alpha helical domain and C-terminal disulphide-bonded loop are highlighted. (**A**) Alignment of A1552 PilA against the 56 unique PilA identified from the NCBI dataset. Strains are organised according to the sequence abundance, with the total number of identical sequences identified shown in brackets after the strain name. (**B**) Alignment of A1552 PilA against the 16 PilA tested in the *pilA*rep experiments. Strains are organised according into aggregation-capable (green) and aggregation-incapable (red) groups.

Figure S13

A

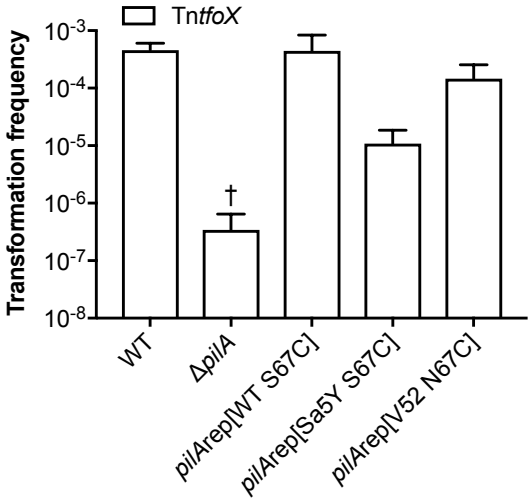

B

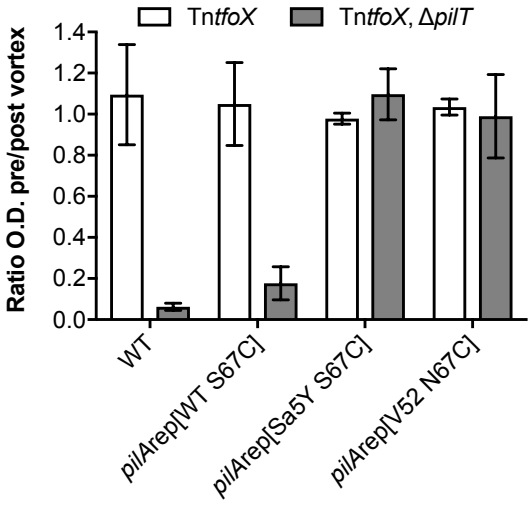

C

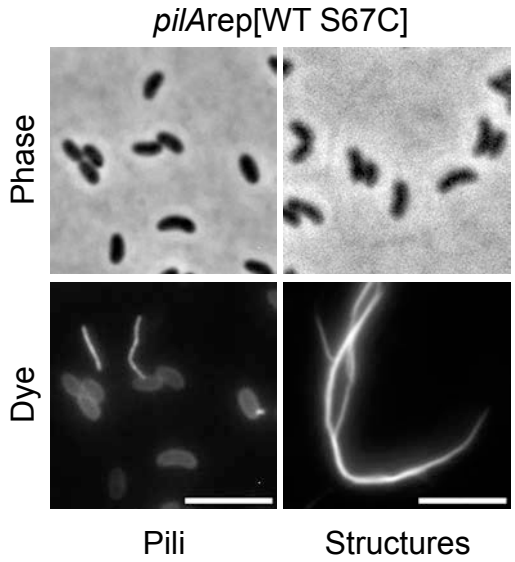

Figure S13. Functionality of *pilA*rep cysteine variants, related to Figure 7.

(**A**-**B**) Functionality of *pilA*rep cysteine variants assessed by transformation frequency and aggregation. Note that ATCC25872 and V52 PilA are identical. (**A**) Chitin-independent transformation assay. WT (A1552-Tn*tfoX*) and *pilA* (A1552-Tn*tfoX*, Δ*pilA*) served as positive and negative controls. Transformation frequencies are the mean of three repeats (±S.D). †, < d.l. in one repeat. (**B**) Aggregation was determined for the WT and each *pilA*rep strain in a *pilT*+ (A1552-Tn*tfoX*) and Δ*pilT* (A1552-Tn*tfoX*, Δ*pilT*) background, as indicated. Aggregation is shown as the ratio of the culture optical density (O.D. $_{600\ nm}$) before and after vortexing, in the presence of *tfoX* induction. Values are the mean of three repeats (±S.D.).

(**C**) Cells of A1552-Tn*tfoX*, *pilA*rep[WT PilA S67C] producing PilA[S67C] were stained with AF-488-Mal. The figure shows labelled pili as well as an example of the large structures that were often observed. Bar = 5 µm.

Supplemental files

File S1. Details of 647 V. *cholerae* genomes used for bioinformatics analyses.

File S2. DNA sequences of *pilA* and the deduced amino acid sequences of the proteins they encode from a collection of 22 environmental and clinical *V. cholerae* strains.

Supplemental movies

Movie S1. DNA uptake pili exhibit rapid assembly dynamics.

Movie of time-lapse series shown in Figure 1L. Cells producing PilA[S67C] (A1552-Tn*tfoX*, PilA[S67C]) were stained with AF-488-Mal and imaged by time-lapse microscopy at 10s intervals for 1 minute. Upper panel shows fluorescence, lower panel shows phase-contrast. The movie is displayed at 1 frame per second. Scale bar (5 µm) and time (min:sec), as indicated.

Movie S2. Additional examples of dynamic DNA uptake pili.

Cells producing PilA[S67C] (A1552-Tn*tfoX*, PilA[S67C]) were stained with AF-488-Mal and imaged by time-lapse microscopy at 10s intervals for 1 minute. Left-hand panels show phase-contrast, right-hand panels show fluorescence. The movie is displayed at 1 frame per second and is a composite of three separate examples. Scale bar (5 µm) and time (min:sec), as indicated.

Movie S3. High time-resolution imaging of pilus extension and retraction.

Cells producing PilA[S67C] (A1552-Tn*tfoX*, PilA[S67C]) were stained with AF-488-Mal and imaged by time-lapse microscopy with continuous illumination. Images were acquired at 1s intervals for 20s to capture complete cycles of extension and retraction. The movie is

displayed at 1 frame per second and is a composite of three separate examples. Scale bar (5 µm) and time (min:sec), as indicated.

Movie S4. Retraction of an unusually long pilus.

Cells producing PilA[S67C] (A1552-Tn*tfoX*, PilA[S67C]) were stained with AF-488-Mal and imaged by time-lapse microscopy at 10s intervals capturing the retraction of an unusually long (8 µm) pilus. Note how the fluorescence of the cell body increases as the pilus retracts. Upper panel shows fluorescence, lower panel shows phase-contrast. The movie is displayed at 1 frame per second. Scale bar (5 µm) and time (min:sec), as indicated.

Movie S5. Pilus retraction followed by DNA-uptake.

Cells producing PilA[S67C] and ComEA-mCherry (A1552-Tn*tfoX*, PilA[S67C], *comEA-mCherry*) were stained with AF-488-Mal, mixed with gDNA and imaged by time-lapse microscopy at 10s intervals. Left-hand panel shows phase-contrast, middle panel shows labelled pili and right-hand panel shows ComEA-mCherry localisation. The switch of ComEA from a peripheral localisation to a focus represents a DNA-uptake event. The movie is displayed at 1 frame per second. Scale bar (5 µm) and time (min:sec), as indicated.

Movie S6. Cells lacking *pilT* produce multiple static pili.

Movie of time-lapse series shown in Figure 1M. Cells producing PilA[S67C] in the absence of *pilT* (A1552-Tn*tfoX*, PilA[S67C], Δ*pilT*) were stained with AF-488-Mal and imaged by time-lapse microscopy at 10s intervals for 1 minute. Upper panel shows fluorescence, lower panel shows phase-contrast. The movie is displayed at 1 frame per second. Scale bar (5 µm) and time (min:sec), as indicated.

Movie S7. Additional examples of static pili in retraction deficient cells.

Cells producing PilA[S67C] in the absence of *pilT* (A1552-Tn*tfoX*, PilA[S67C], Δ*pilT*) were stained with AF-488-Mal and imaged by time-lapse microscopy at 10s intervals for 1 minute. Left-hand panels show phase-contrast, right-hand panels show fluorescence. The movie is displayed at 1 frame per second and is a composite of three separate examples. Scale bar (5 μm) and time (min:sec), as indicated.

Supplemental file S1 - Details of 647 V. cholerae genomes used for bioinformatics analyses

Summary_strains

Strain name	RefSeq	Assembly type	Length	Gap_length
5	GCF_002196165.1	Contig	3960426	0
28	GCF_002196175.1	Contig	4076049	0
31	GCF_001281585.1	Contig	4041947	0
39	GCF_001281595.1	Contig	4024490	0
39	GCF_002204075.1	Contig	3866753	0
43	GCF_001281615.1	Contig	4181484	0
56	GCF_001281665.1	Contig	4105143	0
56	GCF_002204105.1	Contig	3950861	0
76	GCF_001899465.1	Contig	4000689	0
85	GCF_002196255.1	Contig	3979842	0
89	GCF_002196135.1	Contig	4115283	0
102	GCF_002196095.1	Contig	3995638	0
114	GCF_002196225.1	Contig	3971369	0
147	GCF_002196105.1	Contig	4107181	0
153	GCF_002204095.1	Contig	4017602	0
155	GCF_002196155.1	Contig	4117933	0
223	GCF_002196185.1	Contig	4018250	0
433	GCF_002196305.1	Contig	3984043	0
617	GCF_002114205.1	Contig	3960877	0
857	GCF_001729125.1	Contig	3993682	0
866	GCF_002204085.1	Contig	3892514	0
1346	GCF_001253035.1	Scaffold	4069009	65
1362	GCF_001260295.1	Scaffold	4064557	60
1587	GCF_000168895.2	Scaffold	4216194	20339
1627	GCF_001247835.1	Scaffold	4065829	177
4110	GCF_001257035.1	Scaffold	3918727	9043
4111	GCF_001252855.1	Scaffold	3870008	24067
4113	GCF_001259055.1	Scaffold	3925537	10
4121	GCF_001252075.1	Scaffold	3948118	218
4322	GCF_001249315.1	Scaffold	3981548	16707
4339	GCF_001260335.1	Scaffold	4019959	159
4488	GCF_001258555.1	Scaffold	4012653	19
4519	GCF_001248505.1	Contig	4012798	0
4536	GCF_001255835.1	Scaffold	4024336	10
4538	GCF_001259715.1	Scaffold	4022271	72
4551	GCF_001252055.1	Scaffold	4032044	198
4552	GCF_001259235.1	Scaffold	4033126	59
4585	GCF_001252895.1	Scaffold	4028120	43
4593	GCF_001257895.1	Scaffold	4031342	224
4600	GCF_001253055.1	Scaffold	4028076	197
4605	GCF_001259135.1	Scaffold	4018974	7103
4623	GCF_001254635.1	Scaffold	4034153	364
4642	GCF_001250435.1	Scaffold	3996103	15043
4646	GCF_001258995.1	Scaffold	4045251	80
4656	GCF_001258495.1	Scaffold	4035639	7484
4661	GCF_001259875.1	Scaffold	3922782	81849
4662	GCF_001260175.1	Scaffold	4012468	114
4663	GCF_001256015.1	Scaffold	4010680	6928
4672	GCF_001249795.1	Scaffold	3972315	52261
4675	GCF_001254815.1	Scaffold	3985607	52614
4679	GCF_001247245.1	Scaffold	4012494	21881
4784	GCF_001254335.1	Scaffold	4018257	344
6191	GCF_001249515.1	Scaffold	4031393	82333
6193	GCF_001257835.1	Scaffold	4032637	564
6194	GCF_001251935.1	Scaffold	4022708	5804

6197	GCF_001254955.1	Scaffold	4030166	300721
6201	GCF_001261555.1	Scaffold	4022982	2743
6210	GCF_001259475.1	Scaffold	4035607	1691
6212	GCF_001251975.1	Scaffold	4040996	286106
6214	GCF_001248645.1	Scaffold	4031671	236464
6215	GCF_001252775.1	Scaffold	4033005	1620
7684	GCF_001260695.1	Scaffold	4034747	212983
7685	GCF_001255915.1	Scaffold	4024204	22003
7686	GCF_001258535.1	Scaffold	4027393	70424
7687	GCF_001251435.1	Scaffold	4030860	1252
7714	GCF_002076415.1	Scaffold	4022767	263
17609	GCF_002078825.1	Scaffold	4045510	111
19886	GCF_002078715.1	Contig	4039107	0
20390	GCF_002078815.1	Scaffold	4045740	107
20478	GCF_002076785.1	Scaffold	4046809	366
21027	GCF_002078705.1	Contig	4043733	0
5-66	GCF_000754625.1	Contig	4014060	0
8-76	GCF_000736935.1	Contig	4074796	0
39361	GCF_002078635.1	Scaffold	4024330	518
47610	GCF_002076645.1	Contig	4022193	0
47623	GCF_002076485.1	Contig	4022899	0
48055	GCF_002076315.1	Scaffold	4024390	518
87395	GCF_000348085.2	Scaffold	3858111	1494
95412	GCF_000348105.2	Scaffold	4030154	1838
116059	GCF_000348045.2	Scaffold	4017055	1579
116063	GCF_000348065.2	Scaffold	3970379	1444
121291	GCF_000174115.1	Contig	3969506	0
10432-62	GCF_000969265.1	Complete	4077462	0
1074-78	GCF_001857405.1	Contig	3967821	0
1154-74	GCF_000969235.1	Complete	3928357	0
1157-74	GCF_000736875.1	Contig	4012216	0
116-17b	GCF_001292745.1	Contig	4125773	0
11S	GCF_002076185.1	Scaffold	4025935	625
1311-69	GCF_000736855.1	Contig	3973555	0
133-73	GCF_000736765.1	Contig	3866097	0
1421-77	GCF_000736785.1	Contig	3969137	0
1496-86	GCF_001857325.1	Contig	3972280	0
1Mo	GCF_002076425.1	Scaffold	4024350	580
2009V-1046	GCF_000237405.1	Contig	4014220	0
2009V-1085	GCF_000237425.1	Contig	4014382	0
2009V-1096	GCF_000237445.1	Contig	4016479	0
2009V-1116	GCF_000237465.1	Contig	4013388	0
2009V-1131	GCF_000237485.1	Contig	4010678	0
2010AA-142	GCF_000788425.1	Scaffold	4026654	2482
2010AA-143	GCF_000788415.1	Scaffold	4027992	2815
2010AA-144	GCF_000788435.1	Scaffold	4026834	2866
2010AA-145	GCF_000788535.1	Scaffold	4017309	2185
2010AA-146	GCF_000788555.1	Scaffold	4028110	2340
2010AA-147	GCF_000788575.1	Scaffold	4027597	2994
2010AA-148	GCF_000788595.1	Scaffold	4027400	2278
2010AA-150	GCF_000788615.1	Scaffold	4025245	2821
2010AA-151	GCF_000788635.1	Scaffold	4028131	2410
2010EL-1749	GCF_000237505.1	Contig	4009493	0
2010EL-1786	GCF_000166455.1	Complete	4077740	0
2010EL-1792	GCF_000166495.1	Contig	4014995	0
2010EL-1798	GCF_000166475.1	Contig	4016678	0

2010EL-1961	GCF_000237525.1	Contig	4004160	0
2010EL-2010H	GCF_000237545.1	Contig	4018270	0
2010EL-2010N	GCF_000237565.1	Contig	4019650	0
2010V-1014	GCF_000237585.1	Contig	4015902	0
2011EL-1089	GCF_000237605.1	Contig	4013698	0
2011EL-1137	GCF_000237645.1	Contig	4018022	0
2011EL-301	GCF_000257415.2	Contig	4002872	0
2011V-1021	GCF_000237665.1	Contig	4011850	0
2012EL-1759	GCF_000710155.1	Contig	3982946	0
2012EL-2176	GCF_000765415.1	Complete	4258023	0
2012Env-131	GCF_000788655.1	Scaffold	4028252	1196
2012Env-2	GCF_000788495.1	Scaffold	3997495	2857
2012Env-25	GCF_000788515.1	Scaffold	3965905	2916
2012Env-32	GCF_000788675.1	Scaffold	3966360	2077
2012Env-326	GCF_000788695.1	Scaffold	4060530	3557
2012Env-9	GCF_000788715.2	Complete	4061813	0
2012Env-90	GCF_000788735.1	Scaffold	4012614	1353
2012Env-92	GCF_000788755.1	Scaffold	3893268	922
2012Env-94	GCF_000788855.1	Scaffold	4014775	1796
2012HC-07	GCF_000788875.1	Scaffold	4080364	615
2012HC-08	GCF_000789115.1	Scaffold	4078954	576
2012HC-10	GCF_000789135.1	Scaffold	4012032	513
2012HC-11	GCF_000789035.1	Scaffold	4029722	488
2012HC-12	GCF_000789155.1	Scaffold	4022401	689
2012HC-15	GCF_000789075.1	Scaffold	4048930	1174
2012HC-16	GCF_000789055.1	Scaffold	4058831	493
2012HC-17	GCF_000788915.1	Scaffold	4012003	571
2012HC-18	GCF_000788895.1	Scaffold	4024111	1595
2012HC-19	GCF_000789095.1	Scaffold	4010541	1238
2012HC-21	GCF_000788995.1	Scaffold	4026556	1577
2012HC-22	GCF_000789015.1	Scaffold	4015520	2702
2012HC-24	GCF_000788795.1	Scaffold	4017899	1366
2012HC-25	GCF_000788775.1	Scaffold	3965905	2916
2012HC-31	GCF_000788835.1	Scaffold	4012329	1385
2012HC-32	GCF_000788935.1	Scaffold	4014797	676
2012HC-33	GCF_000788975.1	Scaffold	4014752	741
2012HC-34	GCF_000788815.1	Scaffold	4014093	1251
2012HC-35	GCF_000788955.1	Scaffold	4012010	1266
21B	GCF_002076775.1	Scaffold	4045625	264
234-93	GCF_000737005.1	Contig	4033463	0
2479-86	GCF_001857305.1	Contig	4011444	0
2497-86	GCF_001857355.1	Contig	3969967	0
2512-86	GCF_001857245.1	Contig	3999880	0
2523-87	GCF_001857345.1	Contig	3947558	0
254-93	GCF_000737025.1	Contig	3954364	0
2559-78	GCF_001857145.1	Contig	3982589	0
2631-78	GCF_001857225.1	Contig	3943436	0
2633-78	GCF_001857425.1	Contig	3902363	0
2740-80	GCF_000168915.2	Scaffold	4068340	42766
2740-80	GCF_001683415.1	Complete	4088961	0
2740-80	GCF_001729185.1	Contig	3986846	0
2Mo	GCF_002076705.1	Scaffold	4024773	108
31Ki	GCF_002076535.1	Scaffold	4044237	372
3223-74	GCF_001743085.1	Contig	4017920	0
3225-74	GCF_001857365.1	Contig	4002038	0
3272-78	GCF_001857265.1	Contig	3946798	0

3500-05	GCF_000237685.1	Contig	4012828	0
3546-06	GCF_000237705.1	Contig	4012129	0
3554-08	GCF_000237725.1	Contig	4019938	0
3568-07	GCF_001857505.1	Contig	4056633	0
3582-05	GCF_000237765.1	Contig	3975631	0
36KI	GCF_002078055.1	Scaffold	4020592	10
39Ki	GCF_002076475.1	Scaffold	4048610	265
4260B	GCF_000330905.1	Contig	4039222	0
43Ki	GCF_002078595.1	Scaffold	4048514	999
490-93	GCF_000737015.1	Contig	3913946	0
5473-62	GCF_000736795.1	Contig	3913714	0
571-88	GCF_000736945.1	Contig	4291048	0
5Mo	GCF_002076665.1	Scaffold	4023405	108
623-39	GCF_000154005.2	Scaffold	4164181	103685
63-93MO45	GCF_000736845.1	Contig	4018178	0
692-79	GCF_001857285.1	Contig	3938077	0
7Mo	GCF_002076615.1	Scaffold	4022979	469
8Mo	GCF_002076695.1	Contig	4023189	0
981-75	GCF_000736925.1	Contig	4034493	0
984-81	GCF_000736775.1	Contig	3946950	0
9Mo	GCF_002076635.1	Scaffold	4024326	109
A10	GCF_001254655.1	Scaffold	4145031	43
A131	GCF_001259315.1	Scaffold	4039161	98999
A152	GCF_001252875.1	Scaffold	3985453	38039
A154	GCF_001253155.1	Scaffold	3982016	32535
A177	GCF_001249995.1	Scaffold	4009459	19915
A18	GCF_001252495.1	Scaffold	4012358	104
A185	GCF_001253295.1	Scaffold	4009761	86788
A19	GCF_001250235.1	Scaffold	3948101	756
A215	GCF_001259995.1	Scaffold	3936701	10
A22	GCF_001255155.1	Scaffold	3979233	223
A27	GCF_001260995.1	Scaffold	3996840	171
A29	GCF_001253235.1	Scaffold	4000671	289
A31	GCF_001253695.1	Scaffold	4002336	338
A32	GCF_001250455.1	Scaffold	4002262	129
A325	GCF_001254095.1	Scaffold	3966042	310
A330	GCF_001257215.1	Scaffold	4039116	19728
A3461	GCF_001247525.1	Scaffold	4095237	324
A383	GCF_001257975.1	Scaffold	3991423	29027
A4	GCF_001254055.1	Scaffold	3946745	46
A46	GCF_001259555.1	Scaffold	4007597	35366
A4871	GCF_001261535.1	Scaffold	4018875	457
A4881	GCF_001257075.1	Scaffold	4022752	183
A4882	GCF_001250615.1	Scaffold	4017885	30117
A5	GCF_001254675.1	Scaffold	4032311	134
A59	GCF_001254535.1	Scaffold	3990340	27034
A6	GCF_001255575.1	Scaffold	3998598	310
A60	GCF_001248195.1	Scaffold	3997697	28449
A61	GCF_001250935.1	Scaffold	3966297	54550
A66	GCF_001260915.1	Scaffold	4012864	29254
A68	GCF_001259635.1	Scaffold	3977514	29974
A70	GCF_001248905.1	Scaffold	3981994	45273
A76	GCF_001259495.1	Scaffold	4016974	52725
AG-7404	GCF_000348125.2	Scaffold	3915123	838
AG-8040	GCF_000348145.2	Scaffold	3977194	1040
AM-19226	GCF_000153785.2	Scaffold	4053126	15439

Amazonia	GCF_000223095.1	Contig	3925563	0
ATCC11629	GCF_001471455.1	Contig	4216071	0
ATCC14035	GCF_000621645.1	Scaffold	4024517	2672
ATCC25874	GCF_001525525.1	Contig	4071446	0
B33	GCF_000153965.1	Scaffold	4043735	16900
B33	GCF_000174315.1	Scaffold	4154698	42
BJG-01	GCF_000221465.1	Scaffold	3910867	4567
BRV8	GCF_001292785.1	Contig	4109032	0
BX330286	GCF_000174335.1	Contig	4000672	0
C5	GCF_001887395.1	Complete	4102038	0
C6706	GCF_000237785.1	Contig	4001202	0
C6706	GCF_001857435.1	Contig	4019194	0
CIRS101	GCF_000175695.1	Contig	4059686	0
CISM-0005	GCF_002099125.1	Contig	4034250	0
CISM-0008	GCF_002099115.1	Contig	4035087	0
CISM-0010	GCF_002099095.1	Contig	4157755	0
CISM-0014	GCF_002099065.1	Contig	4032716	0
CISM-0015	GCF_002099055.1	Contig	4038651	0
CISM-0016	GCF_002099035.1	Contig	4032775	0
CISM-0017	GCF_002099015.1	Contig	4036556	0
CISM-0018	GCF_002098995.1	Contig	4036015	0
CISM-0019	GCF_002098965.1	Contig	4033489	0
CISM-0034	GCF_002098955.1	Contig	4036351	0
CISM-0035	GCF_002098935.1	Contig	4034640	0
CISM-0074	GCF_002098915.1	Contig	4035667	0
CISM-0079	GCF_002098875.1	Contig	4040112	0
CISM-0091	GCF_002098885.1	Contig	4036548	0
CISM-091	GCF_002098845.1	Contig	4162346	0
CISM-100	GCF_002098835.1	Contig	4040221	0
CISM-101	GCF_002098765.1	Contig	4034875	0
CISM-1019828-5	GCF_002098805.1	Contig	4036202	0
CISM-1019829-2	GCF_002098795.1	Contig	4031863	0
CISM-1020229-6	GCF_002098755.1	Contig	4034980	0
CISM-1020231-9	GCF_002098715.1	Contig	4026090	0
CISM-1020234-0	GCF_002098705.1	Contig	4037201	0
CISM-105	GCF_002098695.1	Contig	4195830	0
CISM-1163068-5	GCF_002097815.1	Contig	4014933	0
CISM-120	GCF_002098675.1	Contig	4036655	0
CISM-121	GCF_002098655.1	Contig	4034073	0
CISM-122	GCF_002098605.1	Contig	4032037	0
CISM-134	GCF_002098625.1	Contig	4194365	0
CISM-146	GCF_002098595.1	Contig	4194205	0
CISM-147	GCF_002098555.1	Contig	4196567	0
CISM-151	GCF_002098525.1	Contig	4037351	0
CISM-152	GCF_002098495.1	Contig	4035506	0
CISM-153	GCF_002098535.1	Contig	4162416	0
CISM-154	GCF_002098515.1	Contig	4032160	0
CISM-178	GCF_002098445.1	Contig	4193944	0
CISM-179	GCF_002098435.1	Contig	4194264	0
CISM-188	GCF_002098415.1	Contig	4196807	0
CISM-189	GCF_002098425.1	Contig	4185376	0
CISM-191	GCF_002098365.1	Contig	4193176	0
CISM-196	GCF_002098355.1	Contig	4195851	0
CISM-296	GCF_002098305.1	Contig	4030126	0
CISM-300043	GCF_002098295.1	Contig	4038332	0
CISM-300055	GCF_002097735.1	Contig	4148676	0

CISM-300205	GCF_002097745.1	Contig	3937137	0
CISM-300208	GCF_002098345.1	Contig	4039049	0
CISM-300209	GCF_002098335.1	Contig	4036397	0
CISM-300215	GCF_002098255.1	Contig	4065320	0
CISM-300506	GCF_002097755.1	Contig	4026639	0
CISM-302015	GCF_002098225.1	Contig	4207521	0
CISM-302029	GCF_002098235.1	Contig	4221472	0
CISM-326	GCF_002098215.1	Contig	4163534	0
CISM-347	GCF_002098195.1	Contig	4049584	0
CISM-374	GCF_002098155.1	Contig	4040267	0
CISM-375	GCF_002098145.1	Contig	4031104	0
CISM-382	GCF_002098135.1	Contig	4038086	0
CISM-398	GCF_002098085.1	Contig	4079517	0
CISM-399	GCF_002098075.1	Contig	4036149	0
CISM-420	GCF_002098055.1	Contig	4029921	0
CISM-505	GCF_002098065.1	Contig	4038667	0
CISM-510	GCF_002098005.1	Contig	4038804	0
CISM-511	GCF_002097985.1	Contig	4034679	0
CISM-655630-3	GCF_002097975.1	Contig	4061319	0
CISM-655664-3	GCF_002097995.1	Contig	4167720	0
CISM-655665-0	GCF_002097925.1	Contig	4037096	0
CISM-710180-8	GCF_002097895.1	Contig	4193899	0
CISM-740115-4	GCF_002097905.1	Contig	4034260	0
CISM-769845-7	GCF_002097915.1	Contig	4195639	0
CISM-770067-4	GCF_002097845.1	Contig	4193261	0
CISM-770180-8	GCF_002097835.1	Contig	4190491	0
CISM-780298-0	GCF_002097825.1	Contig	4194523	0
CISM-S-Nida	GCF_002097765.1	Contig	4195572	0
CMR001	GCF_001860225.1	Scaffold	4022419	829
CMR004	GCF_001858585.1	Scaffold	4021213	1360
CMR007	GCF_001860265.1	Scaffold	4026765	904
CMR008	GCF_001860285.1	Scaffold	4032975	1270
CMR009	GCF_001860295.1	Scaffold	4029303	655
CMR010	GCF_001860315.1	Scaffold	4035994	1260
CMR011	GCF_001860345.1	Scaffold	4024152	1494
CMR012	GCF_001860365.1	Scaffold	4027803	634
CMR013	GCF_001860385.1	Scaffold	4034667	486
CMR014	GCF_001860395.1	Scaffold	4042618	1056
CMR015	GCF_001860425.1	Scaffold	4027621	871
CMR016	GCF_001860445.1	Scaffold	4026175	423
CMR017	GCF_001860465.1	Scaffold	4034135	561
CMR018	GCF_001860485.1	Scaffold	4036389	1682
CMR019	GCF_001858475.1	Scaffold	4028526	576
CMR020	GCF_001858445.1	Scaffold	4034563	1486
CMR021	GCF_001858455.1	Scaffold	4037271	772
CMR022	GCF_001858465.1	Scaffold	4031968	1052
CP10303	GCF_000279555.1	Scaffold	4010577	7706
CP10325	GCF_000279305.1	Contig	3971467	0
CP10336	GCF_000304755.1	Contig	3988132	0
CP10358	GCF_000304915.2	Scaffold	3933356	4769
CP103710	GCF_000302965.1	Scaffold	3922570	6390
CP103811	GCF_000279325.1	Contig	4058268	0
CP104013	GCF_000302985.1	Scaffold	4033944	6929
CP104114	GCF_000279245.1	Contig	4085554	0
CP104215	GCF_000279345.1	Contig	4045377	0
CP104417	GCF_000303045.1	Scaffold	4010199	7722

CP104619	GCF_000281655.1	Contig	4093497	0
CP104720	GCF_000279785.1	Scaffold	4039784	5749
CP104821	GCF_000279395.1	Contig	4091990	0
CP105023	GCF_000303065.1	Scaffold	4024004	5360
CP1110	GCF_000387585.1	Contig	3925419	0
CP1111	GCF_000387625.1	Contig	3927492	0
CP1112	GCF_000387645.1	Contig	3927706	0
CP1113	GCF_000387665.1	Contig	3925787	0
CP1114	GCF_000387685.1	Contig	3925539	0
CP1115	GCF_000387605.1	Contig	3927074	0
CP1116	GCF_000387725.1	Scaffold	3932707	115
CP1117	GCF_000387705.1	Contig	3925548	0
CRC1106	GCF_001887455.1	Complete	4099119	0
CRC711	GCF_001887435.1	Complete	4057520	0
D-35	GCF_000961975.1	Contig	4010503	0
DL4211	GCF_001953365.1	Scaffold	3985387	80
DL4215	GCF_001953375.1	Scaffold	3981208	165
Drakes2013	GCF_001543505.1	Contig	4042766	0
E1162	GCF_001887495.1	Complete	4110872	0
E1320	GCF_001887415.1	Complete	4110440	0
E306	GCF_000487955.1	Scaffold	4165066	9
E506	GCF_001887475.1	Complete	4062508	0
E9120	GCF_001887655.1	Complete	4066727	0
EC-0009	GCF_000348165.2	Scaffold	4028271	963
EC-0012	GCF_000348185.2	Scaffold	4031923	1540
EC-0027	GCF_000348205.2	Scaffold	4027674	476
EC-0051	GCF_000348225.2	Scaffold	4069374	939
EC-051	GCF_001282605.1	Contig	4068854	0
EDC-020	GCF_000348245.2	Scaffold	4028191	916
EDC-022	GCF_000348265.2	Scaffold	4050458	1053
EM-1536	GCF_000348285.2	Scaffold	4053577	1458
EM-1542	GCF_001187255.1	Contig	4055638	0
EM-1543	GCF_001186515.1	Contig	4064052	0
EM-1546	GCF_000348305.2	Scaffold	4061605	1044
EM-1626	GCF_000348325.2	Scaffold	4052965	1147
EM-1626	GCF_001186485.1	Contig	4058026	0
EM-1652A	GCF_001186505.1	Contig	4052192	0
EM-1654	GCF_001186575.1	Contig	4053299	0
EM-1676A	GCF_000348345.2	Scaffold	4007225	1596
EM-1688	GCF_001186565.1	Contig	4054925	0
EM-1690	GCF_001186595.1	Contig	4056072	0
EM-1690A	GCF_001186585.1	Contig	3961642	0
EM-1706	GCF_001186645.1	Contig	3944903	0
EM-1727	GCF_000348365.1	Scaffold	4067194	796
Env-390	GCF_001854425.1	Complete	4050927	0
FC1105	GCF_002194295.1	Contig	3960610	0
FC1225	GCF_002194335.1	Contig	4003412	0
FC1341	GCF_002194265.1	Contig	3999105	0
FC1384	GCF_002194245.1	Contig	4014742	0
FC1817	GCF_002194305.1	Contig	4043413	0
FC1877	GCF_002194155.1	Contig	3984202	0
FC2271	GCF_002194235.1	Contig	4016919	0
FC2273	GCF_002194215.1	Contig	4022199	0
FC3611a	GCF_002194165.1	Contig	4013511	0
FC3611b	GCF_002194185.1	Contig	4013713	0
FDAARGOS-223	GCF_002073335.1	Complete	4042138	0

FJ147	GCF_000963555.1	Complete	4091935	0
G-33	GCF_002102575.1	Contig	3933642	0
GP140	GCF_001253315.1	Scaffold	3919716	147036
GP145	GCF_001250035.1	Scaffold	3946053	4679
GP152	GCF_001249715.1	Scaffold	3964217	4182
GP16	GCF_001251495.1	Scaffold	3968603	5192
GP160	GCF_001254435.1	Scaffold	3986399	22
GP60	GCF_001261335.1	Scaffold	3871365	127092
GP8	GCF_001253575.1	Scaffold	3951857	29492
H1	GCF_000275645.1	Chromosome	4089020	0
HC-02A1	GCF_000221445.1	Scaffold	3949552	1748
HC-02C1	GCF_000305525.2	Scaffold	3935576	1564
HC-06A1	GCF_000234375.1	Contig	4028197	0
HC-17A1	GCF_000304935.2	Scaffold	4174355	9743
HC-17A2	GCF_000305675.2	Scaffold	4023476	1821
HC-19A1	GCF_000234965.1	Scaffold	4033401	3282
HC-1A2	GCF_000304775.1	Contig	3965428	0
HC-20A2	GCF_000279415.1	Contig	4084542	0
HC-21A1	GCF_000234945.1	Scaffold	4030433	2868
HC-22A1	GCF_000234925.1	Scaffold	4034031	2254
HC-23A1	GCF_000234395.1	Contig	4099188	0
HC-28A1	GCF_000234415.1	Contig	4027641	0
HC-32A1	GCF_000234905.1	Scaffold	4033209	2143
HC-33A2	GCF_000234885.1	Scaffold	4024727	1853
HC-36A1	GCF_000474965.1	Contig	3959428	0
HC-37A1	GCF_000305585.2	Scaffold	4029550	1667
HC-38A1	GCF_000221485.1	Scaffold	4036059	1781
HC-39A1	GCF_000302775.1	Scaffold	4022430	5657
HC-40A1	GCF_000221345.1	Scaffold	4031783	1496
HC-41A1	GCF_000302755.1	Scaffold	4027832	11240
HC-41B1	GCF_000304955.2	Scaffold	3883402	1001
HC-42A1	GCF_000279185.1	Scaffold	4024780	5973
HC-43A1	GCF_000234435.1	Contig	4053234	0
HC-43B1	GCF_000279435.1	Contig	3931831	0
HC-44C1	GCF_000305565.2	Scaffold	3876537	1663
HC-46A1	GCF_000279455.1	Contig	4120976	0
HC-46B1	GCF_000305605.1	Contig	3941918	0
HC-47A1	GCF_000279955.1	Scaffold	4031718	9951
HC-48A1	GCF_000221365.1	Scaffold	4032180	1356
HC-48B2	GCF_000234865.1	Scaffold	4024820	1358
HC-49A2	GCF_000220725.1	Contig	4059369	0
HC-50A1	GCF_000302835.1	Scaffold	3939222	9499
HC-50A2	GCF_000304995.1	Scaffold	4030802	7108
HC-51A1	GCF_000303105.1	Scaffold	3929843	5488
HC-52A1	GCF_000302855.1	Scaffold	3937542	9994
HC-55A1	GCF_000302875.1	Scaffold	3932130	6222
HC-55B2	GCF_000305645.2	Scaffold	3934012	1633
HC-55C2	GCF_000305015.2	Scaffold	3940186	1030
HC-56A1	GCF_000302895.1	Scaffold	3934171	6128
HC-56A2	GCF_000279205.1	Scaffold	4029365	9452
HC-57A1	GCF_000303005.1	Scaffold	3934427	6168
HC-57A2	GCF_000279375.1	Scaffold	4025386	7140
HC-59A1	GCF_000305195.2	Scaffold	3934654	1525
HC-59B1	GCF_000305545.2	Scaffold	3934504	1173
HC-60A1	GCF_000305055.2	Scaffold	3938002	433
HC-61A1	GCF_000234455.2	Contig	4067936	0

HC-61A2	GCF_000304795.1	Contig	4000124	0
HC-62A1	GCF_000305075.2	Scaffold	4032880	818
HC-62B1	GCF_000305625.2	Scaffold	4028528	2967
HC-64A1	GCF_000327105.3	Scaffold	4032042	1766
HC-65A1	GCF_000327125.3	Scaffold	4028731	2476
HC-67A1	GCF_000327145.3	Scaffold	4026751	2103
HC-68A1	GCF_000327165.3	Scaffold	4026495	2019
HC-69A1	GCF_000305695.2	Scaffold	4024183	1425
HC-70A1	GCF_000221385.1	Scaffold	4057434	913
HC-71A1	GCF_000327185.3	Scaffold	4028948	2793
HC-72A2	GCF_000327205.3	Scaffold	4028422	1709
HC-77A1	GCF_000305095.2	Scaffold	4040127	784
HC-78A1	GCF_000327225.3	Scaffold	3937766	1859
HC-7A1	GCF_000318485.2	Contig	4074920	0
HC-80A1	GCF_000327245.3	Scaffold	4032382	2581
HC-81A1	GCF_000318505.2	Contig	4084020	0
HC-81A2	GCF_000303125.1	Scaffold	4028931	8323
HCUF01	GCF_000220745.2	Contig	4067550	0
HE-09	GCF_000221405.1	Scaffold	3826131	2323
HE-16	GCF_000303085.1	Scaffold	3911386	5849
HE-25	GCF_000279265.1	Contig	4092530	0
HE-40	GCF_000305115.2	Scaffold	3875898	942
HE-45	GCF_000279285.1	Contig	4125202	0
HE-46	GCF_000305135.2	Scaffold	3874516	843
HE39	GCF_000220765.2	Contig	3937798	0
HE46	GCF_001857515.1	Contig	3978873	0
HE48	GCF_000220785.1	Contig	4179415	0
HFU-02	GCF_000221425.1	Scaffold	4032845	1777
I-1187	GCF_001661905.1	Contig	3957421	0
I-1300	GCF_000967785.1	Chromosome	4033785	83438
I-1471	GCF_000818865.1	Chromosome	4034973	154110
IDHO1-726	GCF_001247885.1	Scaffold	4015875	23136
IEC224	GCF_000250855.1	Complete	4079586	0
InabaG4222	GCF_000338075.1	Chromosome	4202811	2100
InabaPIC018	GCF_001543465.1	Contig	4029307	0
InabaRND18826	GCF_000500735.1	Contig	4036141	0
InabaRND18899	GCF_000500695.1	Contig	3991231	0
InDRE4262	GCF_000953775.1	Contig	4019893	0
InDRE4354	GCF_000953755.1	Contig	4019937	0
INDRE91-1	GCF_000176435.1	Contig	3947707	0
J8YRSKAGUNGA	GCF_002078795.1	Contig	4044226	0
KW3	GCF_001318185.1	Complete	4089020	0
L-3226	GCF_000600255.1	Contig	3991045	0
L11	GCF_001718105.1	Scaffold	4000957	712
L15	GCF_001718095.1	Contig	4083945	0
LMA3984-4	GCF_000195065.1	Complete	3738715	0
M1030	GCF_002196335.1	Contig	3951787	0
M1275	GCF_001517845.1	Contig	4124381	0
M1275D	GCF_001517855.1	Contig	4111077	0
M1337	GCF_002196375.1	Contig	4005292	0
M1429	GCF_000960915.1	Contig	4040011	0
M1501	GCF_001637575.1	Contig	4011026	0
M1518	GCF_001641685.1	Contig	4014173	0
M1524	GCF_001641705.1	Contig	3961165	0
M2140	GCF_001887635.1	Complete	4014863	0
M66-2	GCF_000021605.1	Complete	3938905	0

M888	GCF_001521835.1	Contig	4041101	0
M888D	GCF_001617675.1	Contig	3970532	0
M988	GCF_001515115.1	Contig	3995831	0
MAK676	GCF_000753725.1	Contig	3937648	0
MAK757	GCF_000153865.1	Scaffold	3936003	16585
MBN17	GCF_001250795.1	Scaffold	4019692	9342
MBRN14	GCF_001249085.1	Scaffold	4014074	9755
ME-7	GCF_001515095.1	Contig	3969186	0
MG116025	GCF_001254895.1	Scaffold	4027317	19844
MG116226	GCF_001254355.1	Scaffold	4028960	123
MJ-1236	GCF_000022585.1	Complete	4236368	0
MJ1485	GCF_001250195.1	Scaffold	4112661	67066
MO10	GCF_000152425.1	Scaffold	4079638	45226
MS6	GCF_000829215.1	Complete	4030944	0
MZO-2	GCF_000153985.2	Scaffold	3977246	29422
MZO-2	GCF_001729155.1	Contig	3948633	0
MZO-3	GCF_000168935.2	Scaffold	4137330	17687
N16961	GCF_000006745.1	Complete	4033464	0
NCTC5395	GCF_001887515.1	Complete	4170245	0
NCTC8457	GCF_000153945.1	Scaffold	4082088	18700
NCTC9420	GCF_001887615.1	Complete	4076583	0
Nep-21106	GCF_000348465.2	Scaffold	4031227	1157
Nep-21113	GCF_000348485.2	Scaffold	4042420	733
NHCC-004A	GCF_000348385.2	Scaffold	4031643	864
NHCC-006C	GCF_000348405.2	Scaffold	4028239	1614
NHCC-008D	GCF_000348425.2	Scaffold	3971576	1969
NHCC-010F	GCF_000348445.2	Scaffold	4028811	997
NHCC-011	GCF_001186655.1	Contig	4034922	0
NHCC-019	GCF_001186755.1	Contig	4006456	0
NHCC-021	GCF_001186725.1	Contig	4044257	0
NHCC-04	GCF_001186665.1	Contig	4039258	0
NHCC-042	GCF_001186735.1	Contig	4040251	0
NHCC-048	GCF_001186675.1	Contig	4041973	0
NHCC-05	GCF_001186785.1	Contig	4063046	0
NHCC-068	GCF_001187185.1	Contig	4033814	0
NHCC-078	GCF_001186495.1	Contig	4032908	0
NHCC-079	GCF_001187225.1	Contig	4037755	0
NHCC-080	GCF_001187245.1	Contig	4032145	0
NHCC-081	GCF_001186805.1	Contig	4036135	0
NHCC-083	GCF_001186835.1	Contig	4032941	0
NHCM-01	GCF_001186825.1	Contig	4058157	0
NHCM-012	GCF_001186915.1	Contig	4058997	0
NHCM-013	GCF_001186925.1	Contig	4056172	0
NHCM-016A	GCF_001186965.1	Contig	4054882	0
NHCM-017	GCF_001186985.1	Contig	4270351	0
NHCM-02	GCF_001186855.1	Contig	4058043	0
NHCM-029	GCF_001186995.1	Contig	4058323	0
NHCM-03	GCF_001187265.1	Contig	4061995	0
NHCM-033	GCF_001187065.1	Contig	4091543	0
NHCM-037	GCF_001187025.1	Contig	4053555	0
NHCM-04	GCF_001186905.1	Contig	4051907	0
NHCM-043	GCF_001187085.1	Contig	4054814	0
NHCM-044	GCF_001187015.1	Contig	4031872	0
NHCM-045	GCF_001187095.1	Contig	4036868	0
NHCM-047	GCF_001187145.1	Contig	4041405	0
NHCM-048	GCF_001187175.1	Contig	3956153	0

NHCM-053	GCF_001187105.1	Contig	4056015	0
NHCM-054	GCF_001187165.1	Contig	4037409	0
NHCM-06	GCF_001186885.1	Contig	4065293	0
NIH41	GCF_000736865.1	Contig	3952728	0
NMH2016	GCF_002251495.1	Contig	3754606	0
O1S	GCF_002076155.1	Contig	4024114	0
O2	GCF_002076255.1	Contig	4044276	0
O395	GCF_000016245.1	Complete	4132319	0
O395	GCF_000021625.1	Complete	4135300	0
O3MU	GCF_002076465.1	Scaffold	4025781	10
O3S	GCF_002076575.1	Scaffold	4022861	108
O5MU	GCF_002076585.1	Scaffold	4023442	518
O6MU	GCF_002076175.1	Scaffold	4025207	108
O7MU	GCF_002076545.1	Scaffold	4025010	115
O7S	GCF_002076165.1	Contig	4023827	0
O9S	GCF_002076245.1	Contig	4022009	0
OgawaRND19187	GCF_000500675.1	Contig	4001659	0
OgawaRND19188	GCF_000710445.1	Contig	3999500	0
OgawaRND19191	GCF_000710455.1	Contig	4005480	0
OgawaRND6878	GCF_000500715.1	Contig	4000976	0
OO4	GCF_002076455.1	Contig	4025417	0
P-18748	GCF_002196055.1	Contig	3961379	0
P-18778	GCF_002196065.1	Contig	4012469	0
P-18785	GCF_000338215.2	Contig	3978895	0
P13762	GCF_001639085.1	Contig	4096073	0
PCS-022	GCF_000569115.2	Scaffold	4055383	780
PCS-023	GCF_000348505.2	Scaffold	4031594	1167
PhVC-311	GCF_001027505.1	Contig	3927966	0
PhVC-326	GCF_001027485.1	Contig	3932194	0
PhVE-5	GCF_001027495.1	Contig	3929317	0
PRL5	GCF_001256355.1	Scaffold	3983009	4188
PRL64	GCF_001261075.1	Scaffold	4027134	4528
PS15	GCF_000318075.1	Contig	3910387	0
R17644	GCF_000965285.1	Contig	4020247	0
RC27	GCF_000176395.1	Contig	4011779	0
RC385	GCF_000152445.1	Scaffold	4194697	74564
RC9	GCF_000174275.1	Contig	4211011	0
RND81	GCF_000763075.1	Contig	3956193	0
S12	GCF_001735565.1	Scaffold	4061577	3290
SIO	GCF_001857455.1	Contig	3998588	0
TEM-04-01-001	GCF_002076745.1	Scaffold	4042748	368
TEM-10-01-002	GCF_002076265.1	Scaffold	4044593	107
TEM-12-12-001	GCF_002076735.1	Scaffold	4041711	264
TEM-15-01-005	GCF_002078695.1	Contig	4043231	0
TEM-25-01-004	GCF_002076235.1	Contig	4042340	0
TEM-29-01-003	GCF_002078755.1	Scaffold	4041320	108
TM11079-80	GCF_000174255.1	Contig	4055140	0
TMA21	GCF_000174295.1	Contig	4023772	0
TP	GCF_001857485.1	Contig	4060799	0
V109	GCF_001257255.1	Scaffold	3995420	65518
V212-1	GCF_001248465.1	Scaffold	3945950	7858
V5	GCF_001252675.1	Scaffold	3989146	19340
V51	GCF_000152465.2	Scaffold	4208620	77392
V52	GCF_000167935.2	Scaffold	4045303	36256
V52	GCF_001857545.1	Contig	3988138	0
VC1761	GCF_000299515.2	Contig	4011457	0

VC22	GCF_001729195.1	Contig	4022142	0
VC35	GCF_000299495.2	Contig	3912714	0
VC4370	GCF_000299535.2	Contig	3986677	0
VC48	GCF_001857165.1	Contig	3931795	0
VC53	GCF_001857155.1	Contig	4217958	0
VC56	GCF_001857175.1	Contig	4193045	0
VCC19	GCF_000438805.2	Contig	4134889	0
YB1A01	GCF_001402185.1	Contig	3876619	0
YB1G06	GCF_001402365.1	Scaffold	3938799	17
YB2A05	GCF_001402535.1	Scaffold	3886789	40
YB2A06	GCF_001402375.1	Contig	4033481	0
YB2G01	GCF_001411585.1	Contig	4032885	0
YB2G05	GCF_001402415.1	Scaffold	3888413	13
YB2G07	GCF_001402425.1	Scaffold	3941216	36
YB3B05	GCF_001402545.1	Scaffold	4014368	47
YB3G04	GCF_001402275.1	Scaffold	4031104	11
YB4B03	GCF_001402605.1	Contig	3916598	0
YB4C07	GCF_001402285.1	Contig	4015430	0
YB4F05	GCF_001402265.1	Scaffold	3886413	56
YB4G05	GCF_001402575.1	Scaffold	3927241	13
YB4G06	GCF_001402255.1	Scaffold	4032120	12
YB4H02	GCF_001402585.1	Scaffold	4039090	90
YB5A06	GCF_001402435.1	Scaffold	3886853	66
YB6A06	GCF_001402445.1	Contig	3884851	0
YB7A06	GCF_001402335.1	Scaffold	3881934	100
YB7A09	GCF_001402595.1	Scaffold	3885495	95
YB8E08	GCF_001402655.1	Scaffold	4013838	52
YN2011004	GCF_001029975.1	Scaffold	4057079	1931
YN89004	GCF_001030035.1	Scaffold	3950281	2928
YN97083	GCF_001030015.1	Scaffold	4074242	1275
YN98296	GCF_001184775.1	Scaffold	4004435	2558
ZWU0020	GCF_000812045.1	Contig	4038248	0

Supplemental file S2 - DNA sequences of pilA and the deduced amino acid sequences of the proteins they encode from a

PilA Protein sequences:

>GC#276_ATCC25872
MKAYKNKLQQGFTLIELMIVVAVIGVLAAIAVPQYQNYVKKSEAAAAVATIRSLTTN
IDTFMADTGNFPTDLTTLGAASNMNKLGTITLGTNEVKLVFSNTDSAFASTDEVKMA
KDATSGLWTCTVPTGVTLKGCTASGSGSGSGSGSGSGSGSGSGN

>GC#353_Sa5Y
MKAYKNKLQKGFTLIELMIVVAIIGVLAAIAVPQYQKYVAKSEAAAALASITGHRTN
VETYVLENGSFPAIEDLAPPSASIGTIQYGEAQASGAGSIVFAFGTSGASPSVVNRN
VTLARDENGSWKCTTTIDTKIAPKGCTP

>GC#354_W6G
MKAYKNKQQQGFTLIELMIVVAIIGVLSAIAVPAYKDYVTKSEVASAVASLKSIITP
AELHYQEYGAFPNDSTELERVGVGSNAVKNGTLTFNKTAGTITLALASPSGVSAIIT
RDGSTGWSCAVTGLTNQSNAPKGCPQSDSGTGGTGGTGDTGGSGS

>GC#952_SP7
MKAYKNKLQQGFTLIELMIVVAIIGILAAFAVPAYQNYTKKATLSEFPKALAAAKLA
VEVCAHENASNETTFISNCVSGNNGVPASFTLNNIDIQVITAANAGVSGAVAVEAKA
KIAKGPIAQDESFIMAAVYKPEGLEWKSSCKDAAGKAQTSYCPD

>GC#953_SL6
MKAYKNKLQQGFTLIELMIVVAVIGVLAAIAVPQYQKYTQKAALATALATATALKTN
YEDYVSMSGAAPTSATDIGATSFSIGTISVTSGAINVAINKGPGTGSSVILTRTGLL
GGWGCQISGAQAEVTINGCP

>GC#954_SL5
MKAYKNKLQQGFTLIELMIVVAVIGVLAAIAVPQYQKYTQKAALATALATATALKTN
YEDYVSMSGAAPTSATDIGATSFSIGTISVTSGAINVAINKGPGTGSSVILTRTGLL
GGWGCQISGAQAEVTINGCP

>GC#955_SL4
MKAYKNKLQKGFTLIELMIVVAIIGVLAAIAVPQYQKYVAKSEAAAALASITGHRTN
VETYVLENGSFPAIEDLAPPSASIGTIQYGEAQASGAGSIVFAFGTSGASPSVVNRN
VTLARDENGSWKCTTTIDTKIAPKGCTP

>GC#956_L6
MKAYKNKQQQGFTLIELMIVVAIVGILAAFAVPAYQNYTMRAHASEMLSASSAMKTA
VGICLISGNTNCSSGNGGVPAKQDLGAFSIESLAGASGASPTVQASVDSGQTKGKLV
AGDTIKLTPTLNTAGVTWQVECVKAANQQSSIDDWCPVK

>GC#957_Sa3
MKAYKNKQQQGFTLIELMIVVAIIGVLAAIAVPQYQKYVAKSEAAAALASITGHRTN
VETYVLENGSFPTSSAVPVPSTSTGAITYSSGASGAGSIIFTFAASGASPSVVTKNV
TLARDGDGKWICTSSIGSDFRPKGCAASQ

>GC#959_Sa7
MKAYKNKQQQGFTLIELMIVVAIIGVLAAIAVPAYKDYVTKSELASGFATIKSVITP
AELYFQENGKISASASTVDVLGVSSGANTLGELTITADNTIQFAHDAGAALGAKFVY
TRSSGGWSCTYTQPSAVSAAAPKGCTP

>GC#960_So5
MKAYKNKQQQGFTLIELMIVVAIIGVLSAIAVPAYKDYVTKSEVASAVASLKSIITP
AELHYQEYGAFPNDSTELERVGVGSNAVKNGTLTFNKTAGTITLALASPSGVSAIIT
RDGSTGWSCAVTGLTNQSNAPKGCPQSDSGTGGTGDTGGSGS

>GC#962_W7
MKAYKNKQQQGFTLIELMIVVAIIGVLSAIAVPAYKDYVTKSEVASAVASLKSIITP
AELHYQEYGAFPNDSTELERVGVGSNAVKNGTLTFNKTAGTITLALASPSGVSAIIT
RDGSTGWSCAVTGLTNQSNAPKGCPQSDSGTGGTGGTGDTGGSGS

>GC#963_E7
MKAYKNKQQQGFTLIELMIVVAIIGVLAAIAVPAYKDYVTKSELASGFATIKSVITP
AELYFQENGKISASASTVDVLGVSSGANTLGELTITADNTIQFAHDAGAALGAKFVY
TRSSGGWSCTYTQPSAVSAAAPKGCTP

>GC#964_SP6
MKAYKNKLQKGFTLIELMIVVAVIGVLAAIAVPQYQKYVAKSEAASALATLTGLKTN
AEAYTVETGSFPTDTQQAQLGTPSSAMGTIAYANTGSSGAAGTITFTFSGTVSPSLK
SSAIRLKRDDSGNWSCESNKDATSGIIPKGCNSGTF

>GC#999_TP
MKAYKNKQQQGFTLIELMIVVAVIGVLAAIAVPQYQDYVKKSALGTALASASAYKTI
VEDNIATNNQFPFISESFGIGTIRATSGAIATGNGTNDIVASVTQGSGTGSSVTLKR
DASGNWTCALSGASNITLGGCS

>GC#1000_SIO
MKAYKNKLQKGFTLIELMIVVAIIGVLAAIAVPAYKDYVTKSEVASAVASLKSIITP
AELYYQEQGAFPAQGSDIGIDLTGLSFASNAITLALTSPSGAQATITREDTKGWSCK
VAGLTKPANAPKGCPQ

>GC#2501_DRC186-4
MNAYKNKQQQGFTLIELMIVVAIIGVLAAIAVPAYKDYVTKSEASSAIATLKALQTP
AELLYQENGNLTVSNALAALGTSENANPLGKLEVEGTDGLKFTFTQSGALKDQTITL
QRSGTDGWKCNASDKIEKLKIKSCTTAQ

>GC#3079_DL4215
MKAYKNKLQKGFTLIELMIVVAVIGVLAAIAIPQYQKYVAKAEVASALATLTGIKTN
VEAYAVETGSFPAAGKEGDLGVPTSIPSGTVAFAATSSGAGTITFSFNTSNVSNLIS
GKKFLLNRTSAGVWTCDGAATTPVTDDLLPKNCI

>GC#3081_1587
MKAYKNKQQQGFTLIELMIVVAIIGVLAAVAIPAYKSYVAKSEAATAAATVRGLLTN
IDMYQQEVGSFPTDITKVGGTTTMNAFGSIALASTVSGGTATFTFTDGALKTGGTGN
TAAKIIYTKDNATGWTCTHTINDTSVVPSGC

>GC#3084_DL4211
MKAYKNKLQQGFTLIELMIVVAVIGVLAAIAVPQYQKYTQKAALATALATATALKTN
YEDYVSMSGAAPTSATDIGATSFSIGTISVTSGAINVAINKGPGTGSSVILTRTGLL
GGWGCQISGAQAEVTINGCP

>GC#5537_W10G
MKAYKNKLQKGFTLIELMIVVAIIGVLAAVAIPAYQDYVKKSEAASALATLRALITP
AELFYQEKGVGAAATVAELGSSGTANDLGTITSALVNAKPTLKFEFGANSSMASTDT
LTFTRDTGGWTCAIAGNVPAIDGCQ

>GC#5539_Sa10G
MKAYKNKQQQGFTLIELMIVVAIIGVLAAIAVPAYKDYVTKSELASGFATIKSVITP
AELYFQENGKISASASTVDVLGVSSGANTLGELTITADNTIQFAHDAGAALGAKFVY
TRSSGGWSCTYTQPSAVSAAAPKGCTP

PilA DNA sequences:

>GC#276_ATCC25872
ATGAAAGCGTATAAAAACAAACTACAGCAAGGTTTTACCTTAATTGAATTGATGATT
GTGGTAGCAGTGATTGGTGTATTGGCAGCGATTGCGGTTCCTCAATATCAAAACTAC
GTTAAAAAATCAGAAGCTGCAGCTGCAGTAGCAACAATACGCTCTTTGACTACCAAT
ATCGATACATTCATGGCTGATACCGGAAATTTTCCAACTGATTTAACTACATTGGGT
GCAGCATCAAATATGAATAAACTCGGTACGATTACACTTGGGACAAACGAAGTTAAA
TTAGTTTTCAGTAATACTGACTCCGCTTTTGCTTCAACTGATGAAGTTAAAATGGCT
AAAGATGCAACTTCTGGCCTTTGGACTTGTACTGTACCAACAGGTGTAACACTGAAA
GGATGTACAGCTTCTGGTTCTGGTTCTGGTTCTGGTTCTGGTTCTGGTTCTGGTTCT
GGTTCTGGCAACTAA

>GC#353_Sa5Y
ATGAAAGCGTATAAAAACAAACTACAGAAAGGTTTTACCTTAATTGAATTGATGATT
GTGGTAGCGATTATTGGTGTGTTGGCTGCCATTGCAGTGCCTCAGTACCAAAAATAC
GTCGCAAAAAGTGAGGCAGCAGCAGCACTGGCTTCGATCACTGGACATAGAACAAAC
GTTGAAACATACGTATTGGAAAATGGTTCCTTCCCAGCAATAGAAGATTTAGCCCCG
CCATCAGCAAGTATAGGCACTATTCAATATGGTGAGGCACAAGCATCTGGAGCTGGC
AGCATAGTTTTTGCCTTCGGTACAAGTGGAGCAAGCCCTAGTGTTGTAAATAGAAAT
GTTACTTTAGCTCGTGATGAAAATGGATCGTGGAAATGTACAACCACTATTGATACA
AAAATCGCGCCTAAAGGCTGTACACCATAG

>GC#354_W6G
ATGAAAGCGTATAAAAACAAACAACAGCAAGGTTTTACCTTAATTGAATTGATGATT
GTAGTGGCGATTATTGGTGTGTTGTCAGCAATTGCTGTACCAGCTTATAAAGACTAC
GTAACCAAAAGTGAAGTGGCTTCTGCGGTAGCATCTTTAAAATCGATTATTACTCCA
GCAGAACTTCATTACCAAGAATATGGAGCCTTCCCAAATGACAGCACAGAATTAGAA
AGAGTCGGAGTAGGCTCTAATGCTGTCAAAAATGGTACATTAACATTTAACAAAACA
GCAGGAACTATAACTTTAGCATTAGCCTCACCTTCAGGAGTATCAGCAATTATTACG
AGAGATGGTTCAACAGGTTGGTCATGTGCTGTAACAGGTCTAACCAACCAGAGTAAT
GCACCTAAAGGCTGTCCTCAATCGGATAGCGGCACTGGTGGCACTGGTGGCACTGGC
GACACTGGTGGCTCTGGTAGTTAA

>GC#952_SP7
ATGAAAGCGTATAAAAACAAACTACAGCAAGGTTTTACCTTAATTGAATTGATGATT
GTGGTAGCGATTATTGGCATTTTGGCTGCCTTCGCCGTTCCGGCCTATCAAAACTAT
ACAAAAAAAGCTACTTTATCTGAATTTCCAAAAGCACTAGCCGCAGCCAAGTTAGCA
GTCGAAGTATGCGCTCATGAGAATGCATCAAATGAAACAACCTTCATTTCAAATTGT
GTTTCTGGCAATAATGGCGTTCCAGCGTCGTTTACACTAAACAATATCGACATTCAA
GTAATAACAGCTGCCAATGCTGGCGTTTCAGGTGCGGTGGCTGTTGAAGCCAAGGCA

AAAATTGCTAAAGGCCCAATTGCCCAAGATGAAAGCTTCATTATGGCTGCTGTATAT
AAGCCCGAAGGACTCGAATGGAAAAGTTCTTGTAAAGATGCAGCAGGTAAAGCTCAA
ACATCTTACTGCCCAGACTAA

>GC#953_SL6
ATGAAAGCGTATAAAAATAAACTACAGCAAGGTTTTACCTTAATTGAATTGATGATT
GTAGTGGCAGTGATTGGTGTGTTGGCAGCGATTGCGGTGCCTCAATATCAGAAATAT
ACACAAAAAGCAGCTCTTGCTACTGCTTTAGCTACAGCAACTGCATTAAAAACAAAT
TATGAAGACTATGTATCTATGAGTGGTGCAGCTCCCACATCTGCAACAGATATTGGA
GCAACCAGCTTCAGTATAGGAACTATTTCAGTGACTAGTGGTGCTATAAACGTTGCT
ATAAATAAGGGACCAGGCACTGGCTCATCTGTAATTTTAACTAGAACAGGGCTTCTT
GGTGGCTGGGGATGCCAAATCTCCGGAGCTCAAGCTGAAGTAACAATTAACGGTTGC
CCATAG

>GC#954_SL5
ATGAAAGCGTATAAAAATAAACTACAGCAAGGTTTTACCTTAATTGAATTGATGATT
GTAGTGGCAGTGATTGGTGTGTTGGCAGCGATTGCGGTGCCTCAATATCAGAAATAT
ACACAAAAAGCAGCTCTTGCTACTGCTTTAGCTACAGCAACTGCATTAAAAACAAAT
TATGAAGACTATGTATCTATGAGTGGTGCAGCTCCCACATCTGCAACAGATATTGGA
GCAACCAGCTTCAGTATAGGAACTATTTCAGTGACTAGTGGTGCTATAAACGTTGCT
ATAAATAAGGGACCAGGCACTGGCTCATCTGTAATTTTAACTAGAACAGGGCTTCTT
GGTGGCTGGGGATGCCAAATCTCCGGAGCTCAAGCTGAAGTAACAATTAACGGTTGC
CCATAG

>GC#955_SL4
ATGAAAGCGTATAAAAACAAACTACAGAAAGGTTTTACCTTAATTGAATTGATGATT
GTGGTAGCGATTATTGGTGTGTTGGCTGCCATTGCAGTGCCTCAGTACCAAAAATAC
GTCGCAAAAAGTGAGGCAGCAGCAGCACTGGCTTCGATCACTGGACATAGAACAAAC
GTTGAAACATACGTATTGGAAAATGGTTCCTTCCCAGCAATAGAAGATTTAGCCCCG
CCATCAGCAAGTATAGGCACTATTCAATATGGTGAGGCACAAGCATCTGGAGCTGGC
AGCATAGTTTTTGCCTTCGGTACAAGTGGAGCAAGCCCTAGTGTTGTAAATAGAAAT
GTTACTTTAGCTCGTGATGAAAATGGATCGTGGAAATGTACAACCACTATTGATACA
AAAATCGCGCCTAAAGGCTGTACACCATAG

>GC#956_L6
ATGAAAGCGTATAAAAACAAACAACAGCAAGGTTTTACCTTAATTGAATTGATGATT
GTGGTGGCGATTGTGGGAATTTTGGCTGCTTTTGCCGTTCCTGCATATCAAAATTAC
ACAATGCGAGCTCATGCAAGCGAGATGCTTAGTGCATCTTCAGCCATGAAAACCGCT
GTAGGAATATGTCTAATTAGTGGTAATACAAACTGTTCATCGGGAAATGGTGGAGTT
CCAGCTAAACAAGATCTTGGTGCGTTTTCTATAGAATCTCTTGCAGGGGCTAGCGGC
GCGTCACCAACAGTACAAGCAAGTGTTGATTCTGGGCAAACTAAAGGAAAACTAGTA
GCAGGGGACACAATAAAACTAACACCAACCTTGAACACGGCTGGTGTAACATGGCAG
GTTGAATGTGTGAAGGCGGCAAATCAACAAAGTTCCATTGATGATTGGTGTCCTGTC
AAATAA

>GC#957_Sa3
ATGAAAGCGTATAAAAACAAACAACAGCAAGGTTTTACCTTAATTGAATTGATGATT
GTGGTAGCGATTATTGGCGTGTTGGCTGCCATTGCAGTACCTCAGTACCAAAAATAC
GTTGCGAAAAGTGAAGCAGCAGCAGCACTGGCTTCAATCACCGGGCATAGAACAAAC
GTTGAAACATACGTATTGGAAAATGGTTCGTTCCCAACATCATCTGCCGTGCCTGTT
CCATCAACAAGTACAGGAGCAATTACTTACAGCTCAGGGGCATCTGGTGCAGGCAGC

ATCATCTTCACATTTGCAGCCAGTGGTGCAAGCCCTAGCGTTGTGACTAAAAACGTC
ACTTTAGCTCGAGACGGAGATGGCAAATGGATCTGTACATCTTCTATTGGCTCAGAT
TTCAGACCCAAAGGCTGTGCGGCCTCCCAGTAA

GC#959_Sa7
ATGAAAGCGTATAAAAACAAACAACAGCAAGGTTTTACCTTAATTGAATTAATGATT
GTGGTAGCGATTATTGGTGTGTTGGCAGCGATTGCTGTTCCTGCTTATAAGGATTAT
GTAACCAAGAGCGAATTGGCATCTGGTTTCGCTACTATCAAGTCCGTGATAACTCCA
GCTGAACTTTATTTCCAAGAAAATGGAAAAATAAGTGCAAGCGCAAGCACTGTTGAT
GTTCTCGGTGTATCTTCTGGAGCAAATACTTTAGGTGAACTTACTATAACCGCTGAC
AATACAATTCAATTTGCTCATGATGCTGGTGCTGCATTAGGTGCAAAATTTGTTTAC
ACAAGAAGCTCTGGAGGTTGGAGTTGCACTTACACACAACCATCAGCAGTTAGTGCA
GCAGCTCCTAAGGGCTGTACACCATAG

>GC#960_So5
ATGAAAGCGTATAAAAACAAACAACAGCAAGGTTTTACCTTAATTGAATTGATGATT
GTAGTGGCGATTATTGGTGTGTTGTCAGCAATTGCTGTACCAGCTTATAAAGACTAC
GTAACCAAAAGTGAAGTGGCTTCTGCGGTAGCATCTTTAAAATCGATTATTACTCCA
GCAGAACTTCATTACCAAGAATATGGAGCCTTCCCAAATGACAGCACAGAATTAGAA
AGAGTCGGAGTAGGCTCTAATGCTGTCAAAAATGGTACATTAACATTTAACAAAACA
GCAGGAACTATAACTTTAGCATTAGCCTCACCTTCAGGAGTATCAGCAATTATTACG
AGAGATGGTTCAACAGGTTGGTCATGTGCTGTAACAGGTCTAACCAACCAGAGTAAT
GCACCTAAAGGCTGTCCTCAATCGGATAGCGGCACTGGTGGCACTGGCGACACTGGT
GGCTCTGGTAGTTAA

>GC#962_W7
ATGAAAGCGTATAAAAACAAACAACAGCAAGGTTTTACCTTAATTGAATTGATGATT
GTAGTGGCGATTATTGGTGTGTTGTCAGCAATTGCTGTACCAGCTTATAAAGACTAC
GTAACCAAAAGTGAAGTGGCTTCTGCGGTAGCATCTTTAAAATCGATTATTACTCCA
GCAGAACTTCATTACCAAGAATATGGAGCCTTCCCAAATGACAGCACAGAATTAGAA
AGAGTCGGAGTAGGCTCTAATGCTGTCAAAAATGGTACATTAACATTTAACAAAACA
GCAGGAACTATAACTTTAGCATTAGCCTCACCTTCAGGAGTATCAGCAATTATTACG
AGAGATGGTTCAACAGGTTGGTCATGTGCTGTAACAGGTCTAACCAACCAGAGTAAT
GCACCTAAAGGCTGTCCTCAATCGGATAGCGGCACTGGTGGCACTGGTGGCACTGGC
GACACTGGTGGCTCTGGTAGTTAA

>GC#963_E7
ATGAAAGCGTATAAAAACAAACAACAGCAAGGTTTTACCTTAATTGAATTAATGATT
GTGGTAGCGATTATTGGTGTGTTGGCAGCGATTGCTGTTCCTGCTTATAAGGATTAT
GTAACCAAGAGCGAATTGGCATCTGGTTTCGCTACTATCAAGTCCGTGATAACTCCA
GCTGAACTTTATTTCCAAGAAAATGGAAAAATAAGTGCAAGCGCAAGCACTGTTGAT
GTTCTCGGTGTATCTTCTGGAGCAAATACTTTAGGTGAACTTACTATAACCGCTGAC
AATACAATTCAATTTGCTCATGATGCTGGTGCTGCATTAGGTGCAAAATTTGTTTAC
ACAAGAAGCTCTGGAGGTTGGAGTTGCACTTACACACAACCATCAGCAGTTAGTGCA
GCAGCTCCTAAGGGCTGTACACCATAG

>GC#964_SP6
ATGAAAGCGTATAAAAATAAACTACAGAAAGGTTTTACCTTAATTGAATTGATGATT
GTGGTGGCAGTGATTGGTGTATTGGCAGCGATTGCGGTACCGCAATACCAGAAATAC
GTAGCGAAAAGTGAAGCAGCTTCTGCATTAGCTACGTTAACTGGCTTAAAAACCAAC
GCAGAGGCTTATACCGTTGAAACAGGATCTTTTCCCACAGATACTCAACAAGCTCAA

CTAGGTACACCATCATCTGCAATGGGTACTATTGCATATGCTAATACCGGTAGCAGT
GGTGCTGCAGGAACAATTACATTTACCTTTAGTGGTACGGTTAGCCCTAGTTTGAAA
AGCAGCGCTATCCGTTTAAAACGAGATGATTCAGGAAACTGGTCATGTGAATCCAAC
AAAGATGCAACTAGTGGGATAATACCTAAAGGATGTAATTCTGGCACTTTCTAG

>GC#999_TP
ATGAAAGCGTATAAAAACAAACAACAGCAAGGTTTTACCTTAATTGAATTGATGATT
GTGGTGGCAGTGATTGGTGTATTGGCAGCGATTGCGGTGCCTCAATATCAAGACTAC
GTCAAGAAAAGTGCTTTAGGAACCGCATTGGCTTCAGCATCCGCATACAAAACGATT
GTTGAAGACAATATTGCAACAAATAATCAGTTTCCATTTATATCAGAATCATTTGGT
ATAGGCACAATCCGTGCAACATCAGGAGCTATTGCAACAGGGAATGGCACTAACGAT
ATCGTTGCAAGTGTTACACAAGGATCTGGTACTGGGTCGAGCGTTACTTTAAAACGG
GACGCTTCTGGTAACTGGACATGCGCTCTATCCGGAGCTTCTAATATTACTTTAGGT
GGCTGTTCATAA

>GC#1000_SIO
ATGAAAGCGTATAAAAATAAACTACAGAAAGGTTTTACCTTAATTGAATTGATGATT
GTGGTGGCGATTATTGGTGTGTTAGCAGCGATTGCTGTGCCTGCTTATAAGGATTAT
GTCACCAAGAGTGAAGTCGCATCTGCGGTTGCATCACTAAAATCGATTATTACTCCA
GCAGAACTCTATTATCAAGAGCAAGGAGCATTCCCAGCACAAGGCAGTGATATTGGT
ATCGATCTTACTGGTTTATCTTTTGCTTCTAATGCAATAACTCTAGCATTAACCTCT
CCTTCCGGCGCTCAAGCTACCATAACAAGAGAGGACACGAAAGGTTGGAGTTGTAAA
GTCGCAGGTCTAACCAAACCCGCTAATGCACCTAAAGGTTGCCCTCAATAA

>GC#2501_DRC186-4
ATGAACGCGTATAAAAACAAACAACAGCAAGGTTTTACCTTAATTGAATTGATGATT
GTGGTAGCGATTATTGGTGTGTTAGCAGCGATTGCTGTGCCTGCTTATAAGGATTAT
GTCACTAAGAGTGAAGCATCCTCAGCTATCGCAACACTGAAAGCACTGCAGACCCCT
GCGGAGCTACTCTATCAAGAGAATGGTAATTTAACCGTTAGTAATGCCCTAGCAGCA
TTAGGTACATCAGAAAACGCCAACCCGCTGGGAAAATTGGAGGTAGAGGGTACTGAT
GGGTTAAAGTTTACCTTCACACAATCAGGAGCCTTGAAAGATCAAACCATAACCTTA
CAGAGAAGTGGTACTGACGGTTGGAAATGTAATGCTTCTGACAAAATTGAAAAACTC
AAGATAAAATCTTGTACAACAGCACAATAG

>GC#3079_DL4215
ATGAAAGCGTATAAAAACAAACTACAGAAAGGTTTTACCTTAATTGAATTGATGATT
GTGGTGGCAGTGATTGGTGTTTTGGCAGCGATTGCCATTCCTCAATATCAAAAATAT
GTAGCAAAAGCTGAAGTCGCATCAGCATTAGCTACATTAACTGGGATTAAAACAAAT
GTTGAAGCTTATGCTGTTGAAACAGGAAGTTTTCCAGCAGCAGGAAAAGAGGGAGAC
TTAGGCGTACCTACATCCATTCCATCAGGGACCGTAGCATTTGCTGCGACATCTTCA
GGCGCAGGTACTATTACTTTTAGCTTTAACACATCAAACGTAAGCAATTTGATCTCT
GGCAAAAAATTTCTTCTAAATAGGACAAGCGCAGGCGTTTGGACATGTGACGGCGCA
GCAACTACCCCAGTAACAGATGATTTACTACCTAAAAACTGTATATAA

>GC#3081_1587
ATGAAAGCGTATAAAAACAAACAACAGCAAGGTTTTACCTTAATTGAATTGATGATT
GTGGTGGCGATTATTGGTGTGTTGGCAGCTGTCGCTATTCCTGCTTACAAAAGCTAC
GTTGCAAAGTCTGAGGCAGCAACTGCGGCTGCAACTGTTAGAGGTTTATTAACCAAT
ATTGATATGTACCAACAAGAAGTAGGCAGTTTTCCAACTGATATAACTAAAGTGGGT
GGAACCACAACAATGAATGCTTTCGGTTCAATTGCACTAGCTAGCACCGTTAGTGGA
GGAACAGCAACATTCACTTTCACTGATGGTGCATTAAAAACAGGTGGTACAGGTAAT

ACGGCTGCAAAAATTATTTACACGAAAGATAACGCCACTGGATGGACTTGTACGCAT
ACAATTAATGACACATCTGTAGTGCCATCAGGCTGTTGA

>GC#3084_DL4211
ATGAAAGCGTATAAAAATAAACTACAGCAAGGTTTTACCTTAATTGAATTGATGATT
GTAGTGGCAGTGATTGGTGTGTTGGCAGCGATTGCGGTGCCTCAATATCAGAAATAT
ACACAAAAAGCAGCTCTTGCTACTGCTTTAGCTACAGCAACTGCATTAAAAACAAAT
TATGAAGACTATGTATCTATGAGTGGTGCAGCTCCCACATCTGCAACAGATATTGGA
GCAACCAGCTTCAGTATAGGAACTATTTCAGTGACTAGTGGTGCTATAAACGTTGCT
ATAAATAAGGGACCAGGCACTGGCTCATCTGTAATTTTAACTAGAACAGGGCTTCTT
GGTGGCTGGGGATGCCAAATCTCCGGAGCTCAAGCTGAAGTAACAATTAACGGTTGC
CCATAG

>GC#5537_W10G
ATGAAAGCGTATAAAAACAAGCTACAGAAAGGTTTTACCTTAATTGAATTGATGATT
GTAGTGGCGATTATTGGTGTGTTGGCTGCTGTCGCTATTCCGGCTTATCAAGATTAT
GTAAAAAAATCGGAGGCTGCTTCTGCTTTAGCCACATTAAGAGCATTGATCACTCCT
GCTGAGCTGTTCTATCAAGAAAAAGGAGTTGGAGCCGCAGCTACCGTCGCCGAATTA
GGTTCATCAGGTACTGCCAATGATCTAGGGACTATTACATCCGCTCTAGTCAATGCT
AAACCAACCCTTAAATTTGAGTTTGGTGCCAATAGCTCGATGGCAAGCACTGACACA
TTAACTTTTACTAGAGATACTGGTGGCTGGACATGTGCAATAGCCGGTAATGTTCCA
GCTATTGATGGTTGCCAATAA

>GC#5539_Sa10G
ATGAAAGCGTATAAAAACAAACAACAGCAAGGTTTTACCTTAATTGAATTAATGATT
GTGGTAGCGATTATTGGTGTGTTGGCAGCGATTGCTGTTCCTGCTTATAAGGATTAT
GTAACCAAGAGCGAATTGGCATCTGGTTTCGCTACTATCAAGTCCGTGATAACTCCA
GCTGAACTTTATTTCCAAGAAAATGGAAAAATAAGTGCAAGCGCAAGCACTGTTGAT
GTTCTCGGTGTATCTTCTGGAGCAAATACTTTAGGTGAACTTACTATAACCGCTGAC
AATACAATTCAATTTGCTCATGATGCTGGTGCTGCATTAGGTGCAAAATTTGTTTAC
ACAAGAAGCTCTGGAGGTTGGAGTTGCACTTACACACAACCATCAGCAGTTAGTGCA
GCAGCTCCTAAGGGCTGTACACCATAG